TARGETING EARLY STAGES IN NON-MAMMALIAN ISOPRENOID BIOSYNTHESIS: 1-DEOXY-D-XYLULOSE 5-PHOSPHATE (DXP) SYNTHASE AND REDUCTOISOMERASE ISPC.

by

Jessica M. Smith

A dissertation submitted to The Johns Hopkins University in conformity with the requirements of the degree of Doctor of Philosophy

Baltimore, MD
November 2013

Abstract

This dissertation research is focused on mechanistic studies of early stage, non-mammalian isoprenoid biosynthesis enzymes, toward the development of selective inhibitors that will target serious human pathogens including *Mycobacterium tuberculosis* and *Plasmodium falciparum*. A major focus of this research has been toward elucidating the random sequential, preferred order mechanism of the first enzyme in the pathway, 1-deoxy-D-xylulose 5-phosphate (DXP) synthase, an unprecedented enzyme in the thiamine diphosphate-dependent family of enzymes. Understanding this mechanism has been integral for selective inhibitor design and we have demonstrated, for the first time, selective inhibition of *E. coli* DXP synthase by butylacetylphosphonate (BAP). Further, selective inhibition is conserved in *Y. pestis*, *S. enterica*, and *M. tuberculosis.* This discovery is significant because DXP synthase is underdeveloped as a drug target and few inhibitors of this enzyme exist.

Subsequently, BAP was evaluated as an antimicrobial agent against *E. coli*. Results of these studies demonstrated DXP synthase as an intracellular target of BAP showed that antimicrobial activity is dramatically enhanced in combination with several established antibiotic classes. These results indicate that BAP has the potential to be further developed as a broad spectrum antibiotic. With antibiotic resistance on the rise, this could have great impact in the treatment of resistant bacterial infections.

In addition to mechanistic studies of *E. coli* DXP synthase, initial studies were carried out to understand the mechanism of the *M. tuberculosis* enzyme (Dxs1), as homology modeling (Jürgen Bosch, Ph.D.) suggested differences in the active site of Dxs1 compared to enzymes from *E. coli* and *D. radiodurans*. Mutagenesis and inhibition

studies performed during the course of this research demonstrate interesting differences in the active site of Dxs1 near the cofactor binding site. This is an important consideration for inhibitor development and will contribute to the efforts of those in the field targeting DXP synthase.

DXP reductoisomerase (IspC), the second enzyme in the pathway, was also targeted. In order to overcome poor pharmacokinetics of fosmidomycin, *N*-acetyl fosfoxacin analogs and a FR900098 phosphonamidate prodrug were biochemically evaluated as inhibitors of *E. coli* IspC. Acetohydroxamic acid (AHA) exhibited enhanced activity against IspC in the presence of phosphate. The activated FR900098 phosphonamidate prodrug also exhibited inhibitory activity against IspC, and displayed anti-parasitic activity against *P. falciuparum* comparable to fosmidomycin.

Advisor: Dr. Caren L. Freel Meyers

2nd Reader: Dr. Jürgen Bosch

Acknowledgements

I would like to thank all of the members of Dr. Caren Freel Meyers' lab for technical assistance, helpful discussions, and moral support. Specifically, I would like to thank Leighanne Brammer Basta for providing the E370A DXP synthase variant, as well as assistance with DynaFit analysis. I am especially thankful for Ryan Vierling and the large amount of time he has spent synthesizing acetylphosphonate compounds for biochemical and antimicrobial evaluation. I particularly enjoyed working together in the initial butylacetylphosphonate studies. I would also like to thank Dr. David Meyers for the tremendous effort in the synthesis of IspC inhibitors. Additionally, I would like to thank everyone in the laboratory of Dr. Andrew Koppisch at Northern Arizona University, including Nicole Warrington and Paul Phillips, for assistance in pathogenic studies. Thanks to everyone in the laboratory of Dr. Theresa Shapiro for assistance in *P. falciparum* studies, as well as helpful discussion.

I would also like to give special thanks to Dr. Carolyn Machamer and everyone affiliated with the Biochemistry, Cellular, and Molecular Biology graduate program. My thesis committee is also acknowledged for providing support and critical feedback; I would like to thank Dr. James Stivers, Dr. Jürgen Bosch and Dr. Eric Nuermberger. Dr. Nuermberger is also acknowledged for providing *M. tuberculosis* genomic DNA. I also am extremely grateful for the mentorship of Dr. Caren Freel Meyers, without her guidance and support none of this would have been possible. I recognize how fortunate I am to have such an exceptional advisor that demonstrates such dedication and patience toward her students. I truly appreciate that she took the time throughout my studies to challenge me when it was required and encourage me when I needed it. It is because of

Caren that I am graduating with confidence, as an independent scientist, excited about what the future holds. Lastly, I would like to thank my family and friends for the support they have given me over the past six years. Graduate school is not an easy endeavor, and I am grateful that I have such a supportive network of individuals that helped me through it. Mostly, I would like to thank my husband, Ben, for always being there with support and encouragement, no matter what.

This work was supported by The National Institute of Health: 5T32-GM007445, R01-GM084998, and F31GM099467.

Table of Contents

List of Tables

List of Figures

Chapter 1: Introduction.

Chapter 2: Toward elucidation of 1-deoxy-D-xylulose 5-phosphate (DXP) synthase mechanism.

Chapter 5: Targeting DXP reductoisomerase (IspC) using fosmidomycin analogs.

CHAPTER 1: INTRODUCTION

1.1 Antibiotics and antimicrobial resistance.

Antibiotics are one of the pillars of modern medicine. They target a variety of essential biosynthetic pathways in bacteria and human pathogens. These targets are either different or non-existent in humans, which make antibiotics relatively nontoxic as drugs [(1)]. Antibiotic resistance can occur through a number of different mechanisms (**Figure 1-1**). For example, a large family of efflux pumps can eject an antibiotic from within the cell, effectively lowering intracellular concentration, as observed in linezolid and the AcrABTolC multidrug pump [(2, 3)]. This mechanism of resistance is one of the most common and occurs with most antibiotic classes [(2, 3)]. In another example, tetracycline efflux can occur where tetracycline itself upregulates the transcription of efflux pump, TetA(B) [(2, 3)]. Immunity and bypass can also occur; either the antibiotic or its target becomes bound to a protein that prevents interaction between the antibiotic and target [(2, 3)]. In particular, ribosomal protection proteins (RPPS) that are widely distributed in both Gram-negative and Gram-positive bacteria, mediate tetracycline resistance by dislodging tetracycline from the ribosome and increase the apparent dissociation constant (K_d) of tetracycline binding [(4)]. Microorganisms can also become resistant when there is a mutation in the antibiotic target itself [(2, 3)]. For instance, under normal circumstances vancomycin binds with high affinity to the D-Ala-D-Ala C-terminus of the *N*-acetylmuramyl-pentapeptide and prevents cell wall biosynthesis [(5)]. However, bacteria are able to modify the target of vancomycin to D-Ala-D-lactate, and this results in a ~1000 fold decrease in affinity [(5)].

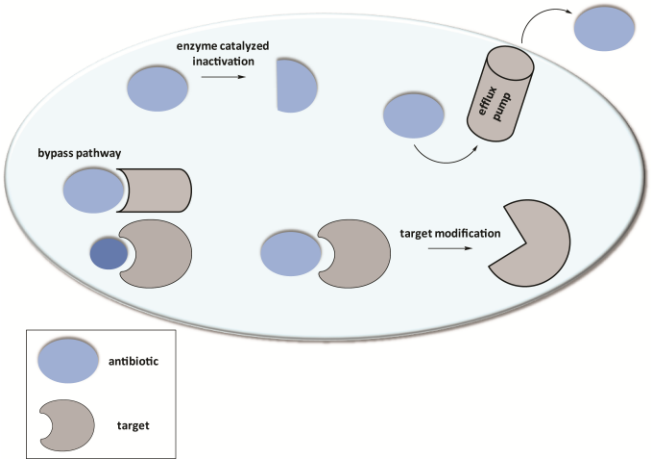

Figure 1-1. Mechanisms of antibiotic resistance.

Finally, enzyme-catalyzed inactivation of an antibiotic is the largest and most specific form of resistance [2, 3]. For example, beta-lactam antibiotics, such as penicillin, can undergo ring-opening, catalyzed by beta-lactamase enzymes, and this deactivates the molecule's antibacterial properties [6]. The 1940s truly were the "Golden Age" of antibiotic discovery, during which many of the antibiotics still used today were deployed [2] (**Table 1-1**). However, the more an antibiotic is used, the higher the incidence of resistance against that antibiotic becomes in response to selective pressure. To date, clinically relevant resistance has been observed for almost every antibiotic class established [2]. This is especially concerning in light of the 40 year innovation gap, following the "Golden Age" of antibiotic discovery during which no new structural classes of antibiotics were developed [2]. The Golden Age took place during World War II; there was a large push to develop antibiotics in order to provide support to troops, as most soilders were dying from infection. Another reason for this gap is that regulatory

authorities started demanding stricter guidelines, which slowed the number of drugs in development [7].

antibiotic class	example	discovered	deployed	resistance observed	targets	effective against
sulfadrugs	prontosil	1932	1936	1942	dihydropteroate synthase	Gram positive
β-lactams	penicllin	1928	1938	1945	cell wall biosynthesis	broad spectrum
aminoglycosides	streptomycin	1943	1946	1946	30S ribosomal subunit	broad spectrum
chloramphenicols	chloramphenical	1946	1948	1950	50S ribosomal subunit	broad spectrum
macrolides	erythromycin	1948	1951	1955	50S ribosomal subunit	broad spectrum
tetracyclines	chlortetracycline	1944	1952	1950	30S ribosomal subunit	broad spectrum
rifamycins	rifampicin	1957	1958	1962	RNA polymerase β-subunit	Gram positive
glycopeptides	vancomycin	1953	1958	1960	cell wall biosynthesis	Gram positive
quinolones	ciprofloxacin	1961	1968	1968	DNA synthesis	broad spectrum
streptogramins	streptogramin B	1963	1998	1964	50S ribosomal subunit	Gram positive
oxazolidinones	linezolid	1955	2000	2001	50S ribosomal subunit	Gram positive
lipopeptides	daptomycin	1986	2003	1987	cell membrane	Gram positive
fidaxomicin		1948	2011	1977	RNA polymerase	Gram positive
diarylquinolone	bedaquiline	1997	2012	2006	F_1F_0-ATPase	*Mycobacterium tuberculosis*

Table 1-1. Timeline of antibiotic discovery and resistance. Adapted from Lewis 2013 [8].

Another reason is that the pharmaceutical industry has cut back antibiotic research programs; antibiotic research is less profitable over time compared to other therapies because antibiotics are typically prescribed for short course treatment, and are not generally prescribed for chronic illness. Typical antibiotic regimens vary depending on the type of infection. For example, treatment of an acute ear infection involves a seven to ten day amoxicillin course [9], while the treatment regimen for an active tuberculosis infection requires several antibiotics taken over the course of six to nine months [10].

Areas of the world most impacted by infectious disease, such as tuberculosis and malaria, include sub-Saharan Africa and parts of Asia, but accessibility to treatments is not always possible at these locations [11]. This specifically impacts antibiotic discovery because there is no "for profit" demand in these developing countries. Although the Food and Drug Administration has implemented a number of programs to entice industry development of antibiotic research programs [12], the well is drying up. To date, only two new antibiotics have been approved in the past 5 years for the treatment of multidrug-resistant gram-negative bacilli and the number of antibiotics approved annually continues to decline [13]. Bedaquiline (diarylquinoline) is the most recent antibiotic approved by the FDA in December of 2012, specifically for the treatment of multi-drug resistant tuberculosis infection [14]. This antibiotic has a novel mechanism of action; targeting the proton pump of ATP synthase [14]. Although bedaquiline represents the first new drug approved to treat tuberculosis in 40 years, there are serious side effects accompanying treatment with this drug. Namely, bedaquiline has been reported to cause QT interval prolongation associated with polymorphic ventricular tachycardia, a potentially fatal event [14].

The antibiotic shortage is a problem because antibiotic resistance represents a serious global public health threat. With the incidence of multidrug resistant bacteria on the rise, the need for more effective anti-infective agents is urgent. Although antibiotics exist for the treatment of tuberculosis and malaria, these infectious diseases continue to account for over 3 million deaths annually [11]. Although antibiotics exist for *M. tuberculosis*, extensively drug-resistant tuberculosis (XDR-TB) is resistant to even the most effective anti-TB drugs and therefore remains very difficult to treat [10]. In addition

to increasing the severity of disease, resistance is also driving up the cost of health care; about $20 billion a year in the United Stated alone [15]. A resistant infection leads to longer hospital stays and treatment with second or third choice medications, which are less effective, more toxic, and more expensive. More efforts are required toward the development of effective anti-infective agents that require shorter treatment durations, smaller doses, and are more cost effective. In order to achieve these goals, new targets for anti-infective medications need to be examined.

1.2 Isoprenoids are essential in Nature.

Isoprenoids are the largest natural product class, comprising over 40,000 compounds [16]. These natural products are essential in all living organisms and are generated from two 5-carbon building blocks [17, 18]: isopentenyl diphosphate (IDP) and its isomer, dimethylallyl diphosphate (DMADP) (**Figure 1-2**).

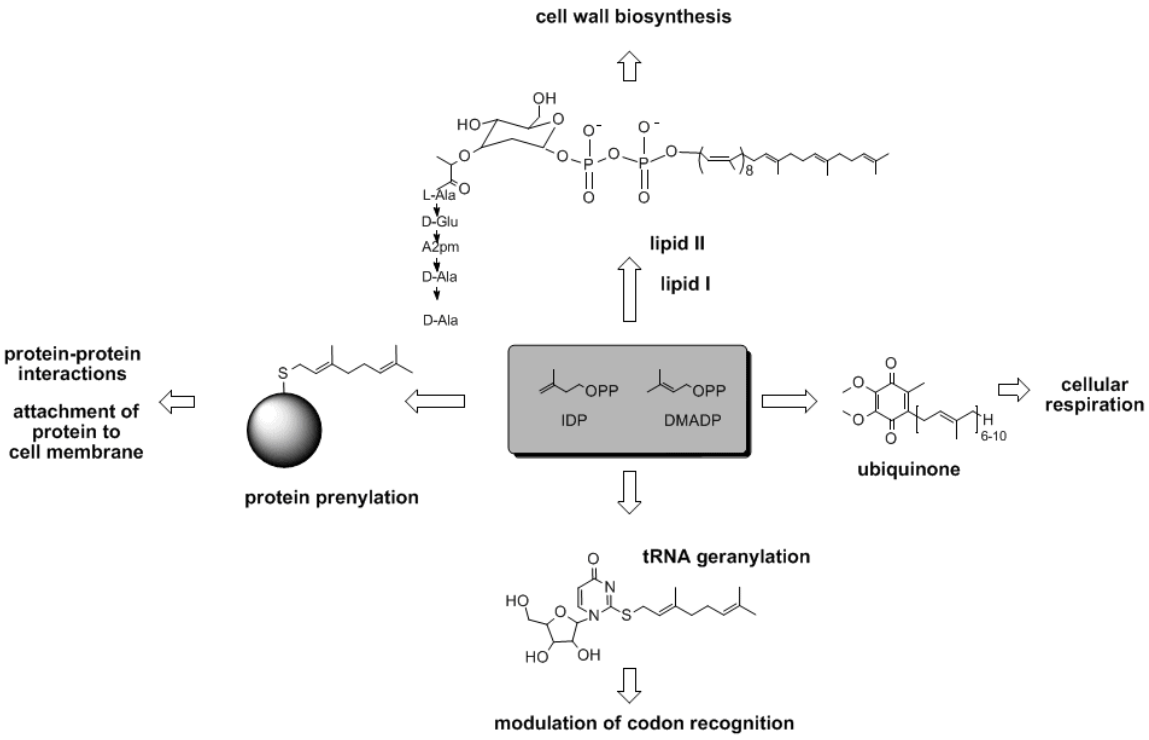

Figure 1-2. Isoprenoid as building blocks for selected metabolites in bacteria and human pathogens.

Isoprene units are assembled and modified in thousands of ways, leading to a high degree of structural diversity within the isoprenoid class. Compounds within this class are classified by the number of isoprene units (C_5H_8) they contain: monoterpenes, $C_{10}H_{16}$; sesquiterpenes, $C_{15}H_{24}$; diterpenes, $C_{20}H_{32}$; triterpenes, $C_{30}H_{48}$; tetraterpenes, $C_{40}H_{64}$; and polyterpenes, $(C_5H_8)_n$ [19]. They are the building blocks that make up cholesterol, steroid hormones, ubiquinone, and fat soluble vitamins, in addition to many secondary metabolites found in all life forms [16] (**Figure 2**). Specifically in bacteria, the MEP pathway generates precursors to Lipid I and II, both of which are essential in bacterial cell wall biosynthesis [20, 21]. Additionally, it was recently proposed that geranylation of tRNA may play a role in modulating codon recognition during bacterial translation [22].

Further, in both bacteria and the malaria parasites, isoprenoids are essential for processes such as protein prenylation, ubiquinone biosynthesis, and GPI anchor biosynthesis [23].

1.3 Isoprenoid precursor biosynthesis.

Although the isoprenoid natural product class is highly diverse structurally, all compounds within this class originate from IDP and DMADP [17, 18]. IDP and DMADP can be generated via the classical mevalonate (MVA) pathway. In this pathway, discovered in 1950 through isotopic labeling in feeding experiments [24, 25], three acetyl coenzyme A (acetyl-CoA) molecules undergo a series of condensation and reduction reactions to generate mevalonate (**Figure 1-3**). After mevalonate is phosphorylated to give mevalonate 5-diphosphate, mevalonate 5-diphosphate decarboxylase generates IDP, which can undergo isomerization to form DMADP. There are a number of drugs that target the mevalonate pathway in humans; specifically, statins are used to decrease cholesterol levels and the nitrogen-containing bisphosphonate class is used to treat various bone degenerative disorders [26]. For decades, it was believed that the mevalonate pathway was the sole source of IDP and DMADP. However, work in bacteria in the 1980s suggested an alternative to the mevalonate pathway existed. Studies to examine incorporation of [1-^{14}C] and [2-^{14}C] acetate (a precursor to acetyl CoA) into the side chain of a bacterial hopanoid were inconsistent with IDP or DMADP derived from the MVA pathway [27]. These experiments were then repeated in *Escherichia coli* and again the isoprenic units of the ubiquinone prenyl chain presented the same labeling pattern, independent of the MVA pathway. Feeding studies of [$^{13}C_6$] glucose were then performed in *Zymomonas mobilis, Methylobacterium fujisawaense*, *E. coli*, and *Alicyclobacillus*

acidoterrestirs [28]. These early studies demonstrated that pyruvate, not acetyl-CoA from the mevalonate pathway, is the precursor of a C_2 subunit in the aforementioned organisms. It also suggested a triose phosphate derivative as a precursor of a C_3 subunit in the aforementioned organisms. Around the same time, an alternative isoprenoid biosynthetic route was also proposed to operate in plants, using the analogous labeling studies [29].

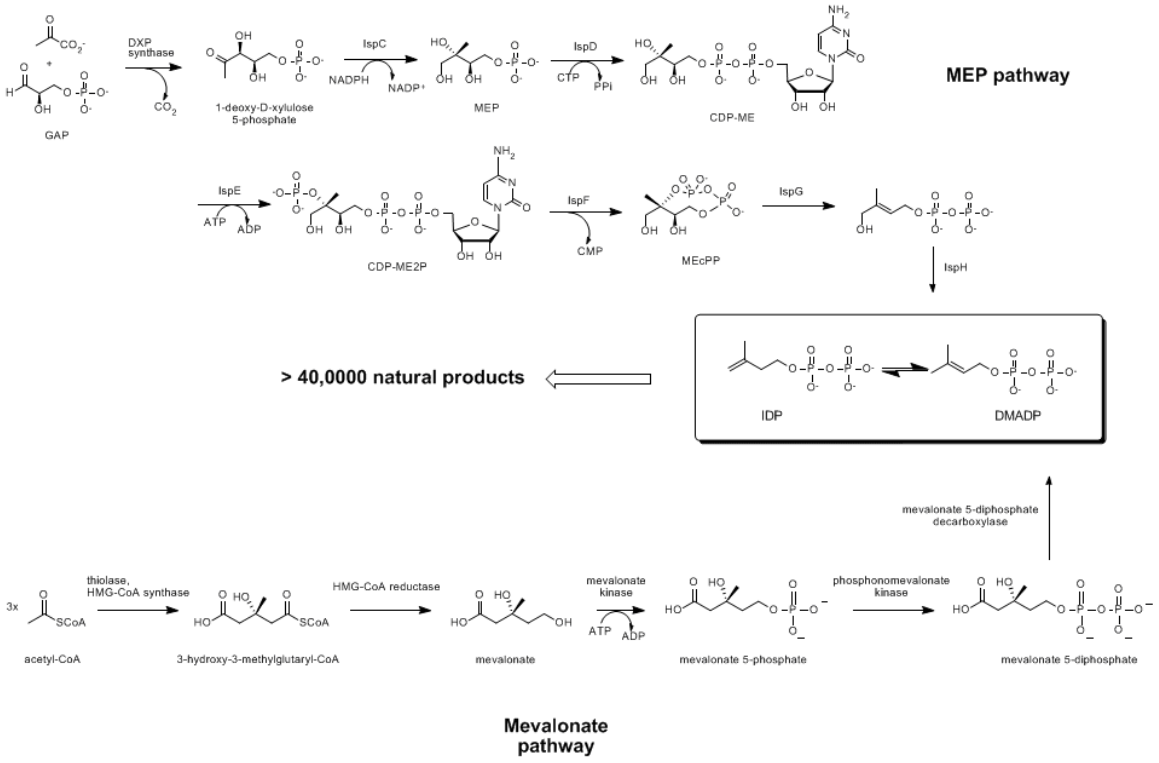

Figure 1-3. Two independent routes to isoprenoid synthesis. The mevalonate pathway is present in plants, mammals and fungi. The methylerythritol phosphate (MEP) pathway is present in plants, bacteria, and apicomplexan parasites.

In 1996, identification of the C_3 subunit was reported using single mutants of *E. coli* that were defective in each enzyme of the triose phosphate pathway and were unable

to catalyze conversions between pyruvate and glycerol [30]. Using labeled and unlabeled pyruvate and glycerol, they examined the labeling patterns in the prenyl chain of ubiquinone. All mutants incorporated the label from pyruvate into the C_2 subunit, while labeling from glycerol was only found in mutants that lacked enolase, phosphoglycerate isomerase, and glyceraldehyde 3- phosphate (GAP) dehydrogenase. The results confirmed the key role of GAP as a precursor to the C_3 subunit. The role of 1-deoxy-D-xylulose (DX) in isoprenoid biosynthesis was first recognized in *E. coli* by Zhou *et al* in 1991; labeled DX was efficiently incorporated into the prenyl side-chain of menaquinone and ubiquinone [31].

It was not until 1997 that the DXP synthase gene (*dxs*) was identified due to its homology with transketolase (TK), another thiamin diphosphate (ThDP)-dependent enzyme [32-34]. Later, it was determined that DXP synthase is the first step in the non-mevalonate, methylerythritol phosphate (MEP) pathway (**Figure 1-3**). It is now known that the MEP pathway generates IDP and DMADP in plants, most bacteria, and apicomplexan protozoa, such as the malaria parasite. The full pathway consists of seven enzymes to produce IDP and DMADP (**Figure 1-3**) and currently each enzyme in this pathway is under investigation as a potential anti-infective drug target. The MEP pathway for isoprenoid biosynthesis is not present in humans, but is essential in bacteria and human pathogens, such as *Mycobacterium tuberculosis* [35, 36] and the malaria parasites, including *Plasmodium falciparum* [37]. Further, it has been shown that this pathway is required for virulence during mycobacterial infection of mice [38]. Therefore, each enzyme in the pathway represents a novel target for the development of anti-infectives and herbicides.

1.4 The methylerythritol phosphate (MEP) pathway as a drug target.

Isoprenoids are diverse in cellular function (see section 1.2), so drugs that target the MEP pathway could act through a number of different cellular mechanisms. For this reason, anti-infective agents that target the MEP pathway have the potential to be developed as broad spectrum antibiotics. Validation for targeting this pathway comes in part from studies of fosmidomycin (3-(*N*-formyl-*N*-hydroxyamino)propyl-phosphonate), a specific, potent inhibitor of the second enzyme in the pathway, DXP reductoisomerase/MEP synthase (IspC). IspC catalyzes the NADPH and Mg^{2+} dependent transformation of DXP into MEP (for more information, see 1.13) [(39)] and fosmidomycin competes for the DXP binding site [(40)]. Fosmidomycin was originally isolated from *Streptomyces lavendulae* culture broths during a 1980 study on organisms that produce phosphonic acid antibiotics [(41)]. In 1999, fosmidomycin was shown to display inhibitory activity against purified *Plasmodium falciparum* IspC and suppress growth of *Plasmodium* in culture [(42)]. Currently, it is in phase 3 clinical trials for the treatment of uncomplicated malaria in combination with clindamycin [(43)]. However, fosmidomycin exhibits poor bioavailability due to its charged phosphonate group, absorption has been found to be only around 20-40% [(44)]. Although it is a promising lead, more efficient antibiotics that target the MEP pathway are required. Studies presented in Chapter 5 focus on addressing the poor pharmacokinetic properties of fosmidomycin and its analogs.

There are several known inhibitors of the MEP pathway, although none have progressed as far in the drug development process as fosmidomycin. 5-Ketoclomazone, a derivative of a soil applied herbicide, weakly inhibits DXP synthase from *Haemophilus*

influenzae and *E. coli* [45]. Additionally, transketolase-based thiamin analogs [46] and fluoropyruvate [42, 47] show inhibitory activity against DXP synthase, but these compounds inhibit the enzyme in a non-specific manner. 2-C-Methyl-D-erythritol 2,4-cyclodiphosphate tranferase (IspD) is modestly inhibited by L-erythritol 4-phosphate [48], but more potent inhibitors are needed against this enzyme that are more drug-like. The fourth enzyme in the pathway 4-(cytidine 5'-diphospho)-2-C-methyl-D-erythritol kinase (IspE), is inhibited by cytidine derivatives and tetrahydrothiophenyl derivatives, but these inhibitors display weak affinity and are non-selective [49]. 2-C-Methyl-D-erythritol 2,4-cyclodiphosphate synthase (IspF), the fifth enzyme in the pathway, was co-crystallized with fluorescent ligands that proved to be inhibitors of this enzyme [50]. Additionally, thiazolopyrimidine inhibitors have also been identified, and are the most potent inhibitors of IspF described to date [50]. HMB-PP synthase (IspG) and HMB-PP reductase (IspH) are inhibited weakly by alkyne-containing compounds that interact with the iron sulfur cluster in these enzymes [51, 52]. Pyridyl inhibitors of IspH also show weak inhibitory effects against this enzyme [53]. With the exception of fosmidomycin and its derivatives, inhibitors designed to target the MEP pathway enzymes are generally weak and non-specific. Although the pathway was discovered over a decade ago and significant progress has been made toward understanding enzyme mechanism throughout the pathway, potent MEP pathway inhibitors that have the potential to become anti-infective agents are lacking.

1.5 Regulatory mechanisms of the MEP pathway.

Despite the progress that has been made to understand the mechanisms of these enzymes, little is known about regulation of expression of the MEP pathway genes or control of flux through the pathway. In most bacteria, the MEP pathway genes are found throughout the genome, with no common motif between them, and no transcriptional regulators have been identified. However, studies carried out in *Mycobacterium tuberculosis* have taken the steps toward understanding pathway regulation in bacteria. Brown *et al* reported that increase in flux through the pathway was observed as a consequence of overexpression of IspG and DXP synthase (Dxs) [(36)]. It was also observed that overexpression of DXP synthase resulted in increased HMB-DP production as well, mediated by increased transcription of the operon for IspC (*dxr*), which also contains *ispG*. These studies suggest that transcriptional control is affected by the first enzyme of the pathway, Dxs1, via an unknown regulator. Additionally, work in the Freel Meyers lab has tested the hypothesis that bacterial isoprenoid biosynthesis is controlled via feedback regulation of cyclodiphosphate synthase (IspF) [(54)]. IspF, the fifth enzyme in the pathway, appears to bind to downstream isoprenoid metabolites (IDP/DMADP, GDP, or FDP) in a hydrophobic cavity as suggested by structural studies [(55-58)]. This suggested that feedback regulation of the MEP pathway might be occurring at the point of IspF. However, work from our lab has demonstrated that MEP is capable of activating and sustaining IspF activity, and only this complex is inhibited by FDP [(54)].

In plants, expression analysis of the MEP pathway genes under different conditions has shown coordinated regulation between genes in the pathway, suggesting common regulatory factors [(59, 60)]. It was also observed that mutants with low transcript

levels of the pathway genes at any step result in a decrease in accumulation of the corresponding proteins, with the exception of Dxs and IspH, who did not show a decrease in protein levels [59, 60]. Additionally, the authors reported that there is a buildup of Dxs protein levels in plants treated with fosmidomycin, and it was proposed that this is in response to changing demand for IDP and DMADP. They postulated that Dxs accumulation observed in these plant studies suggests a post-translational regulatory mechanism of the first enzyme in the pathway and warrants investigation in a bacterial or pathogenic model. Additionally, Sharkey *et al* has demonstrated that DXP synthase from *Populus trichocarpa* is inhibited by IDP and DMADP and both of these metabolites are reported to be competitive with the thiamin diphosphate (ThDP) cofactor [61].

1.6 DXP is a metabolic branch point.

1-deoxy-D-xylulose 5-phosphate (DXP) synthase is the first enzyme in the MEP pathway and represents a metabolic branch point in bacteria and pathogens [29, 32, 62]. DXP is not only a precursor to isoprenoids, but also functions as a precursor in thiamin diphosphate (ThDP, vitamin B_1) in bacteria and Plasmodium, and pyridoxal phosphate (PLP, vitamin B_6) biosynthesis in *E. coli* and a few members of the γ subdivision of proteobacteria [63-65] (**Figure 1-4**). The enzyme is unique in that it catalyzes formation of a precursor its own cofactor, ThDP.

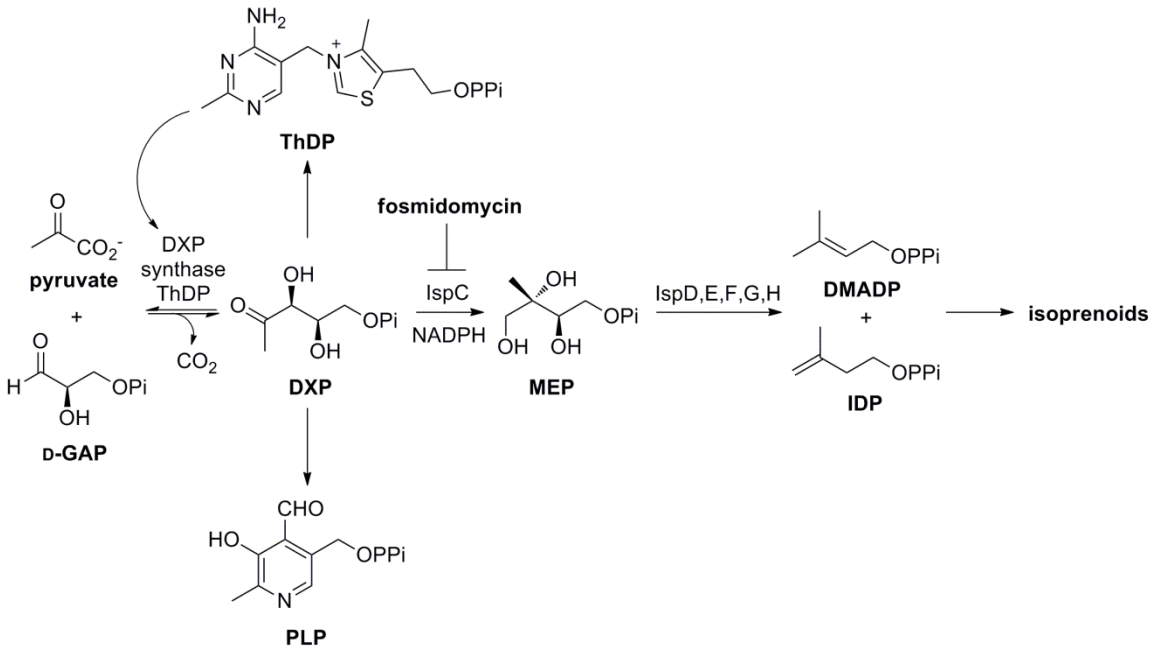

Figure 1-4. DXP synthase catalyzes the first step in IDP/DMADP biosynthesis and represents a branch point in bacterial metabolism [66].

In the thiamin biosynthesis pathway in these organisms (**Figure 1-5**), the sulfur carrier protein ThiS undergoes adenylylation by ThiF, then a sulfur transfer step to yield the ThiS thicarboxylate (ThiS-COSH). After glycine (*E. coli*) or tyrosine (*B. subtilis*) is converted to dehydroglycine, thiazole synthase (ThiG) can then couple together DXP, dehydroglycine, and ThiS thicarboxylate to give the thiazole tautomer, which then aromatizes to form the thiazole phosphate carboxylate tautomer [65, 67]. The pyrimidine ring of thiamin is formed by a rearrangement of 5-aminoimidazole ribotide (AIR) [68] to generate HMP-P, and then ThiD then phosphorylates HMP-P to give HMP-PP. After a decarboxylation step the thiazole and pyrimidine form thiamin phosphate.

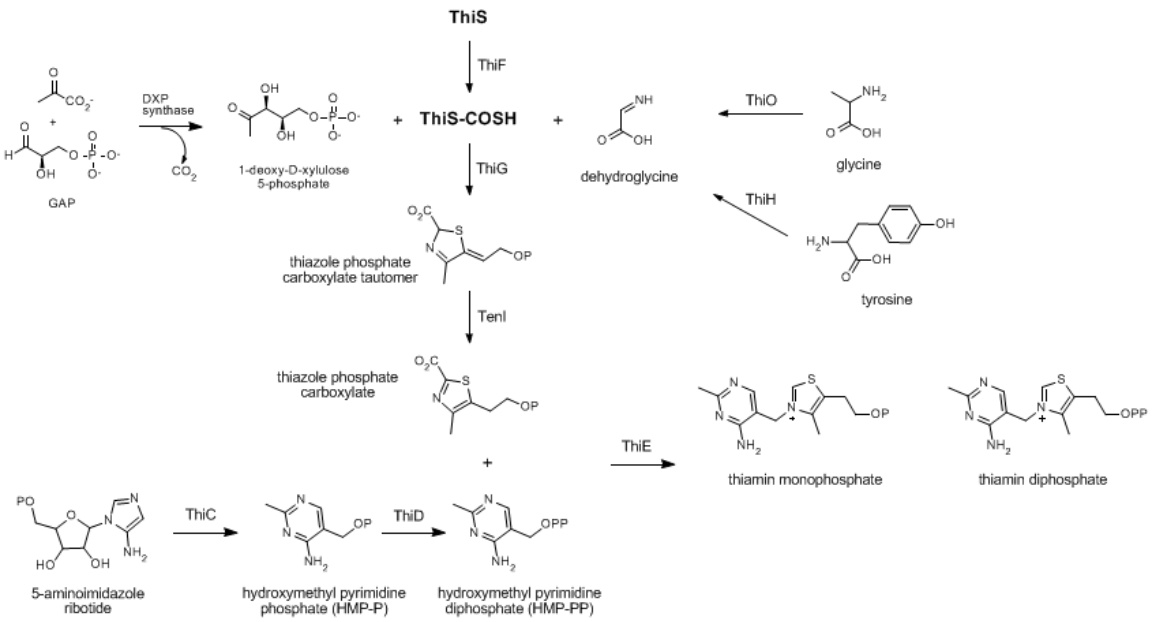

Figure 1-5. Thiamin biosynthesis in bacteria. Adapted from Jurgenson 2009 [(65)].

This metabolic process is regulated by the ThDP riboswitch, one of the most widespread riboswitches found in Nature [(65)]. When the intracellular concentration of ThDP is high, the aptamer domain of the riboswitch adopts a stable metabolite-bound conformation. When ThDP concentration is low, the ThDP dissociates from the riboswitch, leading to the expression of ThDP synthetic genes. Although bacteria and pathogens biosynthesize thiamin, a well-defined salvage pathway does exist in most microorganisms. Exogenous thiamin can be imported via an ATP-binding cassette (ABC), and then converted to thiamin-diphosphate. However, pathogens like *Mycobacterium tuberculosis* lack this salvage pathway [(64)], so inhibitors designed to block thiamin biosynthesis in organisms such as these should result in decreased survival of bacterial growth.

There are two distinct pathways for the biosynthesis of PLP [63]. The DXP-independent (ribose 5-phosphate dependent) route is widely distributed in four kingdoms of life [69-72] and has been extensively studied [73-79]. It uses PLP synthase, an enzyme composed of two subunits that function together as the glutamine amidotransferase. In the presence of ammonia, GAP, and ribose 5-phosphate, PLP is generated in a set of complex reactions. The DXP-dependent pathway for PLP biosynthesis (**Figure 1-6**) is found in *E. coli* and a few members of the gamma subdivision of proteobacteria, including *Salmonella*, *Yersinia*, *V. cholerae*, and *K. pnemoniae* [80]. It requires the convergence of DXP and 1-amino-propan-2-one-3-phosphate, produced from erythrose 4-phosphate, to generate pyridoxine 5-phosphate. Using primarily the *E. coli* model system, the PLP salvage pathway has been well characterized [32, 81-90] and it is generally agreed upon that the various forms of vitamin B_6 are interconvertible. However, the vitamin B_6 transporter has not yet been identified.

Both ThDP and PLP are essential cofactors in all living organisms. Humans depend solely on dietary uptake of thiamin and pyridoxal phosphate, so it is logical that these metabolic networks in bacteria and pathogens are suitable drug targets for anti-infectives. As DXP synthase biosynthesizes a precursor for both of these networks, in addition to the isoprenoid pathway, it makes a promising target for the development of such anti-infectives.

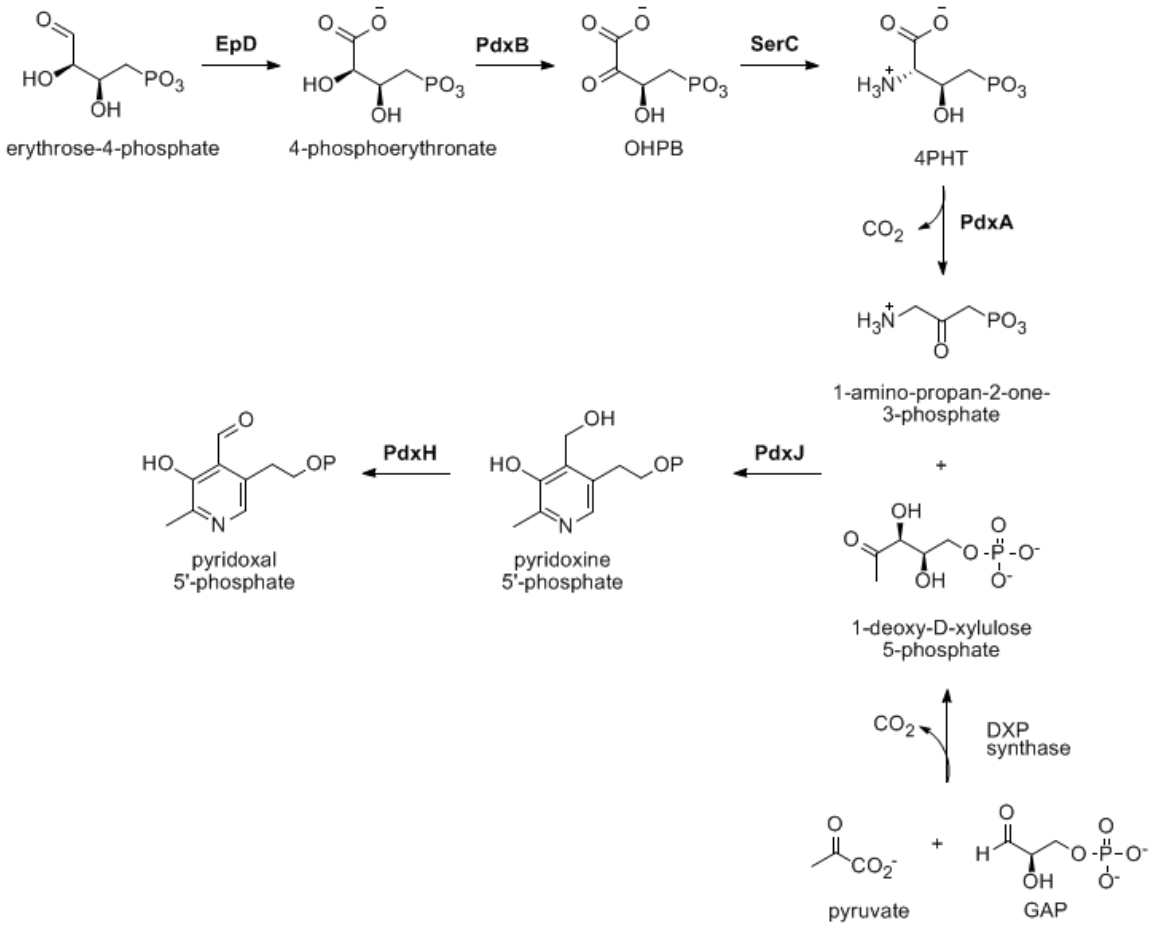

Figure 1-6. The DXP-dependent biosynthetic pathway for pyridoxal phosphate (PLP).

1.7 Alternative pathways for DXP/MEP production.

Although inhibition of the MEP pathway ought to simultaneously reduce flux through multiple essential pathways, the emergence of mechanisms to circumvent such an intervention in bacteria is inevitable. In a recent study by Perez-Gil *et al* [91], the lethal phenotype that was observed in *E. coli* by deleting *dxs* or *ispC* was partially suppressed by mutations in the unrelated genes *aceE* and *ribB*. The *aceE* gene encodes for pyruvate dehydrogenase (PDH), and the E636Q [92], Q408R, L633R, and E636G mutants partially

rescue the deficiency of *dxs*. PDH is thiamin-dependent enzyme that has been previously shown to catalyze the formation of DX from pyruvate and D-glyceraldehyde, albeit very inefficiently [93, 94]. It has also been shown that DX can be phosphorylated to DXP by D-xylulose kinase [95]. Presumably, these mutations within the active site of PDH alter enzyme activity to permit more efficient turnover to generate DX.

The *ribB* gene encodes 3,4-dihydroxy-2-butanone-4-phosphate synthase (DHBPS), whose catalysis involves a series of steps including dehydration, intramolecular rearrangement and rehydration of D-ribulose 5-phosphate to formate and 3,4-dihydroxy-2-butanone 4-phosphate[96]. The authors speculate that the G108S and D113G mutant enzymes are capable of generating DXP by utilizing either D-ribulose 5-phosphate or its isomer D-xylulose 5-phosphate as substrates.

In another study by Erb *et al*, an alternative pathway to DXP was identified in the photosynthetic, facultative anaerobe *Rhodospirillum rubrum* [97]. In this study, the authors linked polyamine metabolism to the MEP pathway by identifying a series of enzymes that catalyze DXP generation from the 5-methylthioadenosine (MTA) byproduct. Under most circumstances, MTA is cleaved and phosphorylated to generate 5-methylthio-D-ribulose 1-phosphate (MTRP), and subsequently methionine [98]. However, in *R. rubrum*, an atypical RLP (rubisco-like protein) isomerizes MTRP to 1-methylthio-D-xylulose 5-phosphate (MTXP), and then MTXP methylsulfurylase (MMS) converts MTXP into DXP. Genomic analysis revealed that enzymes involved in this metabolic shunt are conserved in several groups of bacteria, including *Rhodopseudomonas palustris*, *Methylocella silvestris*, *Rhodomicrobium vannielii*, *Meiothermus silvanus*, and *Meiothermus ruber*. Yet these are photosynthetic, non-pathogenic bacteria so the

relevancy of this shunt remains questionable as a potential mechanism of resistance to anti-infectives targeting the MEP pathway.

1.8 Thiamin-diphosphate (ThDP)-dependent enzymology.

The ThDP cofactor is present in all living systems (see 1.6 for more information regarding thiamin biosynthesis). This essential nutrient was first discovered in the 1930s by Robert Williams through its link to the nervous system disease, Beriberi [99]. ThDP consists of an aminopyridine ring connected via a carbon linker to a thiazole ring, which contains a diphosphate group (**Figure 1-7A**). Reactive intermediates along the reaction coordinate are linked to the cofactor at the C2 position of thiazole ring.

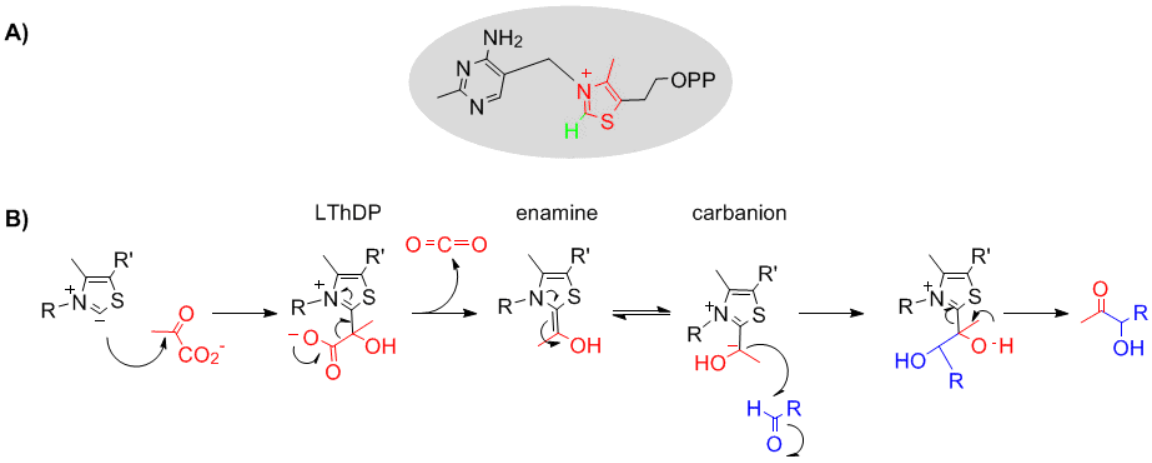

Figure 1-7. The thiamin diphosphate cofactor. A) ThDP shown with the pyrimidine ring in blue, thiazole ring in red, and C2 hydrogen in green. **B**) Enzymology for pyruvate-utilizing ThDP-enzymes. The pyruvate donor substrate is highlighted in red, with the acceptor substrate in blue. The C2α-lactylthiamin diphosphate intermediate is abbreviated LThDP.

Although ThDP-dependent enzymes can differ mechanistically (**Figure 1-8**), common themes are evident in the chemical mechanism of pyruvate-utilizing enzymes [100-102] (**Figure 1-7B**). Deprotonation at the C2 position generates the corresponding ylide intermediate, and the resulting carbanion/enamine is able to act as a nucleophile in this chemical mechanism. The carbanion attacks the carbonyl group on the donor substrate (pyruvate) to generate the lactyl-ThDP (LThDP) tetrahedral intermediate. The positively charged nitrogen on the thiazole ring then acts as an electron sink and drives release of the first product to generate the C2-α carbanion/enamine intermediate. This is a central intermediate in ThDP-dependent enzymology.

ThDP is an important cofactor in several biochemical reactions (**Figure 1-8**), such as: 1) oxidative and nonoxidative decarboxylation of alpha-keto acids (E1 subunit of pyruvate dehydrogenase, pyruvate decarboxylase, benzoylformate decarboxylase) 2) the formation of amino acid precursors (acetolactate synthase) 3) electron transfer reactions (pyruvate oxidase, pyruvate:ferredoxin oxidoreductase/pyruvate synthase) and 4) ketol transfer between sugars (transketolase). The common thread throughout all of these reactions is that the acceptor substrate, the second substrate, cannot enter the active site until the first product is released. This is a classic example of ping-pong kinetics [103].

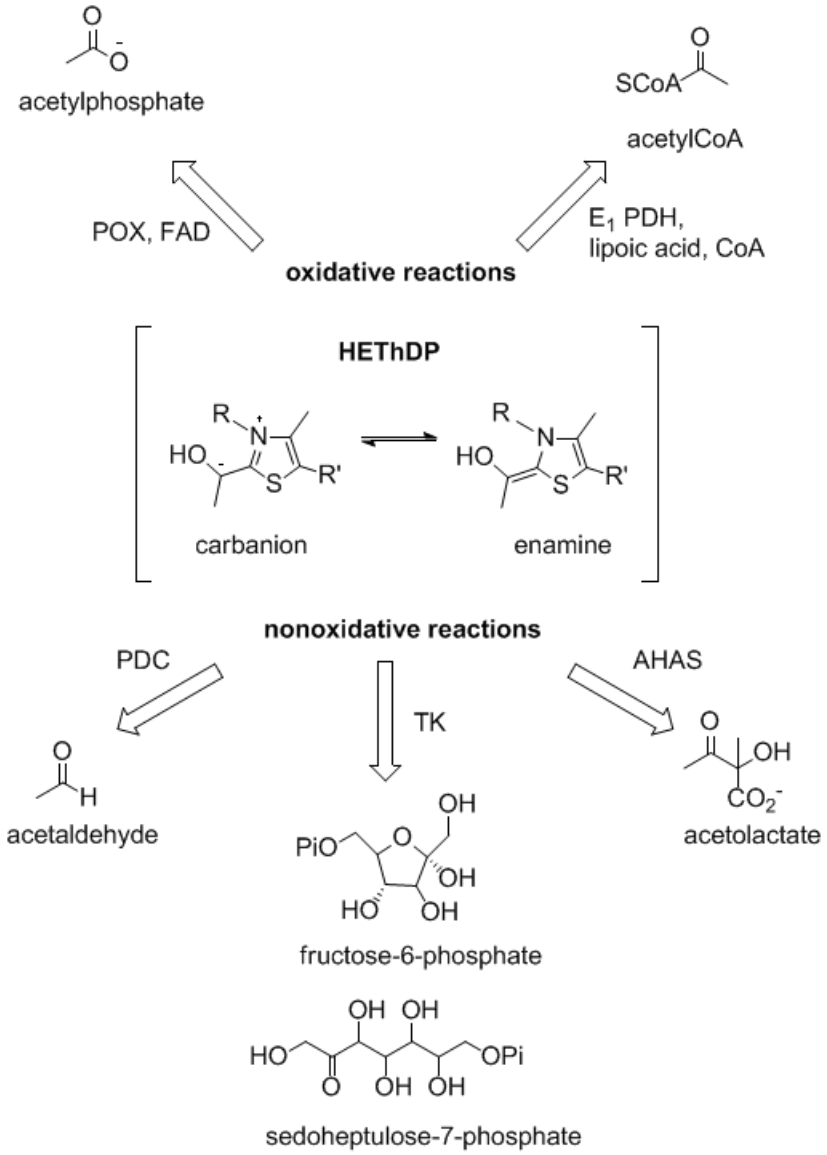

Figure 1-8. ThDP-dependent biochemical reactions. Abbreviations used: Pyruvate oxidase (POX), flavin adenine dinucleotide (FAD), E1 subunit of pyruvate dehydrogenase (E1 PDH), coenzyme A (CoA), pyruvate decarboxylase (PDC), transketolase (TK), acetohydroxyacid synthase (AHAS).

Many studies have focused on ThDP cofactor activation toward understanding factors that drive the initial deprotonation step at the C2 position. Structural evidence shows the presence of a conserved glutamate residue that is in hydrogen bonding distance from the N1' position of the aminopyrimidine ring [104-107]. Site-directed mutagenesis and spectroscopic studies [108-110] show the 4'-aminopyrimidine ring and the highly conserved interaction between a glutamate and the N1' of the cofactor are integral components of a proton relay that promotes ionization at the C2 position and activation of the cofactor (**Figure 1-9**).

Circular dichrosim (CD) studies have identified the tautomeric forms and ionization states of the cofactor for several ThDP-dependent enzymes [111] (**Figure 1-9**). The signature for the 4-aminopyrimidine (AP) form of ThDP is a negative band near 320-330 nm. This CD band is due to a charge transfer transition between the AP ring as a donor and the thiazolium ring as an acceptor. The 1,4-iminopyrimidine (IP) form gives rise to a positive CD band in the 300-314 nm range. There is no electronic absorption characteristic for the APH+ form; however the pK_a for the APH+ coincides with the pH optimum for each enzyme, indicating that all three forms (AP, IP, APH+) must be available during the catalytic cycle. These studies provide evidence for the participation of both aromatic rings in catalysis, specifically the 4-aminopyrmidine ring.

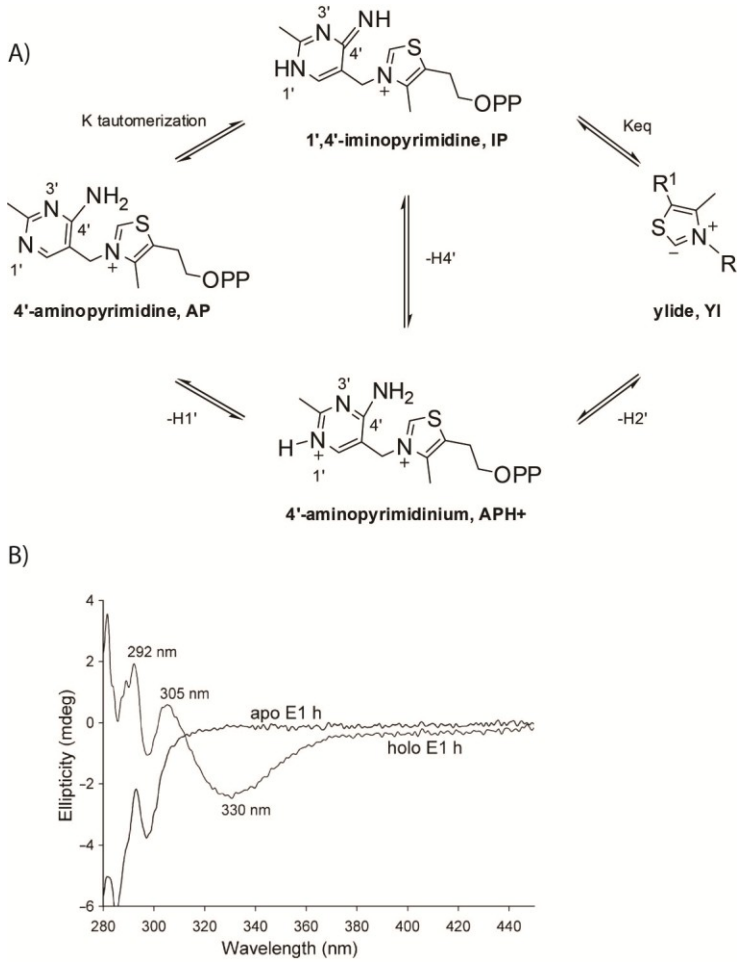

Figure 1-9. ThDP tetrahedral intermediates. A) Tautomerization states **B**) CD spectra of human E1 PDH titrated with ThDP. The spectra revealed the presence of both the IP (305 nm) and AP (330 nm) tautomeric forms of ThDP [(111)].

The ^{1}H-NMR fingerprint approach has also been used to study key intermediates in ThDP-dependent enzymes during catalysis [(112)]. This method directly detects intermediates on the basis of differences in the corresonding ^{1}H-NMR spectra and determines the quantitative distribution in an enzymatic reaction. This approach has been used during mutagenesis studies to determine functional and catalytic residues.

Finally, decarboxylation among ThDP-dependent enzymes has been extensively studied using nonenzymatic LThDP models. For example, Kluger *et al* has measured a rate constant of 4 x 10^{-5} s^{-1} for decarboxylation of a C2α-lactylthiamin [113]. Additionally, a 10^4 – 10^5 fold increase in the rate of decarboxylation has been reported when the 2-(1-carboxy-1-hydroxyethyl)-3,4-dimethyl-thiazolium ion is transferred from water to ethanol [114]. "Spontaneous" decarboxylation has also been reported for C2α-lactylthiazolium salts, with a rate constant of ~ 50 s^{-1} [115]. Collectively, these studies argue that CO_2 is a powerful electrophile, and decarboxylation may be reversible prior to separation of the CO_2 molecule from the residual carbanion. In summary, while there are subtleties in the mechanisms of the ThDP-dependent class of enzymes that remain unknown, they are generally well-studied with a number of methods available to research these enzymes, and common mechanistic themes prevail within this enzyme class.

1.9 Inhibitors of thiamin diphosphate (ThDP)-dependent enzymes.

Although the ThDP-dependent enzymes are well studied, there are few reports of inhibitors that selectively target these enzymes. For example, bacimethrin (**Figure 1-10**) is an analog of hydroxymethylthiamin-PP (HMP), an intermediate in the thiamin biosynthetic pathway [116]. Bacimethrin inhibits ThDP-dependent enzymes non-specifically and requires intracellular activation by enzymes in the thiamin biosynthetic pathway. The low micromolar inhibitiory activity observed by bacimethrin against *E. coli* can be abrogated by supplementing the growth media with low levels of thiamin or HMP. As discussed in section 1.4, inhibitors that have been evaluated against DXP synthase (5-ketoclomazone, transketolase-based thiamin analogs, and fluoropyruvate, **Figure 1-10**)

inhibit ThDP-dependent enzymes in a non-specific manner. Methylacetylphosphonate (MAP) (**Figure 1-10)** is a pyruvate analog that has been extensively used to study the mechanism of ThDP-dependent enzymes, and while it is a relatively potent inhibitor against this enzyme class (average K_i for ThDP enzymes ~ 1 μM), it also inhibits non-specifically [117-124]. The mechanisms of inhibition of fluoropyruvate and MAP will be discussed in more detail in Chapter 2.

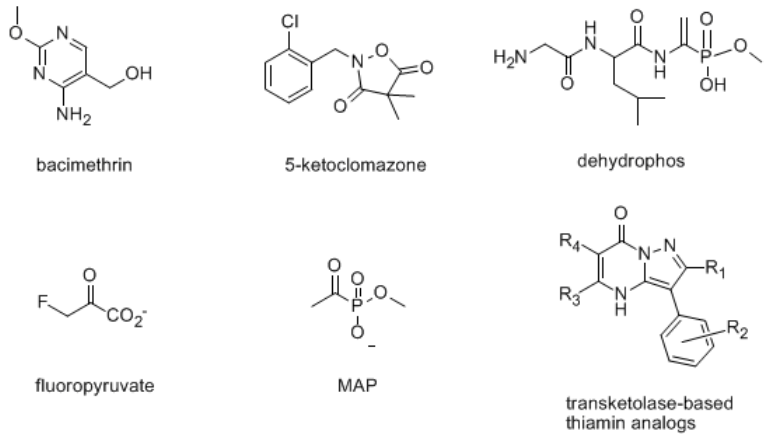

Figure 1-10. Inhibitors of ThDP-dependent enzymes.

Dehydrophos is a phosphonotripeptide natural product from *Streptomyces luridus* that exhibits broad spectrum activity as an antibiotic *in vitro* and also *in vivo* against *Salmonella typhimurium* challenged chickens [125]. It is imported via oligopeptide permeases and subsequently cleaved by intracellular peptidases to release MAP [126]. The peptide moiety of dehydrophos acts as a "Trojan horse" that allows it to be readily taken up by the cell and released after the cleavage event, where it then is believed to inhibit ThDP-dependent enzymes, such as PDH and DXP synthase. Although the charged phosphonate group presumably accounts for poor cellular uptake of MAP, Nature has

found a way to circumvent this by masking this charge in the dehydrophos natural product.

1.10 DXP synthase enzymology.

1.10.1 DXP synthase enzyme characterization.

DXP synthase combines elements of decarboxylase and carboligase ThDP-dependent chemistry by catalyzing the decarboxylation of pyruvate and subsequent condensation of this two carbon donor substrate with D-glyceraldehyde 3-phosphate (D-GAP) (**Figure 1-3**) [32]. DXP synthase enzymes have been identified, cloned, purified, and characterized from a number of bacterial species [42, 45, 47, 127-130] (**Table 1-2**). DXP synthase is also the subject of numerous botanical reports. Differences in the kinetic parameters reported for each of these enzymes appear to be affected by the buffer chosen for each study (for more information on buffer effects, see section 2.2.1). Despite the many reports of DXP synthase enzymes from plants and *Mycobacterium tuberculosis, Haemophilus influenzae*, and *E. coli,* there is a notable gap in the literature for purification of pathogenic DXP synthase enzymes. Characterization of *Mycobacterium tuberculosis, Haemophilus influenzae*, and *E. coli* DXP synthase enzymes are exceptions [45, 127, 129].

species	K_m D-GAP (µM)	K_m pyruvate (µM)	k_{cat} (min^{-1})	reference
Escherichia coli	226	1000	246	(126)
Rhodobacter capsulatus	68	440	114	(47)
Streptomyces coelicolor	300	600	66	(128)
	570	200	66	
Mycobacterium tuberculosis	6	40	N/A	(129)
Haemophilus influenzae	190	190	N/A	(45)
Populus trichocarpa	19	89	30	(61)

Table 1-2. DXP synthase steady-state kinetics. Reported kinetic constants for bacterial characterization of DXP synthase enzymes. **P. trichocarpa* was selected as an example for characterization of the plant enzyme.

M. tuberculosis DXP synthase was first identified in 2002 and partially characterized by Bailey, *et al* [(129)]. In this initial study, the *Rv2682c* (*dxs1*) and *Rv3379c* (*dxs2*) genes were identified as encoding proteins that are similar in primary structure to *E. coli* DXP synthase (~38%). Only two other bacterial species have been discovered that contain two homologs of DXP synthase: *Rhodobacter capsulatus* [(131)] and *Streptomyces coelicolor* [(128)]. However, in these species both *dxs* genes encode functional enzyme. On the basis of an *N*-terminus truncation, it was hypothesized that *dxs2* from *M. tuberculosis* encodes a non-functional enzyme. This was postulated on the basis of the observation that the *N*-terminal deletion results in the absence of a residue that corresponds to H49 in *E. coli* DXP synthase. Although it was previously proposed that H49 is critical to catalysis [(132)], work from our lab shows that H49 is not absolutely essential [(133)]. This warrants further studies on the catalytic activity of Dxs2. For *M. tuberculosis* Dxs1, there are still several questions remaining. Bailey *et al* reported Dxs1 substrate affinity (K_m) values and acceptor substrate specificity, but the catalytic constant (k_{cat}) and turnover

efficiency (k_{cat} / K_m) were not reported in this study [129]. Interestingly the enzyme is capable of turning over both D-glyceraldehyde and L-glyceraldehyde, which is unusual as most transketolases are specific for the D configuration [134]. They also found the enzyme was capable of turning over D-erythrose 5-phosphate, but not D-ribose 5-phosphate. In order to design inhibitors of the enzyme that would exhibit potential as broad spectrum antibiotics, the mechanism of Dxs1 and DXP synthase from additional pathogenic species should be further investigated.

1.10.2 DXP synthase kinetic mechanism.

As a ThDP-dependent enzyme, DXP synthase is underdeveloped as a drug target. This is presumably due to concerns about achieving selective inhibition over mammalian ThDP-dependent enzymes, such as the E1 subunit PDH and TK. Indeed, *E. coli* DXP synthase active site residues are conserved relative to other ThDP-dependent enzymes. These include His-49, proposed to play a role in proton transfer in a manner similar to that of His-30 in transketolase, and Glu-370, thought to be essential for cofactor activation [132]. Yet DXP synthase is a unique enzyme among the ThDP-dependent class, as it exhibits a novel domain architecture and kinetic mechanism [135]. The *Deinococcus radiodurans* DXP synthase crystal structure [135] shows that the enzyme has a distinctive domain arrangement. The active site is located between domains I and II of the same monomer, versus other ThDP-dependent enzymes whose active sites reside at the dimer interface.

Additionally, early work by Eubanks and Poulter on the kinetic mechanism of *Rhodobacter capsulatus* DXP synthase suggests this enzyme is mechanistically distinct

from other ThDP-dependent enzymes [47] despite the similar carboligation transformation it catalyzes. All other ThDP-dependent enzymes are believed to operate via a classical ping-pong mechanism, whereas CO_2 trapping studies have provided compelling evidence for the requirement of a ternary complex in DXP synthase catalysis. Interestingly, slow CO_2 release was observed in the absence of D-GAP, which can be explained by the acetolactate synthase activity as a side reaction of DXP synthase reported by our group in a subsequent study of DXP synthase substrate specificity [127]. Based on these experiments, as well as steady-state kinetic studies, Eubanks and Poulter proposed an ordered substrate binding model, in which pyruvate binds essentially irreversibly to the free enzyme prior to binding of D-GAP (**Figure 1-11A**).

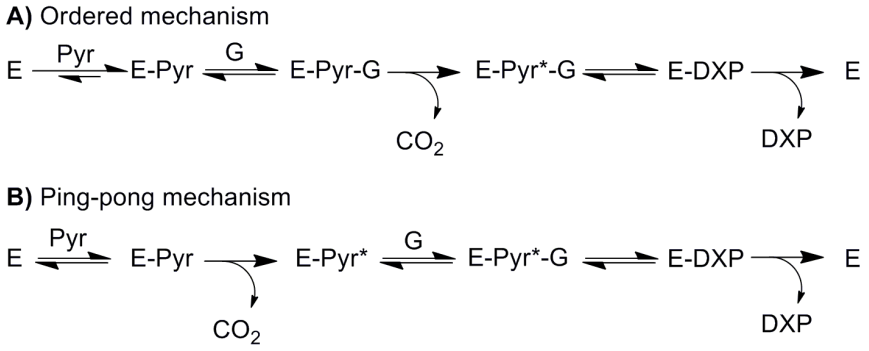

Figure 1-11. Proposed mechanistic models for DXP synthase. E, ThDP-bound enzyme; Pyr, pyruvate; Pyr*, enamine/carbanion; G, D-GAP; E-Pyr-G, catalytically competent ternary complex. **A**) ordered mechanism where pyruvate binds tightly and essentially irreversibly to DXP synthase[47, 136]. **B)** ping-pong mechanism where CO_2 liberation occurs prior to D-GAP binding[45].

A more recent study reported a single-molecule force spectroscopy nanosensor to measure *E. coli* DXP synthase substrate binding and application of single-molecule force spectroscopy for identifying beta-fluoropyruvate as an inhibitor of the enzyme [136]. Using immobilized enzyme and substrate, the authors determined substrate binding constants and suggested that the observed 1.7-fold enhancement in binding of D-GAP to DXP synthase in the presence of soluble pyruvate provides further support for an ordered mechanism. A conflicting report [45] proposes, on the basis of steady-state kinetics, that *E. coli* and *Haemophilus influenzae* DXP synthase operate via a classical ping-pong mechanism in a manner similar to other ThDP-dependent enzymes (**Figure 1-11B**).

1.11 Challenges in antimicrobial development.

With antibiotic resistance on the rise, there has been a recent push to develop new classes of drugs to combat resistant bacteria and pathogens. Nevertheless, there are specific challenges in targeting these organisms that present difficulties in the drug discovery process. For example, in addition to the cellular membrane, prokaryotes have a cell wall composed of peptidoglycan, a waxy polymer consisting of sugars and amino acid building blocks [137]. The peptidoglycan layer makes up 90% of the dry weight of the Gram positive cell. The peptidoglycan layer for Gram negative bacteria is much smaller; the dry weight is only around 10% [138]. Yet cellular transport is especially difficult because Gram negative bacteria typically have a thick outer lipid membrane. This mechanical permeability barrier prevents the entry of small molecules larger than 2 nm [139]. In bacteria, cellular entry of an antibiotic is also restrained by the amphipathic nature of most drugs. Assuming an antibiotic can gain entry through the outer and inner

membrane, the antibiotic can still be ejected by an efflux pump. Entry is especially difficult in Gram negative bacteria, whose barrier contains multi-drug resistant (MDR) pumps that are specific for amphipathic molecules [2, 3]. This poor cellular uptake requires higher doses of antibiotics for effective treatments. Although the affinity of an antibiotic to its purified target is typically comparable to a typical drug for a eukaryotic target, the effective dose is two to three orders of magnitude higher [140]. This can result in higher toxicity, presenting challenges in the drug development and approval process for new classes of antibiotics.

1.12 Antimicrobial combination therapy and synergy.

Antibiotic combinations are used for patients who are either seriously ill and may be septicemic, or to prevent the spread of resistance. For example, combinations of isoniazid and rifampicin have been used for the treatment of tuberculosis for over fifty years [10]. Combinations such as these suppress the emergence of resistance by probability; the chance of bacteria harboring multiple spontaneous, independent resistant mutations to several antibiotics is unlikely. Another benefit is that antibiotics administered in combination usually require a lower dosage, and this reduces dose-related toxicity of these drugs [141]. In most cases, the lower dosage of antibiotics when used in combination was believed to be the result of antibiotic synergy. Although there are several definitions of the term synergy, it generally means that the effect of a drug in combination is greater than the sum of their effects alone [142, 143].

There are several laboratory methods to evaluate the activity of antimicrobial combinations [142-144] and the checkerboard assay is the classical approach. The term

checkerboard refers to the pattern produced by multiple drug dilutions of the two antimicrobials being tested (**Figure 1-12**). Each antimicrobial is serially diluted at concentrations above and below its minimum inhibitory concentration (MIC). The MIC is the amount of antimicrobial required to inhibit overnight growth of the bacterial strain evaluated. From the checkerboard, one obtains a fractional inhibitory concentration (FIC) index, a predictor of synergy between the two antibiotics tested. Synergy involves a four-fold or greater decrease in the minimum inhibitory concentration of each antibiotic when used in combination, which corresponds to an FIC index of < 0.5 (for more information, see Chapter 4). After each organism is scored for growth, an isobologram can be generated (**Figure 1-12**). If the dose pair relationship is below the line of additivity, this is also an indicator of synergy.

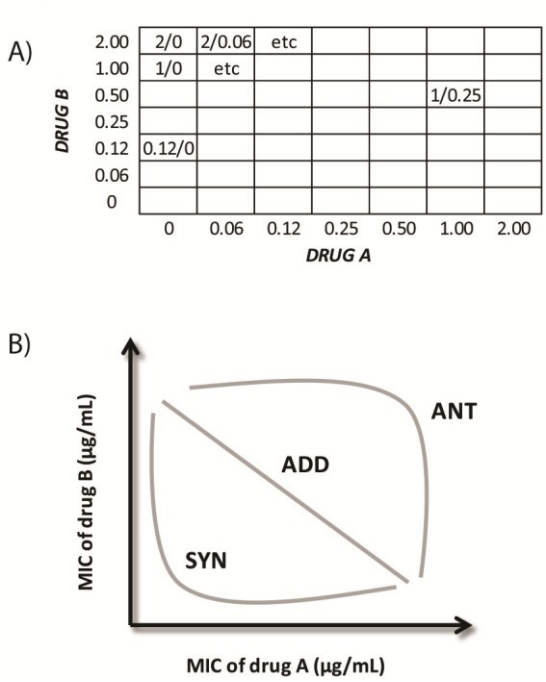

Figure 1-12. Evaluating antibiotic combinations. A) The checkerboard assay is used to determine the fraction inhibitory concentration (FIC) index between two antibiotics tested. An FIC < 0.5 is considered synergistic. **B**) An isobologram is another way to represent the checkerboard data. If the dose pair relationship is below the line of additivity, the relationship is considered synergistic. SYN = synergistic, ADD = additive, ANT = antagonistic [142-144].

In addition to the clinical implications of drug synergy, synergistic relationships have also been used to study drug mechanism of action. Synergy can occur for a number of reasons, as combinations could have: 1) different targets of the same pathway that regulate the same process, 2) different targets of the same pathway that regulate the same target, 3) different targets of related pathways, or 4) the same target itself. When synergy is observed, it can be an indicator that two drug targets are metabolically related [145].

Drug combination studies continue to be a useful tool for researching not only antibiotics, but also for drugs with eukaryotic targets as well.

1.13 Inhibition of DXP reductoisomerase by fosmidomycin and its analogs.

DXP reductoisomerase (IspC) is the first committed step of the MEP pathway. IspC catalyzes the reduction and rearrangement of DXP to generate MEP, and this occurs in an NAPDH and magnesium dependent manner (**Figure 1-13**) [39]. As discussed in section 1.4, fosmidomycin is a potent inhibitor of IspC (K_m^{DXP} = 115 μM; $K_i^{fosmidomycin}$ = 57 nM for *Synechocystis* sp. PCC6803 IspC [146]); it binds tightly in the active site of IspC in a time-dependent manner [147]. The *E. coli* IspC crystal structure shows that fosmidomycin binds in a similar manner as DXP; the flexible loop that is open in the apo form of IspC covers the active site when bound to fosmidomycin or DXP in a phosphate induced mechanism [148]. There are three regions of the substrate binding cavity: a positively charged pocket, which binds the phosphonate moiety, a hydrophobic region around the carbon backbone, and an amphipathic region, which binds to the hydroxamic acid moiety. Structure activity relationship studies show that the phosphonyl and hydroxamic acid groups are essential binding elements, and isosteric replacement of the phosphonyl group abolishes inhibitory activity [149, 150] (**Figure 1-13**). Replacement of the phosphonyl group with sulfonamide, carboxylate, and carboxamide result in a large decrease in inhibitory activity [146]. The phosphoryl analog of fosmidomycin (fosfoxacin) and its *N*-acetyl congener (FR900098) have been shown to be more potent inhibitors of IspC compared to fosmidomycin (**Figure 1-13**) [146].

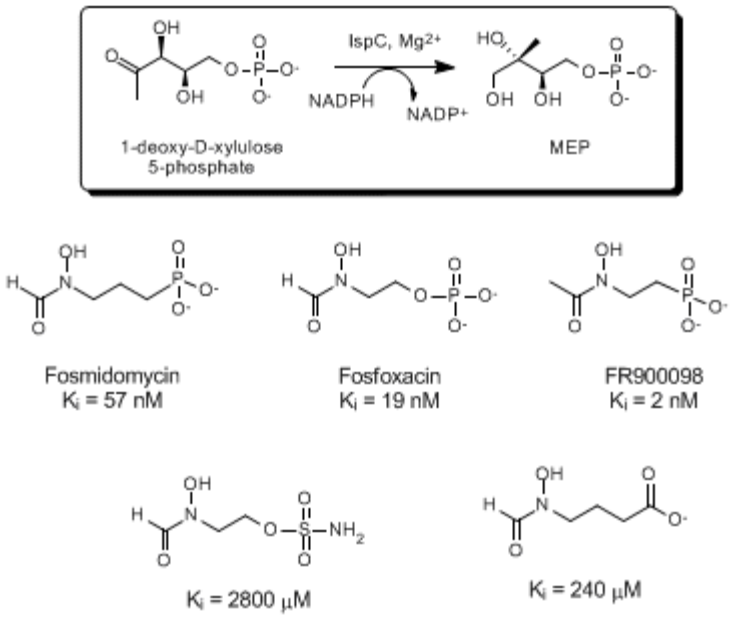

Figure 1-13. Fosmidomycin and its analogs inhibit *Synechocystis* sp. PCC6803 DXP reductoisomerase (IspC). [146]

Although fosmidomycin has shown promise as an anti-malaria agent in combination with clindamycin [43], it displays poor bioavailability, and this presumably results from poor cellular permeability [44]. Several strategies have been explored to increase the permeability of fosmidomycin. Alpha-substituted lipophilic analogs increase permeability, but decrease inhibitory activity against purified IspC [151]. Other studies have centered on generating fosmidomycin/FR900098 prodrugs, employing biodegradable delivery groups that rely upon two bioactivation steps catalyzed by esterases or phosphatases [152, 153]. Although these prodrugs resulted in improved bioavailability, esters such as these are unstable in serum, leading to premature, extracellular activation and formation of membrane impermeable intermediates [154]. Further, the second bioactivation to release fully unmasked drug is often slow. In order

to improve the efficacy of fosmidomycin, more work is needed to overcome the difficulties presented by the charged moiety of this compound.

Results of our studies support the unique requirement for ternary complex formation in DXP synthase catalysis and highlight the flexibility of this enzyme for aliphatic acceptor substrates. Taken together, these observations have guided the design of a new class of DXP synthase inhibitors, acetylphosphonates. The unnatural bisubstrate analog, butylacetylphosphonate (BAP), exhibits selective inhibition of DXP synthase over ThDP-dependent enzymes. Further, BAP displays antimicrobial activity and is shown to act in synergy with other antimicrobial agents. These results suggest a new approach for selective inhibition of early stage isoprenoid biosynthesis, toward development of new anti-infective agents. Additionally, work presented here proposes new strategies to overcome bioavailability issues of fosmidomycin and improve its efficacy as an antibiotic.

References

1. Rouveix, B. Antibiotic Safety Assessment. *Int. J. Antimicrob. Agents*. **21**, 215-221 (2003).

2. Walsh, C. T. Antibiotics: actions, origins, resistance. 335, (Washington, 2003).

3. Alekshun, M. and Levy, S. Molecular mechanisms of antibacterial multidrug resistance. *Cell*. **128**, 1037-1050 (2007).

4. Connell, S. R., Tracz, D. M., Nierhaus, K. H. & Taylor, D. E. Ribosomal Protection Proteins and Their Mechanism of Tetracycline Resistance. *Antimicrob. Agents Chemother*. **47**, 3675-3681 (2003).

5. Pootoolal, J., Neu, J. & Wright, G. Glycopeptide antibiotic resistance. *Ann. Rev. Pharmacol. Toxicol.* **42**, 381-408 (2002).

6. Drawz, S. and Bonomo, R. Three decades of beta-lactamase inhibitors. *Clin. Microbiol. Rev.* **23**, 160-201 (2010).

7. U.S. Food and Drug Administration. A history of the FDA and drug regulation in the United States. (2012).

8. Lewis, K. Platforms for antibiotic discovery. *Nat. Rev. Drug Discovery*. **12**, 371-87 (2013).

9. American Academy of Pediatrics Subcommittee on Management of Acute Otitis Media. Diagnosis and management of acute otitis media. *Pediatrics*. **113**, 1451-1465 (2004).

10. Centers for Disease Control and Prevention. Core curriculum on tuberculosis: what the clinician should know. **24** (2011).

11. World Health Organization. Global report for research on infectious disease of poverty. (2012).

12. Infectious Disease Society of America. IDSA Summary of antibiotic incentives in the FDA Safety and Innovation Act. (2012).

13. Boucher, H., *et al*. 10 x '20 Progress--development of new drugs active against gram-negative bacilli: an update from the Infectious Diseases Society of America. *Clin Infect Dis.* **56**, 1685-94 (2013).

14. World Health Organization. The use of bedaquiline in the treatment of multidrug-resistant tuberculosis: interim policy guidance, executive summary. (2013).

15. Infectious Disease Society of America. Antibiotic resistance fact sheet. (2012).

16. Rohmer, M. The discovery of a mevalonate-independent pathway for isoprenoid biosynthesis in bacteria, algae, and higher plants. *Nat. Prod. Rep*. **16**, 565-574 (1999).
17. Heuston, S., Begley, M., Gahan, C. & Hill, C. Isoprenoid biosynthesis in bacterial pathogens. *Microbiology*. **158**, 1389-1401 (2012).

18. Kuzuyama, T. and Seto, H. Two distinct pathways for essential metabolic precursors for isoprenoid biosynthesis. *Proc Jpn Acad Ser B Phys Biol Sci*. **88**, 41-52 (2012).

19. Holstein, S. A. and Hohl, R. J. Isoprenoids: Remarkable diversity of form and function. *Lipids*. **39**, 293-309 (2004).

20. Anderson, R. G., Hussey, H. & Baddiley, J. The mechanism of wall synthesis in bacteria. The organization of enzymes and isoprenoid phosphates in the membrane. *Biochem. J*. **127**, 11-25 (1972).

21. Mahapatra, S., *et al*. Mycobacterial lipid II is composed of a complex mixture of modified muramyl and peptide moieties linked to decaprenyl phosphate. *J. Bacteriol*. **187**, 2757 (2005).

22. Dumelin, C., Chen, Y., Leconte, A., Chen, Y. & Liu, D. Discovery and biological characterization of geranylated RNA in bacteria. *Nat. Chem. Biol*. **8**, 913 (2012).

23. Rodríguez-Concepción, M. The MEP Pathway: A New Target for the Development of Herbicides, Antibiotics and Antimalarial Drugs. *Curr. Pharm. Des*. **10**, 2391-2400 (2004).

24. Cornforth, J. W. and Popjak, G. Mechanism of biosynthesis of squalene from sesquiterpenoids. *Tetrahedron Lett*. **19**, 29-35 (1959).

25. Chaykin, S., Law, J., Phillips, A. H., Tchen, T. T. & Bloch, K. Phosphorylated intermediates in the synthesis of squalene. *Biochemistry*. **44**, 998-1003 (1958).

26. Thurnher, M., Nussbaumer, O. & Gruenbacher, G. Novel Aspects of Mevalonate Pathway Inhibitors as Antitumor Agents. *Clin Cancer Res*. **18**, 3524-3531 (2012).

27. Flesch, G. and Rohmer, M. Prokaryotic hopanoids: the biosynthesis of the bacteriohopane skeleton. *Eur. J. Biochem*. **175**, 405-411 (1988).

28. Rohmer, M., Knani, M., Simonin, P., Sutter, B. & Sahm, H. Isoprenoid biosynthesis in bacteria: a novel pathway for the early steps leading to isopentenyl diphosphate. *Biochem*
J. **15**, 517-524 (1993).

29. Arigoni, D., *et al*. Terpenoid biosynthesis from 1-deoxy-d-xylulose in higher plants by
intramolecular skeletal rearrangement. *Proc. Natl. Acad. Sci. U. S. A*. **94**, 10600-10605 (1997).

30. Rohmer, M., Seemann, M., Horbach, S., Bringer-Meyer, S. & Sahm, H. Glyceraldehyde 3-phosphate and pyruvate as precursors of isoprenic units in an alternative non-mevalonate pathway for terpenoid Biosynthesis. *J. Am. Chem. Soc*. **118**, 2564 (1996).

31. Zhou, D. and White, R. H. Early steps of isoprenoid biosynthesis in *Escherichia coli*. *Biochem J*. **273**, 627-634 (1991).

32. Sprenger, G. A., *et al*. Identification of a thiamin-dependent synthase in *Escherichia coli* required for the formation of the 1-deoxy-D-xylulose 5-phosphate precursor to isoprenoids, thiamin, and pyridoxol. *Proc. Natl. Acad. Sci. U. S. A*. **94**, 12857 (1997).

33. Lois, L. M., *et al*. Cloning and characterization of a gene from *Escherichia coli* encoding a transketolase-like enzyme that catalyzes the synthesis of D-1-deoxyxylulose 5-phosphate, a common precursor for isoprenoid, thiamin, and pyridoxol biosynthesis. *Proc. Natl. Acad. Sci. U. S. A*. **95**, 2105 (1998).

34. Lange, B. M., Wildung, M. R., McCaskill, D. & Croteau, R. A family of transketolases that directs isoprenoid biosynthesis via a mevalonate-independent pathway. *Proc. Natl. Acad. Sci. U. S. A*. **95**, 2100-4 (1998).

35. Brown, A. and Parish, T. Dxr is essential in *Mycobacterium tuberculosis* and fosmidomycin resistance is due to a lack of uptake. *BMC Microbiol*. **8**, 78 (2008).

36. Brown, A. C., Eberl, M., Crick, D. C., Jomaa, H. & Parish, T. The nonmevalonate pathway of isoprenoid biosynthesis in *Mycobacterium tuberculosis* is essential and transcriptionally regulated by Dxs. *J Bacteriol*. **192**, 2424-2433 (2010).

37. Lange, B. M., Rujan, T., Martin, W. & Croteau, R. Isoprenoid biosynthesis: The evolution of two ancient and distinct pathways across genomes. *Proc. Natl. Acad. Sci. U. S. A*. **97**, 13172-7 (2000).

38. Shin, S. J., Wu, C., Steinberg, H. & Talaat, A. M. Identification of novel virulence determinants in *Mycobacterium tuberculosis* by screening a library of insertional mutants. *Infect. Immun*. **74**, 3825-3833 (2006).

39. Takahashi, S., Kuzuyama, T., Watanabe, H. & Seto, H. A 1-deoxy-D-xylulose 5-phosphate reductoisomerase catalyzing the formation of 2-C-methyl-d-erythritol 4-phosphate in an alternative nonmevalonate pathway for terpenoid biosynthesis. *Proc. Natl. Acad. Sci. U. S. A*. **95**, 9879-9884 (1998).

40. Steinbacher, S., *et al*. Structural basis of fosmidomycin action revealed by the complex with 2-C-methyl-d-erythritol 4-phosphate synthase (IspC): Implications for the catalytic mechanism and anti-malaria drug development. *J. Biol. Chem*. **278**, 18401-18407 (2003).

41. Okuhara, M., *et al*. Studies on new phosphonic acid antibiotics. *J. Antibiot*. **33**, 13 (1980).

42. Altincicek, B., *et al*. Tools for discovery of inhibitors of the 1-deoxy-D-xylulose 5-phosphate (DXP) synthase and DXP reductoisomerase: an approach with enzymes from the pathogenic bacterium *Pseudomonas aeruginosa*. *FEMS Microbiol Lett*. **190**, 329-333 (2000).

43. Albert Schweitzer Hospital. Efficacy of fosmidomycin-clindamycin for treating malaria in gabonese children. Clinical trial number NCT00214643. (2009).

44. Na-Bangchang, K., Ruengweerayut, R., Karbwang, J., Chauemung, A. & Hutchinson, D. Pharmacokinetics and pharmacodynamics of fosmidomycin monotherapy and

combination therapy with clindamycin in the treatment of multidrug resistant falciparum malaria. *Malaria Journal*. **6**, 70 (2007).

45. Matsue, Y., *et al*. The herbicide ketoclomazone inhibits 1-deoxy-D-xylulose 5-phosphate synthase in the 2-*C*-methyl-D-erythritol 4-phosphate pathway and shows antibacterial activity against *Haemophilus influenzae*. *J. Antibiot*. **63**, 583-8 (2010).

46. Mao, J., *et al*. Structure–activity relationships of compounds targeting *Mycobacterium tuberculosis* 1-deoxy-D-xylulose 5-phosphate synthase. *Bioorg. Med. Chem. Lett*. **18**, 5320-5323 (2008).

47. Eubanks, L. M. and Poulter, C. D. *Rhodobacter capsulatus* 1-deoxy-D-xylulose 5-phosphate synthase: steady-state kinetics and substrate binding. *Biochemistry*. **42**, 1140-9 (2003).

48. Lillo, A. M., Tetzlaff, C. N., Sangari, F. J. & Cane, D. E. Functional expression and characterization of EryA, the erythritol kinase of *Brucella abortus*, and enzymatic synthesis of L-erythritol-4-phosphate. *Bioorg. Med. Chem. Lett*. **13**, 737-739 (2003).

49. Crane, C. M., *et al*. Synthesis and characterization of cytidine derivatives that inhibit the kinase IspE of the non-mevalonate pathway for isoprenoid biosynthesis. *Chem. Med. Chem*. **3**, 91-101 (2008).

50. Crane, C. M., *et al*. Fluorescent inhibitors for IspF,an enzyme in the non-mevalonate pathway for isoprenoid biosynthesis and a potential target for antimalarial therapy. *Ang. Chem. Int*. *Ed*. **45**, 1069-1074 (2006).

51. Liu, Y., *et al*. Structure, function and inhibition of the two- and three-domain 4Fe-4S IspG proteins. *Proc. Natl. Acad. Sci. U. S. A*. **109**, 8558-8563 (2012).

52. Wang, W., *et al*. Bioorganometallic mechanism of action, and inhibition, of IspH. *Proc. Natl. Acad. Sci. U. S. A*. **107**, 4522-4527 (2010).

53. Wang, W., Li, J., Wang, K., Smirnova, T. I. & Oldfield, E. Pyridine inhibitor binding to the 4Fe-4S protein *A. aeolicus* IspH (LytB): A HYSCORE investigation. *J. Am. Chem. Soc.* **133**, 6525-6528 (2011).

54. Bitok, J. and Meyers, C. F. 2-C-methyl-D-erythritol 4-phosphate enhances and sustains cyclodiphosphate synthase IspF activity. *ACS Chem. Biol*. **7**, 1702 (2012).

55. Richard, S. B., et al. Structure and mechanism of 2- C-methyl-D-erythritol 2,4-cyclodiphosphate synthase. *J. Biol. Chem*. **277**, 8667-8672 (2002).
56. Kemp, L. E., Bond, C. S. & Hunter, W. N. Structure of 2C-methyl-d-erythritol 2,4-cyclodiphosphate synthase: An essential enzyme for isoprenoid biosynthesis and target for antimicrobial drug development. *Proc. Natl. Acad. Sci. U. S. A*. **99**, 6591-6596 (2002).

57. Kemp, L. E., *et al*. The identification of isoprenoids that bind in the intersubunit cavity of *Escherichia coli* 2C-methyl-D-erythritol-2,4-cyclodiphosphate synthase by complementary biophysical methods. *Acta Crystallogr., Sect. D: Biol. Crystallogr*. **61**, 45-52 (2005).

58. Ni, S., Robinson, H., Marsing, G. C., Bussiere, D. E. & Kennedy, M. A. Structure of 2C-methyl-D-erythritol-2,4- cyclodiphosphate synthase from *Shewanella oneidensis* at 1.6 A:
Identification of farnesyl pyrophosphate trapped in a hydrophobic cavity. *Acta Crystallogr., Sect. D: Biol. Crystallogr.* **60**, 1949-57 (2004).

59. Guevara-Garcı´a, A. A., *et al*. The characterization of the Arabidopsis clb6 mutant illustrates the importance of posttranscriptional regulation of the methyl-D-erythritol 4-phosphate pathway. *The Plant Cell*. **17**, 628-643 (2005).

60. Sauret-Gueto, S., *et al*. Plastid cues posttranscriptionally regulate the accumulation of key enzymes of the methylerythritol phosphate pathway in Arabidopsis. *Plant Physiol*. **141**, 75-84 (2006).

61. Banerjee, A., *et al*. Feedback inhibition of deoxy-D-xylulose-5-phosphate synthase regulates the methylerythritol 4-phosphate pathway. *J. Biol. Chem*. **288**, 16926-36 (2013).

62. Hill, R. E., *et al*. The biogenetic anatomy of vitamin B6. A 13C NMR investigation of the biosynthesis of pyridoxolin in *E. coli*. *J. Biol. Chem*. **271**, 30426 (1996).

63. Mukherjee, T., Hanes, J., Tews, I., Ealick, S. E. & Begley, T. P. Pyridoxal phosphate: biosynthesis and catabolism. *Biochimica et Biophysica Acta*. **1814**, 1585–1596 (2011).

64. Du, Q., Wang, H. & Xie, J. Thiamin (vitamin B1) biosynthesis and regulation: A rich source of antimicrobial drug targets. *Int. J. Biol. Sci*. **7**, 41-52 (2011).

65. Jurgenson, C. T., Begley, T. P. & Ealick, S. E. The structural and biochemical foundations of thiamin biosynthesis. *Annu Rev Biochem*. **78**, 569-603 (2009).

66. Smith, J. M., *et al*. Targeting DXP synthase in human pathogens: enzyme inhibition and antimicrobial activity of butylacetylphosphonate. *J. Antibiot*. 2013. Advance online publication. doi: 10.1038/ja.2013.105.

67. Park, J. H., *et al*. Biosynthesis of the thiazole moiety of thiamin pyrophosphate (vitamin B1). *Biochemistry*. **42**, 12430-8 (2003).

68. Lawhorn, B. G., Mehl, R. A. & Begley, T. P. Biosynthesis of the thiamin pyrimidine: the reconstitution of a remarkable rearrangement reaction. *Org. Biomol. Chem., OBC*. **2**, 2538-46 (2004).

69. Ehrenshaft, M., Bilski, P., Li, M. Y., Chignell, C. F. & Daub, M. E. A highly conserved sequence is a novel gene involved in de novo vitamin B6 biosynthesis. *Proc. Natl. Acad. Sci. U. S. A*. **96**, 9374-8 (1999).

70. Cane, D., Shoucheng, D., Robinson, J. K., Hsiung, Y. & Spenser, I. D. Biosynthesis of vitamin B6: enzymatic conversion of 1-deoxy-d-xylulose-5-phosphate to pyridoxol phosphate. *J. Am. Chem. Soc.* **121**, 7722-7723 (1999).

71. Sakai, A., Kita, M., Katsuragi, T., Ogasawara, N. & Tani, Y. yaaD and yaaE are involved in vitamin B6 biosynthesis in *Bacillus subtilis*. *J Biosci Bioeng*. **93**, 309-12 (2002).

72. Wetzel, D. K., Ehrenshaft, M., Denslow, S. A. & Daub, M. E. Functional complementation between the PDX1 vitamin B6 biosynthetic gene of *Cercospora nicotianae* and pdxJ of *Escherichia coli*. *FEBS*. **564**,143-6 (2004).

73. Tambasco-Studart, M., *et al.* Vitamin B6 biosynthesis in higher plants. *Proc. Natl. Acad. Sci. U. S. A*. **102**, 13687-92 (2005).

74. Burns, K. E., Xiang, Y., Kinsland, C. L., McLafferty, F. W. & Begley, T. P. Reconstitution and biochemical characterization of a new pyridoxal-5'-phosphate biosynthetic pathway. *J. Am. Chem. Soc*. **127**, 3682-3 (2005).

75. Bauer, J. A., Bennett, E. M., Begley, T. P. & Ealick, S. E. Three-dimensional structure of YaaE from *Bacillus subtilis*, a glutaminase implicated in pyridoxal-5'-phosphate biosynthesis. *J. Biol. Chem*. **279**, 2704-11 (2004).

76. Gengenbacher, M., *et al*. Vitamin B6 biosynthesis by the malaria parasite *Plasmodium falciparum*: biochemical and structural insights. *J. Biol. Chem*. **281**, 3633-41 (2006).

77. Raschle, T., Amrhein, N. & Fitzpatrick, T. B. On the two components of pyridoxal 5′-phosphate synthase from *Bacillus subtilis*. *J. Biol. Chem*. **280**, 32291-300 (2005).

78. Strohmeier, M., *et al.* Structure of a bacterial pyridoxal 5′-phosphate synthase complex. *Proc. Natl. Acad. Sci. U. S. A*. **103**, 19284-9 (2006).

79. Wrenger, C., Eschbach, M. L., Müller, I. B., Warnecke, D. & Walter, R. D. Analysis of the vitamin B6 biosynthesis pathway in the human malaria parasite. *J. Biol. Chem*. **280** ,5242-8 (2005).

80. Mittenhuber, G. Phylogenetic analyses and comparative genomics of vitamin B6 (pyridoxine) and pyridoxal phosphate biosynthesis pathways. *J. Mol. Microbiol. Biotechnol*. **3**, 1-20 (2001).

81. Banks, J. and Cane, D. E. Biosynthesis of vitamin B6: direct identification of the product of the PdxA-catalyzed oxidation of 4-hydroxy-l-threonine-4-phosphate using electrospray ionization mass spectrometry. *Bioorg. Med. Chem. Lett.* **14**, 1633-36 (2004).

82. Cane, D. E., Du, S. C. & Spenser, I. D. Biosynthesis of vitamin B6: origin of the oxygen atoms of pyridoxol phosphate. *J. Am. Chem. Soc.* **122**, 4213-14 (2000).

83. Fitzpatrick, T. B., *et al.* Two independent routes of de novo vitamin B6 biosynthesis: not that different after all. *Biochem J.* **407**, 1-13 (2007).

84. Franco, M. G., Laber, B., Huber, R. & Clausen, T. Structural basis for the function of pyridoxine 5'-phosphate synthase. *Structure*. **9**, 245-53 (2001).

85. Garrido-Franco, M., Huber, R., Schmidt, F. S., Laber, B. & Clausen, T. Crystallization and preliminary X-ray crystallographic analysis of PdxJ, the pyridoxine 5'-phosphate synthesizing enzyme. *Acta Crystallogr D Biol Crystallogr*. **56**, 1045-8 (2000).

86. Garrido-Franco, M., Laber, B., Huber, R. & Clausen, T. Enzyme–ligand complexes of pyridoxine 5′-phosphate synthase: implications for substrate binding and catalysis. *J. Mol. Biol*. **4**, 601-12 (2002).

87. Sivaraman, J., *et al*. Crystal structure of *Escherichia coli* PdxA, an enzyme involved in the pyridoxal phosphate biosynthesis pathway. *J. Biol. Chem*. **278**, 43682-90 (2003).

88. Tazoe, M., Ichikawa, K. & Hoshino, T. Biosynthesis of vitamin B6 in Rhizobium: *in vitro* synthesis of pyridoxine from 1-deoxy-D-xylulose and 4-hydroxy-L-threonine. *Biosci. Biotechnol. Biochem.* **66**, 934-936 (2002).

89. Yeh, J. I., Du, S., Pohl, E. & Cane, D. E. Multistate binding in pyridoxine 5′-phosphate synthase: 1.96 Å crystal structure in complex with 1-deoxy-D-xylulose phosphate. *Biochemistry*. **41**, 11649-57 (2002).

90. Zhao, G. and Winkler, M. E. Kinetic limitation and cellular amount of pyridoxine (pyridoxamine) 5′-phosphate oxidase of *Escherichia coli* K-12. *J. Bacteriol*. **177**, 883-891 (1995).

91. Perez-Gil, J., *et al*. Mutations in *Escherichia coli aceE* and *ribB* genes allow survival of strains defective in the first step of the isoprenoid biosynthesis pathway. *PLoS ONE*. 7, 43775 (2012).

92. Sauret-Güeto, S., Uros, E. M., Ibanez, E., Boronat, A. & Rodriguez-Concepcion, M. A mutant pyruvate dehydrogenase E1 subunit allows survival of *Escherichia coli* strains defective in 1-deoxy-D-xylulose 5-phosphate synthase. *FEBS Lett.* **580**, 736-740 (2006).

93. Yokota, A. and Sasajima, K. I. Formation of 1-deoxyketoses by pyruvate dehydrogenase and acetoin dehydrogenase. *Agric. Biol. Chem*. **50**, 2517-2524 (1986).

94. Schoerken, U. and Sprenger, G. A. Thiamin-dependent enzymes as catalysts in chemoenzymatic syntheses. *Biochim. Biophys. Acta*. **1385**, 2517-24 (1998).

95. Wungsintaweekul, J., *et al*. Phosphorylation of 1-deoxy-D-xylulose by D-xylulokinase of *Escherichia coli*. *Eur J Biochem*. **268**, 310-16 (2001).

96. Bacher, A., Eberhardt, S., Fisher, M., Kis, K. & Richter, G. Biosynthesis of vitamin B2 (riboflavin). *Annu Rev Nutr*. **20**, 153-67 (2000).

97. Erb, T., *et al*. A RubisCO-like protein links SAM metabolism with isoprenoid biosynthesis. *Nat. Chem. Biol*. **8**, 926 (2012).

98. Parveen, N. and Cornell, K. A. Methylthioadenosine/S-adenosylhomocysteine nucleosidase, a critical enzyme for bacterial metabolism. *Mol Microbiol.* **79**, 7-20 (2011).

99. Carpenter, K. J. The discovery of thiamin. *Ann Nutr Metab*. **61**, 219-23 (2012).

100. Breslow, R. On the mechanism of thiamine action: IV. Evidence from studies on model systems. *J. Am. Chem. Soc* .**80**, 3719-26 (1958).

101. Breslow, R. Rapid deuterium exchange in thiazolium salts. *J. Am. Chem. Soc*. **79**, 1762 (1957).

102. Kluger, R. and Tittmann, K. Thiamin diphosphate catalysis: enzymic and nonenzymic covalent intermediates. *Chem. Rev*. **108**, 1797–1833 (2008).

103. Frank, R. A., Leeper, F. J. & Luisi, B. F. Structure, mechanism and catalytic duality of thiamine-dependent enzymes. *Cell Mol Life Sci.* **64**, 892-905 (2007).

104. Hasson, M. S., *et al.* The crystal structure of benzoylformate decarboxylase at 1.6 A resolution: diversity of catalytic residues in thiamin diphosphate-dependent enzymes. *Biochemistry*. **37**, 9918-30 (1998).

105. Muller, Y. A. and Schulz, G. E. Structure of the thiamine- and flavin-dependent enzyme pyruvate oxidase. *Science*. **259**, 965-7 (1993).

106. Chabrière, E., et al. Crystal structures of the key anaerobic enzyme pyruvate:ferredoxin oxidoreductase, free and in complex with pyruvate. *Nat Struct Biol.* **6**, 182-90 (1999).

107. Lindqvist, Y., Schneider, G., Ermler, U. & Sundström, M. Three-dimensional structure of transketolase, a thiamine diphosphate dependent enzyme, at 2.5 A resolution. *EMBO J.* **11**, 2373-9 (1992).

108. Jordan, F., Zhang, Z. & Sergienko, S. Spectroscopic evidence for participation of the 1',4'- imino tautomer of thiamine disphosphate in catalysis by yeast pyruvate decarboxylase. *Bioorg. Chem*. **30**, 188-98 (2002).

109. Killenberg-Jabs, M., König, S., Eberhardt, I., Hohmann, S. & Hübner, G. Role of Glu51 for cofactor binding and catalytic activity in pyruvate decarboxylase from yeast studied by site-directed mutagenesis. *Biochemistry*. **36**, 900-5 (1997).

110. Schellenberger, A. The amino group and steric factors in thiamin catalysis. *Ann N Y Acad Sci.* **378**, 51-62 (1982).

111. Nemeria, N. S., Chakraborty, S., Balakrishnan, A. & Jordan, F. Reaction mechanisms of thiamin diphosphate enzymes: Defining states of ionization and tautomerization of the cofactor at individual steps. *FEBS Lett.* **76**, 2432-3446 (2009).

112. Tittmann, K., *et al*. NMR analysis of covalent intermediates in thiamin diphosphate enzymes. *Biochemistry*. **42**, 7885-91 (2003).

113. Kluger, R., Chin, J. & Smyth, T. Thiamin-catalyzed decarboxylation of pyruvate. Synthesis and reactivity analysis of the central, elusive intermediate, .alpha.-lactylthiamin. *J. Am. Chem. Soc*. **103**, 884-888 (1981).

114. Crosby, J., Stone, R. & Lienhard, G. E. Mechanisms of thiamine-catalyzed reactions. Decarboxylation of 2-(1-carboxy-1-hydroxyethyl)-3,4-dimethylthiazolium chloride. *J. Am. Chem. Soc*. **92**, 2891-900 (1970).

115. Zhang, S., Liu, M., Yan, Y., Zhang, Z. & Jordan, F. C2-alpha-lactylthiamin diphosphate is an intermediate on the pathway of thiamin diphosphate-dependent pyruvate decarboxylation. Evidence on enzymes and models. *J. Biol. Chem.* **279**, 54312-8 (2004).

116. Zilles, J. L., Croal, L. R. & Downs, D. M. Action of the thiamine antagonist bacimethrin on thiamine biosynthesis. *J Bacteriol.* **182**, 5606-10 (2000).

117. Arjunan, P., *et al.* A thiamin-bound, pre-decarboxylation reaction intermediate analogue in the pyruvate dehydrogenase E1 subunit induces large scale disorder-to-order transformations in the enzyme and reveals novel structural features in the covalently bound adduct. *J. Biol. Chem.* **281**, 15296 (2006).

118. O'Brien, T. A., Kluger, R., Pike, D. C. & Gennis, R. B. Phosphonate analogues of pyruvate. Probes of substrate binding to pyruvate oxidase and other thiamin pyrophosphate-dependent decarboxylases. *Biochimica et Biophysica Acta (BBA) Enzymology*. **613**, 10-17 (1980).

119. Kale, S., Arjunan, P., Furey, W. & Jordan, F. A Dynamic Loop at the Active Center of the Escherichia coli Pyruvate Dehydrogenase Complex E1 Component Modulates Substrate Utilization and Chemical Communication with the E2 Component. *J. Biol. Chem*. **282**, 28106-28116 (2007).

120. Gish, G., Smyth, T. & Kluger, R. Thiamin diphosphate catalysis. Mechanistic divergence as a probe of substrate activation of pyruvate decarboxylase. *J. Am. Chem. Soc.* **110**, :6230-4 (1988).

121. Flournoy, D. S. and Frey, P. A. Inactivation of the pyruvate dehydrogenase complex of *Escherichia coli* by fluoropyruvate. *Biochemistry*. **28**, 9594-602 (1989).

122. Kluger, R. and Pike, D. C. Active site generated analogs of reactive intermediates in enzymic reactions. Potent inhibition of pyruvate dehydrogenase by a phosphonate analog of pyruvate. *J. Am. Chem. Soc.* **99**, 504-6 (1977).

123. Nemeria, N. S., Korotchkina, L. G., Chakraborty, S., Patel, M. S. & Jordan, F. Acetylphosphinate is the most potent mechanism-based substrate-like inhibitor of both the human and *Escherichia coli* pyruvate dehydrogenase components of the pyruvate dehydrogenase complex. *Bioorg. Chem*. **34**, 362-379 (2006).

124. Nemeria, N., *et al.* The 1',4'-iminopyrimidine tautomer of thiamin diphosphate is poised for catalysis in asymmetric active centers on enzymes. *Proc. Natl. Acad. Sci. U. S. A*. **104**, 78-82 (2007).

125. Johnson, R. D., Kastner, R. M., Larsen, S. H. & Ose, E. E. Antibiotic A53868 and process for production thereof. U.S. patent 4,482,488. (5 April 1984).

126. Circello, B., Miller, C., Lee, J., van der Donk, W. & Metcalf, W. The antibioticdehydrophos is converted to a toxic pyruvate analog by peptide bond cleavage in *Salmonella enterica*. *Antimicrob Agents Chemother*. **55**, 3357 (2011).

127. Brammer, L. A. and Meyers, C. F. Revealing substrate promiscuity of 1-deoxy-d-xylulose 5-phosphate synthase. *Org Lett*. **11**, 4748-51 (2009).

128. Cane, D. E., Chow, C., Lillo, A. & Kang, I. Molecular cloning, expression and characterization of the first three genes in the mevalonate-independent isoprenoid pathway in *Streptomyces coelicolor*. *Bioorg.Med.Chem*. **9**, 1467-1477 (2001).

129. Bailey, A. M., Mahapatra, S., Brennan, P. J. & Crick, D. C. Identification, cloning, purification, and enzymatic characterization of *Mycobacterium tuberculosis* 1-deoxy-d-xylulose 5-phosphate synthase. *Glycobiology*. **12**, 813-820 (2002).

130. Kuzuyama, T., Takagi, M., Takahashi, S. & Seto, H. Cloning and characterization of 1-deoxy-D-xylulose 5-phosphate synthase from streptomyces sp. strain CL190, which

uses both the mevalonate and nonmevalonate pathways for isopentenyl diphosphate biosynthesis. *J Bacteriol.* **15**, 891 (2000).

131. Hahn, F. M., *et al.* 1-deoxy-D-xylulose 5-phosphate synthase, the gene product of open reading frame (ORF) 2816 and ORF 2895 in *Rhodobacter capsulatus*. *J. Bacteriol*. **183**, 1-11 (2001).

132. Querol, J., Rodriguez-Concepcion, M., Boronat, A. & Imperial, S. Essential role of residue H49 for activity of *Escherichia coli* 1-deoxy-D-xylulose 5-phosphate synthase, the enzyme catalyzing the first step of the 2-C-methyl-D-erythritol 4-phosphate pathway for isoprenoid synthesis. *Biochem. Biophys. Res. Commun*. **289**, 155-160 (2001).

133. Brammer, L. A. Toward investigating 1-deoxy-D-xylulose 5-phosphate (DXP) synthase as an anti-infective target. Ph.D., Johns Hopkins University (2012).

134. Sprenger, G. A., Schörken, U., Sprenger, G. & Sahm, H. Transketolase a of *Escherichia coli* K12. *Eur. J. Biochem*. **230**, 525-32 (1995).

135. Xiang, S., Usunow, G., Lange, G., Busch, M. & Tong, L. Crystal structure of 1-deoxy-D-xylulose 5-phosphate synthase, a crucial enzyme for isoprenoids biosynthesis. *J. Biol Chem*. **282**, 2676-2682 (2007).

136. Sisquella, X., *et al*. A single-molecule force spectroscopy nanosensor for the identification of new antibiotics and antimalarials. *FASEB J*. **24**, 4203-4217 (2010).

137. Wang, S. and Shaevitz, J. W. The mechanics of shape in prokaryotes. Front Biosci (Schol Ed). 564-74, (2013).

138. Hogan, C. M. Bacteria. Encyclopedia of Earth. (National Council for Science and the Environment, Washington DC, 2010).

139. Demchick, P. H. and Koch, A. L. The permeability of the wall fabric of *Escherichia coli* and *Bacillus subtilis*. *J. Bacteriol*. **178**, 768-73 (1996).

140. Pea, F. and Viale, P. Bench-to-bedside review: Appropriate antibiotic therapy in severe sepsis and septic shock-does the dose matter? *Crit Care*. **13**, 214 (2009).

141. Rahal, J. Novel antibiotic combinations against infections with almost completely resistant *Pseudomonas aeruginosa* and Acinetobacter species. *Clin Infect Dis*. 43S95-S99 (2006).

142. Pillai, S. K., Moellering, R. C. & Eliopoulos, G. M. in Antimicrobial combinations. *Antibiotics in Laboratory Medicine* (ed V. Lorian) (Lippincott Williams & Wilkins 2005).

143. Moody, J. in Synergism testing: broth microdilution checkerboard and broth macrodilution methods. *In* H. D. Isenberg, Clinical microbiology procedures handbook, vol. 2. American Society for Microbiology, Washington, DC. p. 5.12.1-5.12.23., (2004).

144. Kalan, L. and Wright, G. D. Antibiotic adjuvants: multicomponent anti-infective strategies. *Expert Rev Mol Med.* **13** (2011).

145. Jia, J., *et al*. Mechanisms of drug combinations: interaction and network perspectives. Nat *Rev Drug Discov.* **8**, 111-28 (2009).

146. Woo, Y. H., Fernandes, R. P. & Proteau, P. J. Evaluation of fosmidomycin analogs as inhibitors of the Synechocystis sp. PCC6803 1-deoxy-D-xylulose 5-phosphate reductoisomerase. *Bioorg Med Chem*. **14**, 2375-85 (2006).

147. Kuzuyama, T., Shimizu, T., Takahashi, S. & Seto, H. Fosmidomycin, a specific inhibitor of 1-deoxy-d-xylulose 5-phosphate reductoisomerase in the nonmevalonate pathway for terpenoid biosynthesis. *Tetrahedron Lett*. **39**, 7913-7916 (1998).

148. Mac Sweeney, A., *et al*. The Crystal structure of *E. coli* 1-deoxy-d-xylulose-5-phosphate reductoisomerase in a ternary complex with the antimalarial compound fosmidomycin and NADPH reveals a tight-binding closed enzyme conformation. *J. Mol. Biol.* **345**, 115-127 (2005).

149. Zingle, C., Kuntz, L., Tritsch, D., Grosdemange-Billiard, C. & Rohmer, M. Isoprenoid biosynthesis via the methylerythritol phosphate pathway: structural variations around phosphonate anchor and spacer of fosmidomycin, a potent inhibitor of deoxyxylulose phosphate reductoisomerase. *J. Org. Chem.* **75**, 3203-3207 (2010).

150. Umeda, T., *et al.* Molecular basis of fosmidomycin's action on the human malaria parasite *Plasmodium falciparum. Sci Rep*. 1-9 (2011).

151. Haemers, T., *et al.* Synthesis of alpha-substituted fosmidomycin analogues as highly potent *Plasmodium falciparum* growth inhibitors. *Bioorg Med Chem Lett.* **16**, 1888-91 (2006).

152. Uh, E., *et al.* Antibacterial and antitubercular activity of fosmidomycin, FR900098, and their lipophilic analogs. *Bioorg Med Chem Lett*. **21**, 6973-6 (2011).

153. Ortmann, R., *et al.* Acyloxyalkyl ester prodrugs of FR900098 with improved *in vivo* anti-malarial activity. *Bioorg Med Chem Lett*. **13**, 2163-6 (2003).

154. Huttunen, K. M., Raunio, H. & Rautio, J. Prodrugs- from serendipity to rational design. *Pharmacol Rev*. **63**, 750-71 (2011).

Chapter 2: Toward elucidation of 1-deoxy-D-xylulose 5-phosphate (DXP) synthase mechanism.

Introduction:

1-deoxy-D-xylulose 5-phosphate (DXP) synthase is a ThDP-dependent enzyme that catalyzes the decarboxylation of a pyruvate and subsequent condensation of the two carbon donor substrate with the D-glyceraldehyde 3-phosphate acceptor substrate to generate DXP [(1)]. Combining elements of carboligase and decarboxylase chemistry, it shares weak sequence homology (~20%) with transketolase and the E1 subunit of pyruvate dehydrogenase [(2)]. The DXP synthase-catalyzed reaction is reminiscent of acetolactate synthase and glyoxylate carboligase, which generate acetohydroxyacid and tartronate semialdehyde, respectively, via similar decarboxylation and carboligation chemistry, as well as transketolase whose acceptor substrate is also an aldehyde. Although DXP synthase is essential in most bacteria and human pathogens [(3-5)], it is undeveloped as a drug target. This is most likely due to perceived challenges in targeting a ThDP-dependent enzyme; examples of selective inhibitors against this class are lacking. However, DXP synthase is unique among ThDP-dependent enzymes. In addition to a novel domain arrangement [(2)], there have also been reports that the kinetic mechanism is distinct [(6, 7)]. Yet there are discrepancies in the literature regarding this mechanism that warrant further investigation of this enzyme.

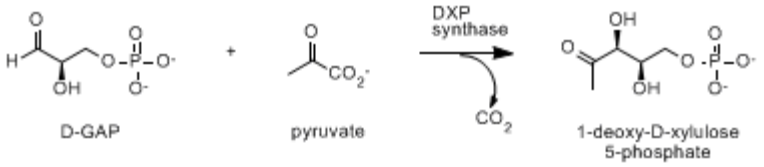

Figure 2-1. Reaction catalyzed by DXP synthase.

Previous mechanistic studies on DXP synthase that have relied primarily upon kinetic analysis concluded that the enzyme follows a ping-pong mechanism [8], similar to all other ThDP-dependent enzymes. In this ping-pong mechanism, pyruvate is proposed to bind to the enzyme first, undergo decarboxylation, and then D-GAP enters the active site and the C-C forming reaction can proceed (**Figure 2-2A**). However, Eubanks *et al* used kinetic analysis and CO_2 trapping studies to provide evidence for ternary complex formation in a proposed ordered mechanism, with pyruvate binding first, tightly and essentially irreversibly [6] (**Figure 2-2B**).). These studies, as well as work presented in this chapter, presume that decarboxylation is an essentially irreversible event. However, CO_2 release has been proposed to be reversible for other ThDP-dependent enzymes (see 1.8). Similar studies have not yet been carried out for DXP synthase. The ternary complex represents a ThDP-bound enzyme conformation in which both substrates are bound to the active site prior to catalysis. During the course of this work, we have undertaken studies of *E. coli* DXP synthase toward resolving the mechanism.

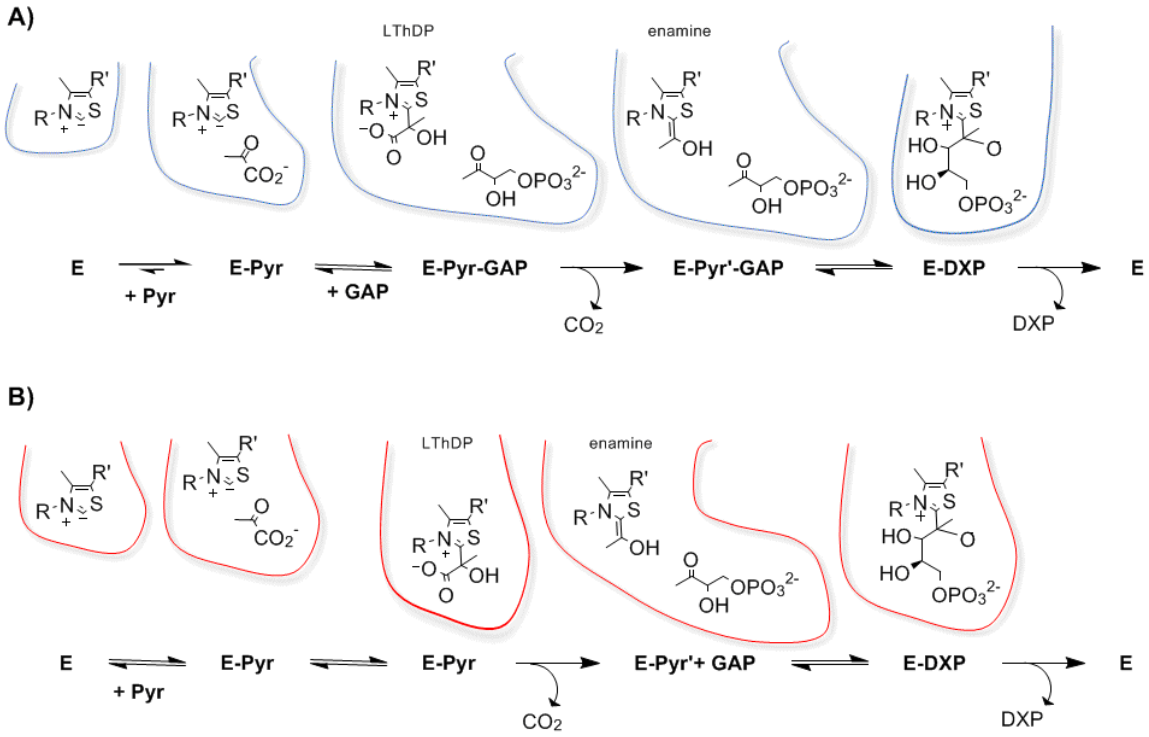

Figure 2-2. Proposed kinetic mechanisms for DXP synthase. E, ThDP-bound enzyme; Pyr, pyruvate; Pyr', enamine; GAP, D-GAP; E-Pyr-G, catalytically competent ternary complex. **A**) Ordered mechanism where pyruvate binds tightly and essentially irreversibly to DXP synthase[6]. **B)** Ping-pong mechanism where CO_2 liberation occurs prior to D-GAP binding [8].

Ultimately, our interest in pursuing the development of selective DXP synthase inhibitors requires knowledge of the kinetic mechanism and catalysis. Features that distinguish DXP synthase from other ThDP-dependent enzymes can be exploited in the development of new anti-infective agents that target this first essential step in pathogen isoprenoid biosynthesis. Ideally, inhibitors of *E. coli* DXP synthase will be effective against DXP synthase enzymes from different pathogens and therefore have the potential to be developed as broad spectrum antibiotics. DXP synthase has been characterized from

a number of organisms, including plants [11, 12] or non-pathogenic bacteria [6, 13, 14], primarily for the purpose of bioengineering. Although some work has been performed to understand the mechanism of DXP synthase from *R. capsulatus* [6] and *Mycobacterium tuberculosis* [15], mechanistic studies from additional pathogens are required to investigate the generality of mechanism. In addition to mechanistic studies on *E. coli* DXP synthase, this work concentrates on *Yersinia pestis*, *Salmonella typhimurium*, and *Mycobacterium tuberculosis* DXP synthase. Both *S. typhimurium* and *Y. pestis* DXP synthase have similar primary amino acid sequence identity with the *E. coli* enzyme (~90%) (**Table 2-1**). *Mycobacterium tuberculosis* DXP synthase (Dxs1) is the least similar to each of the three (~40%).

	M. tuberculosis	***S. enterica***	***E. coli***
Y. pestis	38%	83%	83%
M. tuberculosis		40%	40%
S. enterica			96%

Table 2-1. **DXP synthase primary amino acid sequence identity [16].**

Y. pestis is the causative agent of the plague, of which there are still thousands of cases a year reported to the World Health Organization (WHO). Due to the possibility of a bioterrorist aerosolized release, *Y. pestis* also represents a potential bioterrorism threat and is categorized as a category A pathogen (Center for Disease Control, CDC) [17]. *S. typhimurium* is a Gram negative bacterium and its serotypes form a group of pathogens that can result in gastroenteritis, typhoid fever, among other diseases. S. *typhimurium* (*S. enterica* serovar Typhimurium) is of particular interest in anti-infective development due to the emergence of the definitive phage type (DT) 104 [18]. This phage type strain is multidrug resistant (MDR); it commonly harbors resistance to ampicillin,

chloramphenicol/florfenicol, spectinomycin/streptomycin, sulfonamides, and tetracyclines. Several outbreaks have already occurred since 1996 in the United States and Canada, and *S. enterica* serovar Typhimurium DT 104 represents a global health problem. Although antibiotics exist for *M. tuberculosis*, extensively drug-resistant tuberculosis (XDR-TB) is resistant to even the most effective anti-TB drugs and therefore remains very difficult to treat. Currently, one third of the world's population infected with TB [(19)]; thus, new more effective treatments are desperately needed.

The focus of this chapter is the elucidation of the mechanism of *E. coli* DXP synthase using inhibition kinetics, model discrimination analysis (in collaboration with Leighanne Brammer Basta, PhD), and molecular docking to distinguish between ordered and ping-pong kinetic mechanisms. The generality of the kinetic mechanism is then explored amongst DXP synthase from more pathogenic species: *M. tuberculosis*, *S. typhimurium*, and *Y. pestis*. We take initial steps to evaluate subtleties in the cofactor binding site of *M. tuberucloisis* Dxs1 using site-directed mutagenesis. Collectively, our results suggest the enzyme proceeds via novel rapid equilibrium, random sequential preferred order mechanism that is conserved among DXP synthase from a variety of bacteria.

Results:

2.1. Kinetics using natural substrates of E. coli DXP synthase.

2.1.1. Buffer optimization studies.

Prior to beginning kinetic studies toward elucidating the mechanism of *E. coli* DXP synthase, buffer optimization studies were carried out to ensure optimal enzyme activity conditions. In our buffer optimization study, decreased turnover efficiency was observed when reactions were performed in Tris (2-amino-2-hydroxymethyl-propane-1,3-diol) and citrate, buffers reported previously for mechanistic studies of DXP synthase [6, 8]. In Tris buffer, $K_m^{\text{D-GAP}}$ values increased with increasing Tris concentration (**Table 2-2**). This can be attributed to D,L-GAP instability in Tris, presumably a consequence of the reactivity of the aldehyde group of D,L-GAP toward the primary amine group of Tris [20].

Buffer	$K_m^{\text{D-GAP}}$ (μM)	K_m^{pyruvate} (μM)	k_{cat} (min^{-1})	$k_{cat}/K_m^{\text{D-GAP}}$ ($\mu M^{-1}\ min^{-1}$)	$k_{cat}/K_m^{\text{pyruvate}}$ ($\mu M^{-1}\ min^{-1}$)
40 mM HEPES	30 ± 5	79 ± 5	230 ± 7	7.6 ± 0.9	3.0 ± 0.2
100 mM HEPES	24 ± 2	49 ± 8	154 ± 7	6.9 ± 0.4	3.2 ± 0.5
40 mM Tris	53 ± 8	86 ± 16	146 ± 13	3.1 ± 0.2	1.6 ± 0.2
100 mM Tris	279 ± 7	75 ± 7	209 ± 6	0.8 ± 0.04	2.7 ± 0.2*
100 mM TEA	36 ± 5	129 ± 13	173 ± 11	5.6 ± 0.6	1.2 ± 0.1
100 mM phosphate	226 ± 32	1100 ± 300	246 ± 13		

Table 2-2. Summary of kinetics parameters for wild type *E. coli* DXP synthase in different buffer systems [21]**.** *Performed in duplicate.

Citrate buffer was found to inhibit DXP synthase and IspC (**Figure 2-3**) which is consistent with its properties as a magnesium chelator [22]. Previous mechanistic reports

describe kinetic experiments performed at higher varying substrate concentrations relative to concentration ranges of natural substrates in the present study. Presumably, these conditions were required to overcome the inhibitory effects and reactivity of these buffered systems.

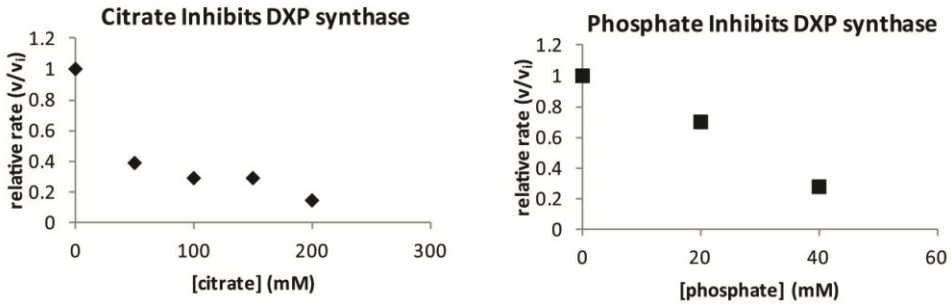

Figure 2-3. Inhibition of *E. coli* DXP synthase by citrate and phosphate [21].

2.1.2. D-GAP and pyruvate exhibit substrate inhibition.

Mechanistic insight was obtained through kinetic analysis of wild-type *E. coli* DXP synthase. DXP formation was monitored using the IspC-coupled reaction [23], and double-reciprocal plots of the natural substrates at varying concentrations were generated by plotting inverse initial velocities of DXP formation as a function of inverse substrate concentration at fixed concentrations of the second substrate in each case (**Figure 2-4**). In both a ping-pong and an ordered mechanism, in which pyruvate binds first, a competitive profile should be apparent with respect to both pyruvate and D-GAP [24-26]. For a rapid equilibrium, random sequential mechanism in which either substrate is capable of binding in the active site the absence of the other, a noncompetitive profile should be evident with respect to both substrates. Likewise, an ordered mechanism in which pyruvate binds first, tightly and essentially irreversibly, also predicts a noncompetitive relationship for both substrates [6]. However, a strictly ordered

mechanism such as this is in disagreement with recent equilibrium binding studies that show pyruvate binds reversibly to the active site [27, 28] . Interestingly, the double-reciprocal plots shown in **Figure 2-4** exhibit apparently different trends at higher concentrations of the fixed second substrate. Under conditions where D-GAP is the varied substrate, the slopes exhibit a noncompetitive relationship at low concentration of pyruvate (12.3–36.8 μM) but appear to increase subtly with increasing fixed pyruvate concentrations (49.0–98.0 μM), suggesting substrate inhibition by pyruvate [24-26]. The apparent increase in slopes is more pronounced when pyruvate is varied at fixed, sub-saturating concentrations of D-GAP (48.0–73.0 μM), suggesting substrate inhibition by D-GAP also takes place.

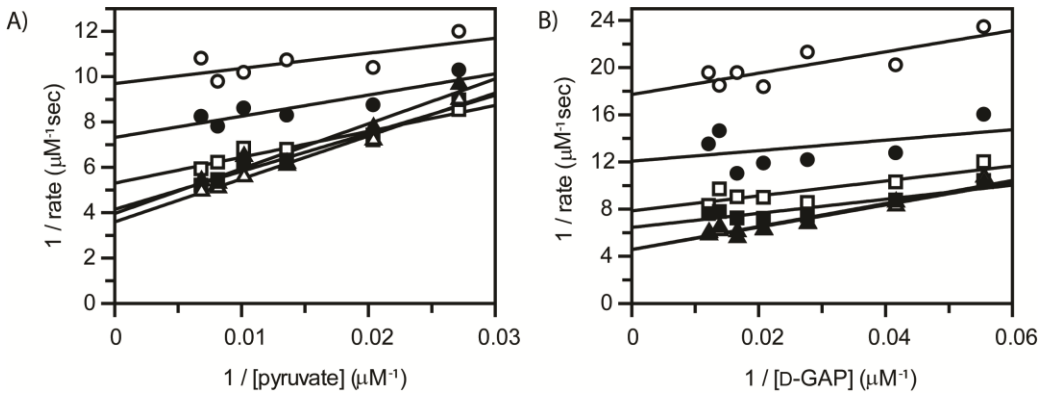

Figure 2-4. Double reciprocal analysis of initial velocities under conditions where either D-GAP or pyruvate is varied at different fixed concentrations of the co-substrate [21]. Kinetic analyses were performed by varying subsaturating concentrations of D-GAP: 18 (○), 24 (●), 36 (□), 48 (■), 60 (△), 72 (▲) μM at varying sub-saturating pyruvate concentrations: 12.3 (○), 24.5 (●), 36.8(□), 49 (■), 73.5 (△), and 98 (▲) μM.

The kinetic data were re-evaluated by a global non-linear regression analysis using the computer simulation program DynaFit (Leighanne Brammer Basta, PhD) [29]. Several mechanistic models for a two substrate, two product (Bi Bi) system were examined in a model discrimination analysis by the Akaike Information Criterion method, including rapid equilibrium ordered (where pyruvate binds first), rapid equilibrium ordered (where D-GAP binds first), ordered (where pyruvate binds first and irreversibly), rapid equilibrium random sequential, and rapid equilibrium ping pong. All models investigated presumed irreversible decarboxylation of LThDP. In this analysis, model discrimination supported a rapid equilibrium, random sequential mechanism of DXP synthase (**Figure 2-5**). However, inspection of this global fit reveals apparent deviation of the empirical data from predicted trends in a random sequential mechanism, suggestive of substrate inhibition and in agreement with the Lineweaver-Burk analyses. We have previously reported a side reaction of DXP synthase involving the formation of acetolactate from two molecules of pyruvate [30], which is consistent with the notion of substrate inhibition by pyruvate. Indeed, a random sequential model considering this side reaction is supported in a model discrimination analysis by DynaFit and provides an improved curve fit (**Figure 2-5**). Although incubation of DXP synthase with D-GAP in the absence of pyruvate does not result in new product formation or enzyme-dependent depletion of D-GAP, a rapid equilibrium, random sequential mechanistic model considering the reversible substrate inhibition by D-GAP provides significantly improved curve fits in the non-linear regression analysis and is supported by model discrimination analysis.

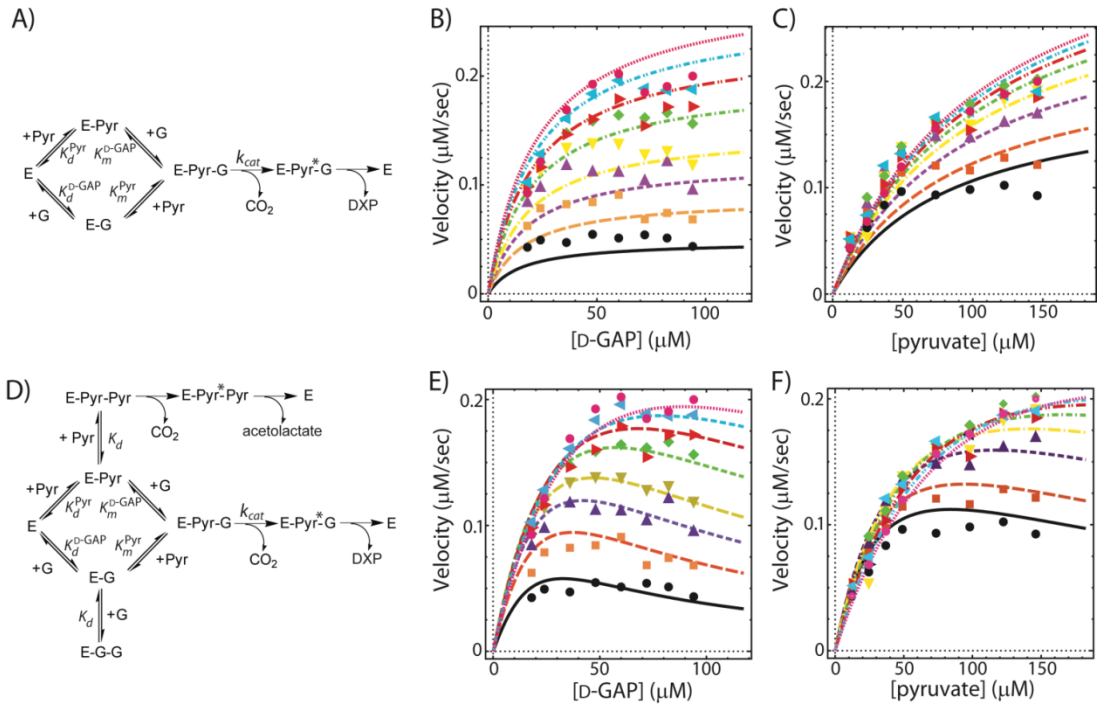

Figure 2-5. **Global non-linear regression analysis of control data for a random sequential mechanism** [21]**.** Panels **A-C**: Random sequential mechanism. Panels **B** and **E:** Varying D-GAP at fixed pyruvate concentrations: 18.0 (●), 24.0 (■), 36.0 (▲), 48.0 (▼), 60.0 (♦), 72.0 (►), 82.3 (◄), 94.0 (●) μM pyruvate.) Panels **C** and **F**: Varying pyruvate at fixed D-GAP concentrations: 12.3 (●), 24.5 (■), 36.8 (▲), 49.0 (▼), 73.5 (♦), 98.0 (►), 122.5 (◄), 146.0 (●) μM D-GAP. Panels **D-F**: Global fit analysis of kinetic data for a random sequential mechanism considering substrate inhibition by D-GAP (nonproductive reaction) and pyruvate (formation of acetolactate).

2.2. Pyruvate analogs inhibit E. coli DXP synthase.

2.2.1. Inhibition of DXP synthase by β-fluoropyruvate and methylacetylphosphonate

β -Fluoropyruvate and phosphonate analogs of 2-oxo acids have been extensively used to study ThDP-dependent decarboxylating enzymes and their mechanisms [31-37].

Unlike β-fluoropyruvate, which undergoes a catalytic step to release carbon dioxide and subsequently eliminates fluoride following activation by ThDP, MAP is incapable of undergoing decarboxylation (**Figure 2-6**).

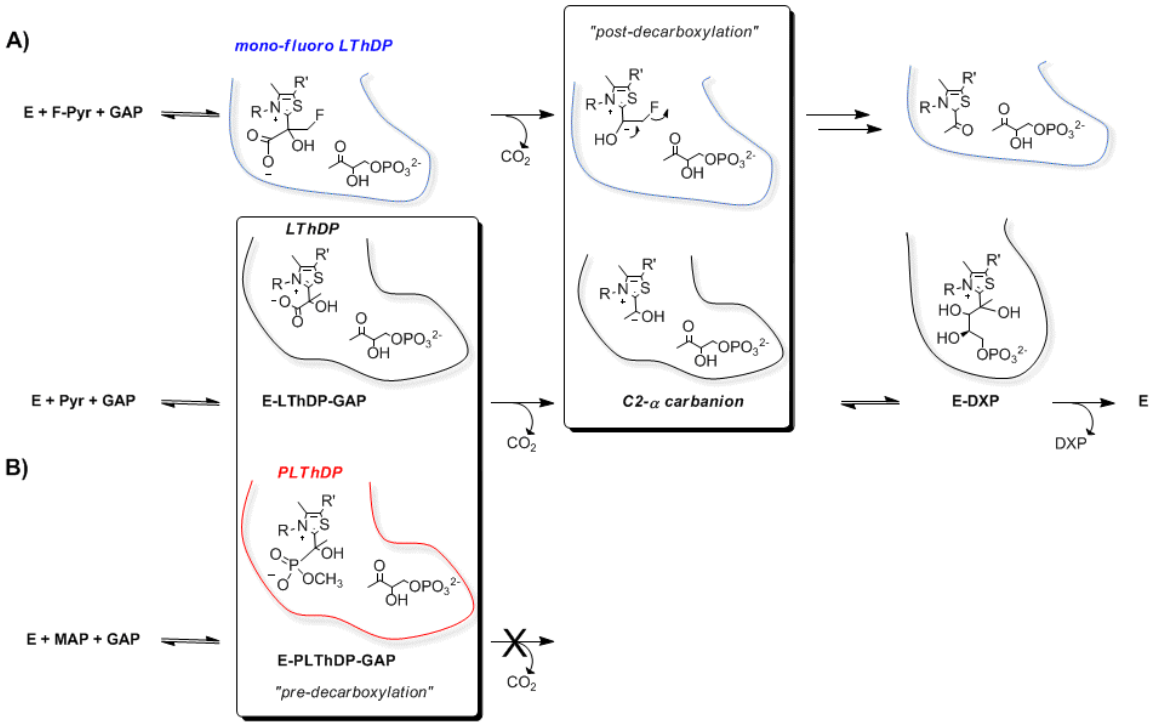

Figure 2-6. β-Fluoropyruvate and MAP shown as pyruvate mimics in a mechanism requiring ternary complex formation. A) DXP synthase is presumed to adopt a "post-decarboxylation" state similar to the C2-α carbanion formed upon decarboxylation of LThDP. **B**) DXP synthase is presumed to adopt a "pre-decarboxylation" state following the formation of the phosphono-2-lactyl-ThDP (PLThDP) intermediate. **E**, ThDP-bound enzyme; **Pyr**, pyruvate; **G**, D-GAP.

Pyruvate analogs β-fluoropyruvate and methylacetylphosphonate (MAP) were evaluated as DXP synthase inhibitors to provide further support for a random sequential

mechanism favored by the global fit. For a random sequential mechanism, β-fluoropyruvate and MAP are predicted to behave as competitive inhibitors with respect to pyruvate but will exhibit a noncompetitive profile with respect to D-GAP [24-26]. Initial rates of DXP formation were monitored using the IspC coupled assay at sub-saturating, varied concentrations of one substrate, at fixed concentrations of the second substrate and in the presence of varying inhibitor concentrations (β-fluoropyruvate or MAP). The results (**Figure 2-7**) show that MAP is a competitive inhibitor with respect to pyruvate (apparent K_i^{MAP} = 715 ± 108 nM). When D-GAP is the varied substrate, the trend is noncompetitive, as expected for a random sequential mechanism. A similar inhibition profile was observed for β-fluoropyruvate ($K_i^{\beta\text{-FPYR}}$ = 430 ± 135 nM) (**Figure 2-8**).

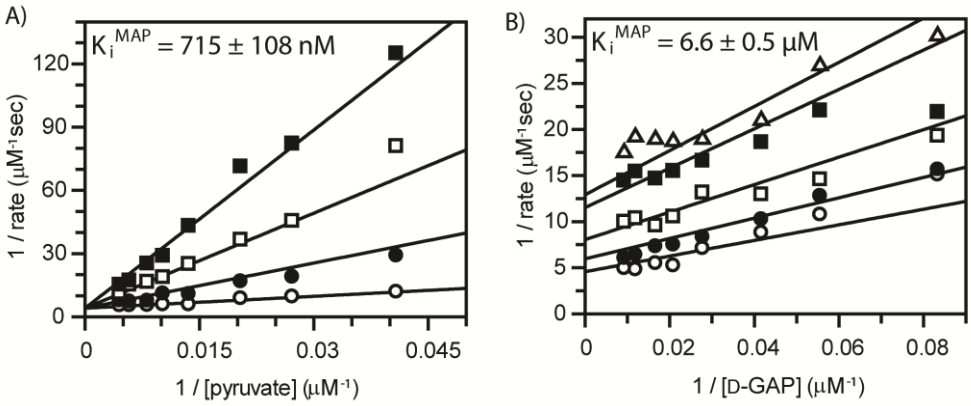

Figure 2-7. Inhibition of DXP synthase by MAP [21]. A) The concentration of pyruvate was varied at a fixed concentration of D-GAP (120 μM), with increasing concentrations of MAP: 0 (○), 2 (●), 5 (□), 10 (■) μM. **B**) The concentration of D-GAP was varied at a fixed concentration of pyruvate (240 μM), with increasing concentrations of MAP: 0 (○), 2 (●), 5 (□), 10 (■), 12 (△) μM.

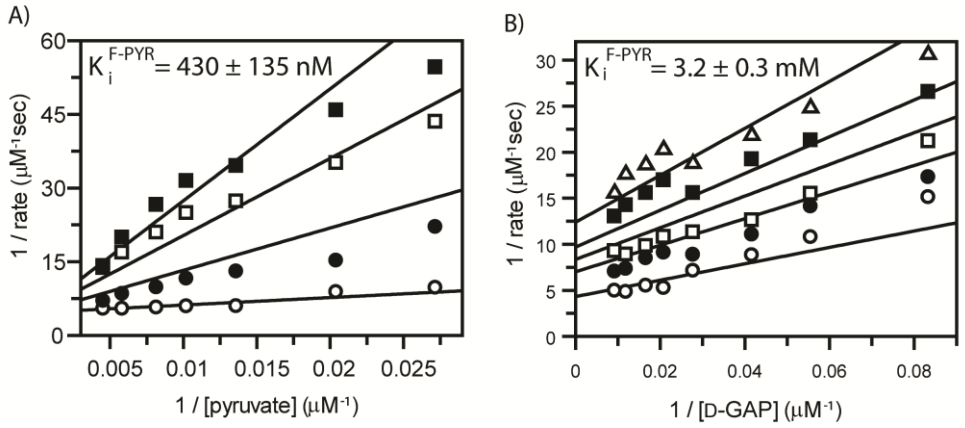

Figure 2-8. Inhibition of DXP synthase by β-fluoropyruvate [21]**. A**) The concentration of β-fluoropyruvate was varied at a fixed concentration of D-GAP (120 μM), with increasing concentrations of MAP: 0 (○), 2 (●), 3 (□), 4 (■), 6 (△) μM. **B**) The concentration of D-GAP was varied at a fixed concentration of pyruvate (240 μM), with increasing concentrations of MAP: 0 (○), 2 (●), 4 (□), 6 (■) μM.

2.2.2. Inhibition by D-glyceraldehyde reveals important binding determinants.

D-Glyceraldehyde was selected for inhibition studies as it is a commonly used D-GAP analog [6, 14, 15, 38]. A random sequential kinetic mechanism predicts this analog to exhibit a competitive inhibition pattern with respect to D-GAP in a Lineweaver-Burk analysis and a noncompetitive profile with respect to pyruvate [24-26]. However, D -glyceraldehyde exhibits a similar trend to MAP and β-fluoropyruvate, indicating competitive inhibition with respect to pyruvate (**Figure 2-9**, apparent $K_i^{\text{D-glyceraldehyde}}$ = 3.2 ± 0.4 mM). It has been suggested that D-glyceraldehyde also acts as a substrate inhibitor competing for the pyruvate binding site at considerably higher concentrations [6]. Clearly, removal of the phosphoryl moiety impacts the binding and recognition profile of

this substrate analog, suggesting D-glyceraldehyde may not be an ideal alternative substrate for D-GAP in mechanistic studies of DXP synthase.

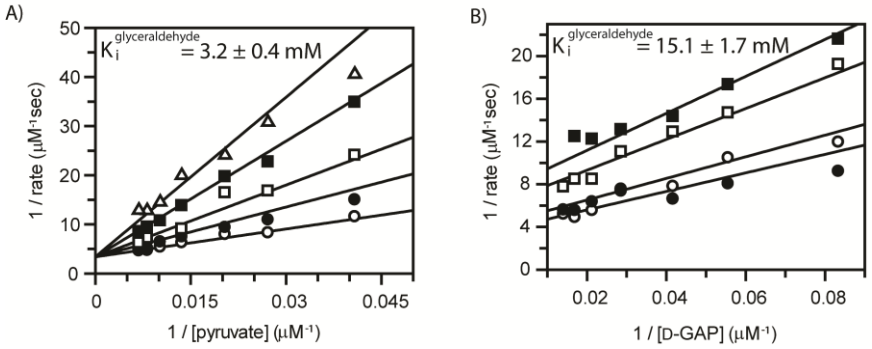

Figure 2-9. Inhibition of DXP synthase by D-glyceraldehyde [21]**. A**) The concentration of pyruvate was varied at a fixed concentration of D-GAP (120 μM), with increasing concentrations of glyceraldehyde: 0 (○), 2.5 (●), 5 (□), 10 (■), 15 (△) mM. **B**) The concentration of D-GAP was varied at a fixed concentration of pyruvate (240 μM), with increasing concentrations of glyceraldehyde: 0 (○), 2.5 (●), 10 (■), 15 (△) mM.

2.3. Exploring the mechanism of DXP synthase from *Mycobacterium tuberculosis, Yersinia pestis, and* Salmonella *typhimurium*.

2.3.1. Overexpression and purification of pathogenic DXP synthase.

Overexpression plasmids encoding the *dxs* gene from *Y. petis* and *S. typhimurium* were provided by Dr. Misty Kuhn and Prof. Wayne Anderson (Center for Structural Genomics of Infectious Diseases, Northwestern Feinberg School of Medicine).
The *M. tuberculosis* DXP synthase (*dxs1*) overexpression plasmid was generated as previously reported [15], with one exception: 5% dimethyl sulfoxide (DMSO) was added to the polymerase chain reaction (PCR) amplification from H37Rv genomic DNA (provided by Dr. Eric Nuermberger, Johns Hopkins University, Dept. of Medicine). The

overexpression and purification of Dxs1 required considerable troubleshooting. Initially, the method reported by Bailey *et al* [15] was pursued. Unfortunately, the majority of protein produced using this overexpression protocol was insoluble. As most *M. tuberculosis* proteins are difficult to overexpress and purify in the *E. coli* model system, this outcome was not unsurprising. In fact, many researchers address this problem through the use of an *M. smegmatis* strain that is engineered for overexpression of *M. tuberculosis* proteins [39, 40]. In order to address solubility issues for heterologous expression in *E. coli*, a number of growth conditions were modified. Overexpression was investigated from a variety of cell types (see below) at 15°C, 25°C, and 37°C. Induction with IPTG was pursued for 5, 16, and 24 hours at concentrations ranging from 0 to 1 mM, with 25 μM being the lowest concentration tested.

Further attempts were made to obtain soluble Dxs1 from various *E. coli* overexpression cells lines, including: BL21 (DE3), single step KRX competent cells (Promega), BL21 Star plus pRIL cells (Agilent), Rosetta 2 cells (Merck), and Arctic Express cells (Agilent). The KRX cell line permits tighter control of the T7 RNA polymerase gene because it is under control of a rhamnose promoter, rather than IPTG. In contrast, T7 RNA polymerase is induced by IPTG, similar to the T7 promoter upstream from *dxs1* in the other cell lines. By tightly controlling T7 RNA polymerase, premature expression of *dxs1* should be negligible prior to induction. We also considered the possibility of codon bias, or the under-abundance of tRNAs required to express *dxs1* in *E. coli* which would effectively stall expression. The BL21 Star plus pRIL cells are engineered to contain extra copies of genes that encode the tRNAs for AGG/AGA, AUA and CUA codons, while Rosetta 2 cells supply tRNAs for 7 rare codons (AGA, AGG,

AUA, CUA, GGA, CCC, and CGG). Lastly, expression of Dxs1 was investigated in Arctic Express cells, as they have been optimized to grow at cooler temperatures (10-13°C) and contain the Cpn60/Cpn10 chaperones from *Oleispira antarctica*, designed to overcome protein misfolding and insolubility. Attempts to overexpress Dxs1 in all cell types resulted in either lack of protein or largely insoluble protein, with the exception of expression in the Arctic Express cell line (**Figure 2-10**). For a detailed description of the overexpression and purification method used, see Material and Methods.

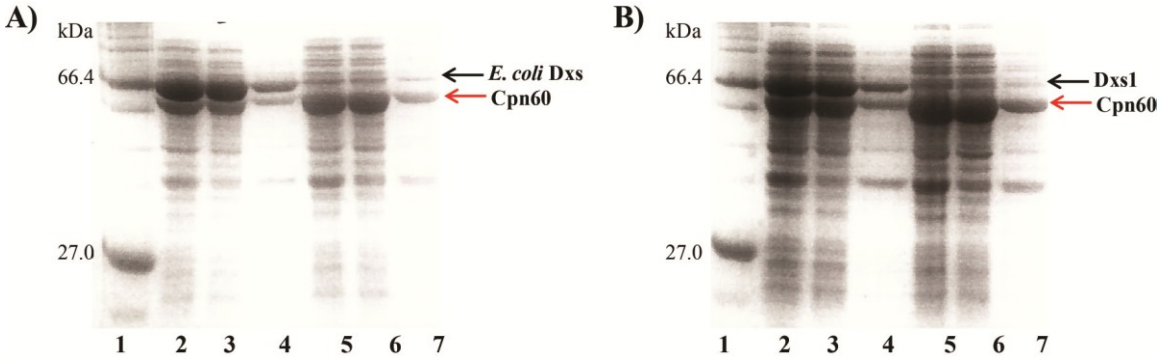

Figure 2-10. Overexpression of *E. coli* DXP synthase and *M. tuberculosis* Dxs1 in Arctic Express cells. A) *E. coli* dxs-pET37b [30] was overexpressed in Arctic Express cells as a positive control. Lanes 2-4 show cells induced with 0.1 mM IPTG, lanes 5-7 were not induced. 1) 2-212 kDa ladder 2) whole cell 3) soluble fraction 4) insoluble fraction 5) whole cell 6) soluble fraction 7) insoluble fraction. **B**) *M. tuberculosis* Dxs1 overexpression. Lanes 2-4 show cells induced with 0.25 mM IPTG, lanes 5-7 were not induced. 1) 2-212 kDa ladder 2) whole cell 3) soluble fraction 4) insoluble fraction 5) whole cell 6) soluble fraction 7) insoluble fraction.

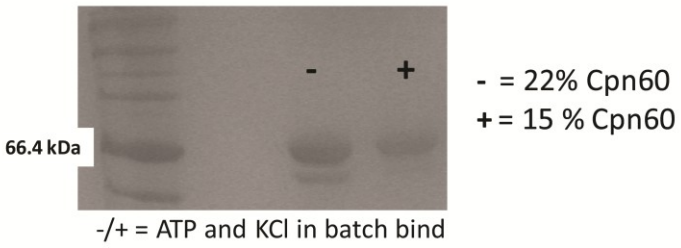

Figure 2-11. Unsuccessful removal of Cpn60 chaperone during Dxs1 purification.

Although soluble protein was obtained at a reasonable working concentration, there appeared to be ~15% contaminating Cpn60 in the final enzyme stock post purification and concentration. To ensure that the Cpn60 chaperone does not interfere with the activity of Dxs1, a dose-response experiment was carried out in which Cpn60 was added up to 1 μM; Cpn60 does not appear to exert any effects at these concentrations. However, for these experiments the Dxs1 stock solution already contained 15% Cpn60. In attempts to remove Cpn60 from Dxs1 stock solutions, the enzyme was purified in the presence or absence of 10 mM adenosine-triphosphate (ATP) and 150 mM potassium chloride (KCl) prior to binding of the protein to the Ni-NTA resin (Pierce). These concentrations of ATP and KCl have been reported to remove Cpn60 during the Ni-NTA column purification process [(41)]. However, this treatment did not remove the Cpn60 chaperone from Dxs1 and also caused apparent 40% reduction in the initial rate of Dxs1. This is in agreement with experiments that show that ATP inhibits either DXP synthase and/or IspC in the coupled assay at concentrations as low as 5 mM (**Figure 2-12**).

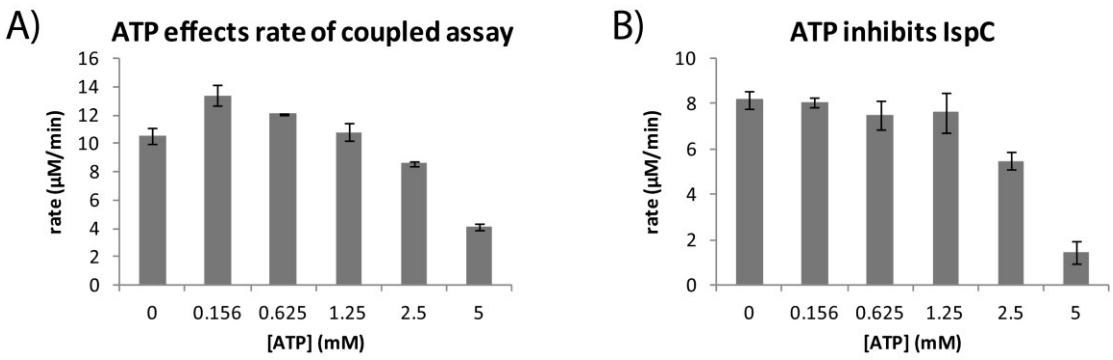

Figure 2-12. Adenosine-triphosphate (ATP) inhibits M. tuberculosis DXP synthase (Dxs1) and/or E. coli IspC. A) ATP inhibits the IspC coupled assay to monitor the Dxs1 reaction. Conditions used: 100 mM HEPES, 1 mg/mL BSA, 5 mM NaCl, 2 mM $MgCl_2$, 2.5 mM TCEP, 1 mM TPP, 0.25 μM Dxs1, 1 μM IspC, 0.1 mM NAPDH, 84 μM pyruvate, 38 μM D-GAP (2-fold K_m substrates). **B**) ATP inhibits IspC. Condition used: 100 mM HEPES, 0.15 mM DXP, 0.18 mM NADPH, 2 mM $MgCl_2$, 50 nM IspC (K_m substrates).

2.3.2. Characterization of pathogenic DXP synthase enzymes.

Using a tri-buffered system (2-(N-morpholino)ethanesulfonic acid (MES), ethylmorpholine, diethanolamine) [42], the pH optimum was determined for *M. tuberculosis* DXP synthase. As changes in pH are also expected to reduce DXP reductoisomerase (IspC) activity, a discontinuous, HPLC-based assay was used for these studies [30] that permits direct detection of derivatized substrates and products. For *M. tuberculosis* Dxs1, the pH optimum = 8.0, comparable to the *E. coli* enzyme (**Figure 2-13**).

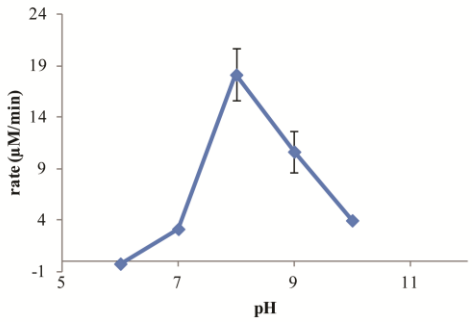

Figure 2-13. pH-rate profile analysis of *M. tuberculosis* Dxs1.

All DXP synthase enzymes were kinetically characterized using the enzyme coupled assays as previously described [21, 23] and the results are shown in **Table 2-3**. The K_m values obtained for Dxs1 from *M. tuberculosis* in this study ($K_m^{\text{pyruvate}} = 81 \pm 3$ and $K_m^{\text{D-GAP}} = 16.6 \pm 0.9$) (**Figure 2-14**) are comparable to those previously reported [15]. K_m^{pyruvate} and $K_m^{\text{D-GAP}}$ determined for DXP synthase from *Y. pestis* ($K_m^{\text{pyruvate}} = 51 \pm 6$ and $K_m^{\text{D-GAP}} = 26 \pm 3$) and *S. typhimurium* ($K_m^{\text{pyruvate}} = 76 \pm 19$ and the $K_m^{\text{D-GAP}} = 12 \pm 1$) (**Figure 2-14**) are also comparable to kinetic constants measured for other DXP synthase enzymes [15, 21]

species	substrate	K_m (μM)	k_{cat} (min^{-1})
Y. pestis	pyruvate	51 ± 6	112 ± 7
	D-GAP	26 ± 3	
M. tuberculosis	pyruvate	81 ± 3	48 ± 1
	D-GAP	17 ± 1	
S. enterica	pyruvate	76 ± 19	140 ± 20
	D-GAP	12 ± 1	

Table 2-3. Kinetic analysis of DXP synthase from *Y. pestis*, *M. tuberculosis*, and *S. typhimurium* DXP synthase [16].

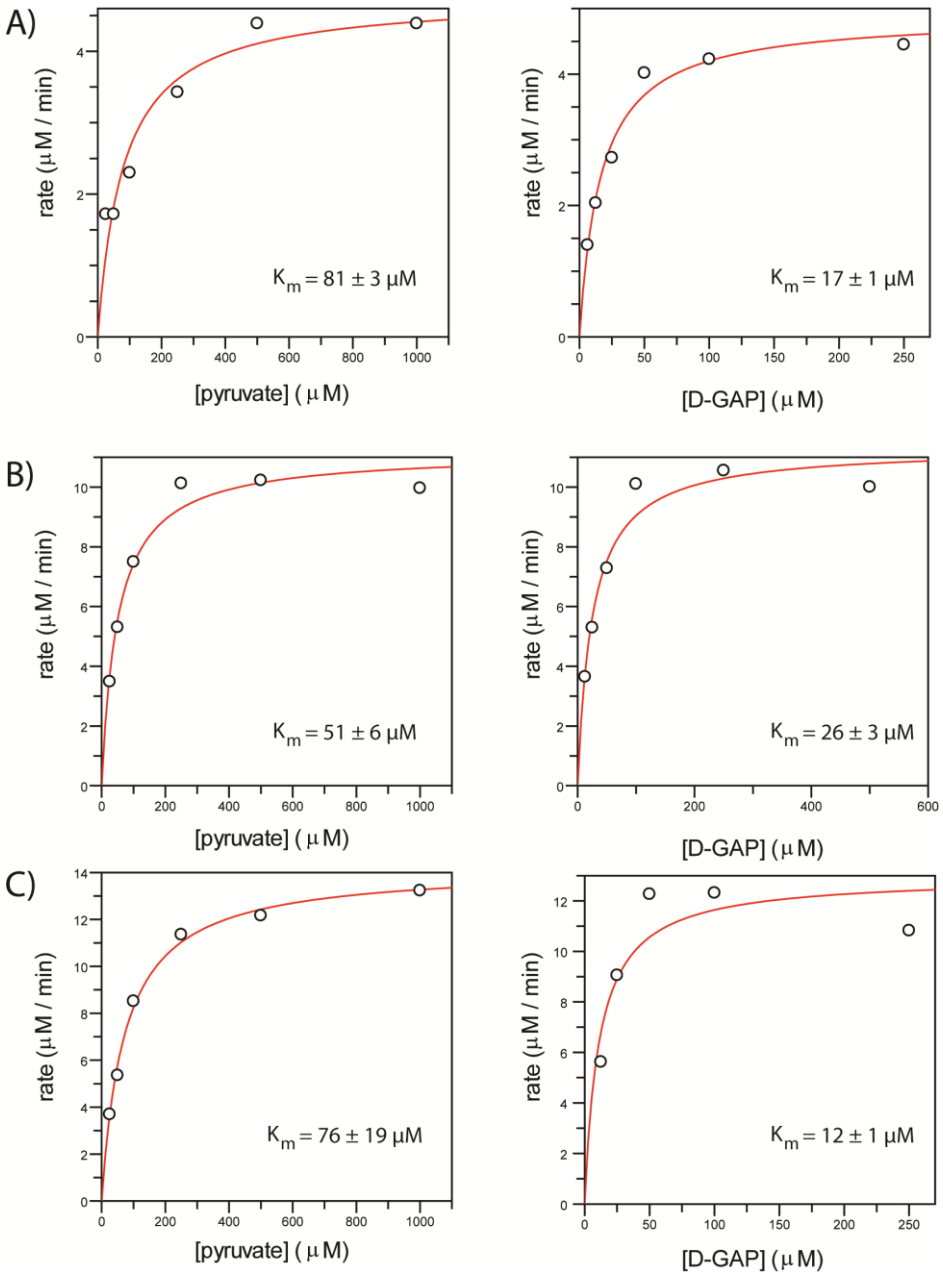

Figure 2-14. **Kinetic characterization of DXP synthase enzymes** [16]**.** DXP synthase was obtained from **A**) *Mycobacterium tuberculosis* (Dxs1) **B**) *Yersinia pestis* **C**) *Salmonella enterica* serovar Typhimurium. The mean and standard deviation of three replicates was used to calculate K_m, and the average of the three replicates (representative curves) is shown.

2.3.3. Homology modeling reveals differences near the M. tuberculosis Dxs1 ThDP cofactor binding site.

To investigate structural similarities and differences amongst the pathogenic DXP synthase enzymes examined in this study, homology modeling was carried out (Lauren Boucher and Prof. Jürgen Bosch, Johns Hopkins University, School of Public Health) (**Figure 2-15**). Modeled to the *D. radiodurans* and *E. coli* DXP synthase crystal structures [(2)], both the *S. typhimurium* and *Y. pestis* enzymes appear to be structurally similar. However, the *M. tuberculosis* enzyme (Dxs1) presented challenges in modeling around the cofactor binding site, specifically around the Y177 residue (**Figure 2-15**). Interestingly, this position usually contains a bulky hydrophobic residue such as leucine, isoleucine, or methionine. This residue is believed to be responsible for maintaining the V-conformation of the cofactor that is universally conserved among all ThDP-dependent enzymes [(43-45)]. In most other DXP synthase enzymes, this residue is an isoleucine. Previous reports suggest that this isoleucine residue and a neighboring isoleucine, both conserved in most ThDP enzymes, stabilize the thiazolium ring of the thiamine cofactor [(2)]. Based on these differences, the Y177 residue was therefore selected for mutagenesis studies.

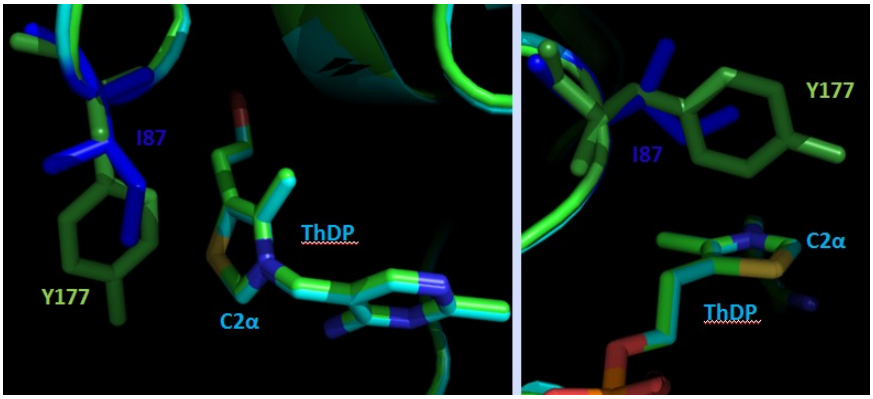

Figure 2-15. *M. tuberculosis* Dxs1 (green) modeled to *D. radiodurans* DXP synthase (dark blue) (Protein Data Bank code 2O1X [2]). The Y177 residue presents challenges in modeling around the cofactor binding site. This residue is an isoleucine in DXP synthase from other organisms (I187 in the 2O1X structure shown here), and a bulky hydrophobic (Leu, Ile, Met) residue in all other ThDP-dependent enzymes [43-45].

2.3.4. M. tuberculosis Dxs1 mutagenesis.

Y177F displays a 1.8-fold reduction in catalytic activity compared to wild type (k_{cat} = 6.3 ± 0.25 min^{-1}), but substrate affinity is not affected (**Table 2-4**). It is possible that this mutation is interfering with the rate-limiting generation of the LThDP cofactor. Interestingly, although Y177I does not contain an aromatic ring, it displays higher turnover compared to the Y177F enzyme (k_{cat} = 26.5 ± 1 min^{-1}, **Table 2-4**). When the tyrosine residue is introduced on the *E. coli* enzyme at this position (I185Y), the K_m value is comparable to wild type Dxs1 (K_m $^{\text{D-GAP}}$ = 19.0 ± 4.6 µM; K_m $^{\text{pyruvate}}$ = 42.0 ± 9.5 µM, **Table 2-4**), and wild type *E. coli* DXP synthase (K_m $^{\text{D-GAP}}$ = 23.5 ± 1.7 µM; K_m $^{\text{pyruvate}}$ = 40.8 ± 4.6 µM) [46]. However, the k_{cat} for I185Y *E. coli* DXP synthase is approximately 5-fold lower (**Table 2-4**).

To examine the role of the tyrosine hydroxyl group, Y177S and Y177T were also evaluated (**Table 2-4**). Y177T displays a ~19-fold reduction in catalytic activity compared to wild type (k_{cat} = 5.9 ± 0.3 min^{-1}), but substrate affinity is not affected (**Table 2-4**). In contrast, Y177S exhibits a 183-fold reduction in turnover (k_{cat} = 0.66 ± 0.16 min^{-1}), but an apparent ~190-fold increase in substrate affinity for pyruvate, and ~1900-fold increase for D-GAP ($K_m^{\text{D-GAP}}$ = 0.01 ± .002 μM; K_m^{pyruvate} = 0.22 ± 0.01 μM) (**Table 2-4**). The relative size of serine and threonine are vastly different than the bulky tyrosine. Although a hydroxyl group is re-introduced in these variants, the smaller nature of these residues might not cover enough of a hypothetical distance to potentially hydrogen bond with an unknown partner in the same manner as wild type. As expected, introducing a charge at this position also results in a dramatic change in rate, as evidenced by the Y177E mutant (**Table 2-4**).

From these results it can be concluded that in the absence of Tyr-177, a large hydrophobic residue is preferred over the smaller residues that contain a hydroxyl group. The role of the hydroxyl group in catalytic proton transfer can be better investigated using the CD method described in chapter 1, section 8 (see Discussion). Further, these results are in agreement with a recent study by Andrews *et al* [47], who reported crystal structures for variants at this position using the benzoylformate decarboxylase (BFDC) enzyme. They found that although a large hydrophobic residue was preferred for catalysis, it is not required to maintain the V-conformation that is conserved in ThDP-dependent enzymes.

enzyme	varied substrate	K_m (μM)	k_{cat} (min^{-1})	k_{cat}/K_m ($min^{-1}μM^{-1}$)
wt Dxs1	pyruvate	42.0 ± 9.48	110.7 ± 3.00	6.2 ± 1.6
	D-GAP	19.0 ± 4.56	117.0 ± 2.33	3.0 ± 0.3
Y177E Dxs1	*no activity at 1, 5, 10 μM enzyme and 0.1 - 2.0 mM substrates*			
Y177F Dxs1	pyruvate	70.7 ± 8.27	6.8 ± 0.23	0.78 ± 0.08
	D-GAP	7.32 ± 0.66	5.8 ± 0.31	0.10 ± 0.01
Y177I Dxs1	pyruvate	256 ± 51	28.1 ± 0.48	0.27 ± 0.05
	D-GAP	91.9 ± 16.7	24.6 ± 1.46	0.11 ± 0.02
Y177S Dxs1	pyruvate	0.22 ± 0.01	0.63 ± 0.13	13 ± 10
	D-GAP	0.01 ± 0.02	0.68 ± 0.18	2.8 ± 0.6
Y177T Dxs1	pyruvate	88 ± 22	5.2 ± 1.0	1.1 ± 0.8
	D-GAP	6.0 ± 3.8	6.6 ± 2.7	0.06 ± 0.02
E. coli I185Y Dxs	pyruvate	12.0 ± 5.5	24 ± 0.8	1.9 ± 0.9
	D-GAP	30.2	21.6	0.62 ± 0.15
Y387F Dxs1	pyruvate	46.5 ± 2.3	62.9 ± 0.8	0.43 ± 0.07
	D-GAP	142 ± 19	61.0 ± 4.8	1.3 ± 0.07

Table 2-4. Kinetic parameters for *M. tuberculosis* Dxs1 enzymes.

Y387 Dxs1 was also selected for mutagenesis, as this residue is believed to be involved in acceptor substrate binding and is the focus of a recent mutagenesis study on *E. coli* DXP synthase (Y392) [28]. Using time-resolved CD spectroscopy and NMR experiments, it was found that Y392 appears to contribute to D-GAP affinity. However, Y392 is not absolutely required for the formation of the LThDP intermediate or its subsequent decarboxylation promoted by D-GAP [28]. In this work, Y387F appears to effect D-GAP affinity on *M. tuberculosis* Dxs1, as there is a 7.5-fold increase in the K_m for D-GAP for this enzyme variant (wild type Dxs1 $K_m^{\text{D-GAP}} = 19.0 \pm 4.6$ μM; Y387F Dxs1 $K_m^{\text{D-GAP}} = 142 \pm 20$ μM, **Table 2-4**). This is comparable to the 9-fold increase that is observed for the *E. coli* DXP synthase variant at this position (wild type $K_m^{\text{D-GAP}} =$

23.5 ± 1.7 μM; Y392F $K_m^{\text{D-GAP}}$ = 210 ± 20 μM; Y392F $K_m^{\text{D-GAP}}$ = 280 ± 30 μM by CD) [28].

Conclusions:

Despite its potential as an anti-infective target, selective inhibitors of DXP synthase are lacking, and reports on the kinetic mechanism are conflicting. The development of selective inhibitors requires knowledge of the characteristics that distinguish this enzyme from other ThDP-dependent enzymes. The work in this chapter takes important steps toward understanding the unique mechanism of DXP synthase. In addition to providing insight regarding order of substrate binding, the results of kinetic analysis suggest pronounced substrate inhibition by D-GAP (**Figure 2-4**). The observed inhibition by both natural substrates at reasonably low concentrations underscores the complexity of substrate equilibrium binding profiles and highlights a promiscuous active site of DXP synthase. The discrepancies between the trends in the double-reciprocal analysis reported here and those reported previously [6, 8] may be explained by differences in reaction conditions. As substrate inhibition is most evident at lower concentrations of the varied substrate, it is anticipated that the subtle inhibitory effects of pyruvate and D-GAP are not observed under conditions where more pronounced inhibition by citrate buffer or removal of D-GAP by reaction with Tris buffer is taking place.

Unexpectedly, we determined that D-glyceraldehyde is competitive with pyruvate but not with D-GAP (**Figure 2-9**). Although D-glyceraldehyde has been used previously as an alternative substrate for D-GAP [6, 14, 15, 38], it has also been suggested that D-

glyceraldehyde can compete for the pyruvate binding site as a substrate inhibitor at high millimolar concentrations [6]. Here, we have shown that removal of the phosphoryl group of D-GAP changes the binding mode of the aldehyde such that it fails to compete for the D-GAP binding site. This result highlights the impact of the phosphoryl moiety on substrate recognition and binding and may underscore the importance of using the natural substrate D-GAP for mechanistic studies of this enzyme. In addition, this result further highlights the promiscuous active site of this enzyme, suggesting opportunities to develop selective inhibitors.

Additionally, methylacetylphosphonate (MAP), a catalytically unreactive analog of pyruvate, was prepared to aid in elucidation of substrate binding order on the GAP binding preferences. MAP is a well characterized inhibitor of many ThDP-dependent enzymes [31-37]. MAP exhibits a clear competitive mode of inhibition with respect to pyruvate, and a noncompetitive mode of inhibition with respect to D-GAP (**Figure 2-7**). The observed potent inhibition of DXP synthase by this pyruvate analog raises the intriguing ideas about the utility of acetyl phosphonate derivatives as selective inhibitors targeting the unique conformations of this mechanistically distinct ThDP-dependent enzyme, a concept further detailed in Chapter 3.

While this work was in progress, a study describing single- molecule force spectroscopy for the identification of novel DXP synthase inhibitors was reported [7]. The method allows measurement of adhesion forces between immobilized substrates and enzyme. The authors suggest a possible dissociation of substrate recognition properties and substrate transformation properties that could permit the use of this catalytically less active nanosensor as a tool for identifying high affinity ligands without the need for

substrate turnover. Interestingly, Sisquella *et al.* reported binding of GAP tethered through the phosphoryl moiety and enhancement of its affinity for the enzyme in the presence of soluble pyruvate. This is particularly interesting, in light of our finding that removal of the phosphoryl moiety inverts the binding mode of the acceptor aldehyde. It is possible that immobilization of DXP synthase effects changes in the active site that promote the binding of an unnatural immobilized substrate. Alternatively, it is conceivable that the immobilized monoanionic phosphate diester binds in a similar manner to D-GAP, suggesting that an acceptor substrate bearing a monoanionic substituent is sufficient to retain the natural binding mode.

The unequivocal distinction between the previously proposed mechanisms [6, 7] and the random sequential mechanism proposed by our laboratory is difficult on the basis of kinetic analysis alone. However, the kinetic analyses presented in this work do argue against ping-pong or rapid equillibirum ordered mechanisms, yet support either a rapid equilibrium, random sequential mechanism or an ordered mechanism, in which pyruvate binds tightly and essentially irreversibly. Both of these mechanisms require the formation of a ternary complex. Molecular docking studies provide additional support for the formation of this ternary complex; *Deinococcus radiodurans* DXP synthase [2] (Protein Data Bank code 2O1X) can easily accommodate both substrates near the C2 position of ThDP (**Figure 2-16**) because the active site of DXP synthase is large. In agreement with this, our group has reported active site calculations indicating that the active site of DXP synthase is 2.5-fold larger than other ThDP-dependent enzymes, pyruvate dehydrogenase and transketolase [48]. This docking analysis also suggests that the phosphate moiety of D-GAP is anchored in the active site by two residues, *D.*

radiodurans DXP synthase R480 and R423. Subsequent work by our lab has used *E. coli* DXP synthase to confirm the involvement of R478 (analogous to R480) and R420 (analogous to R423) in D-GAP binding [28].

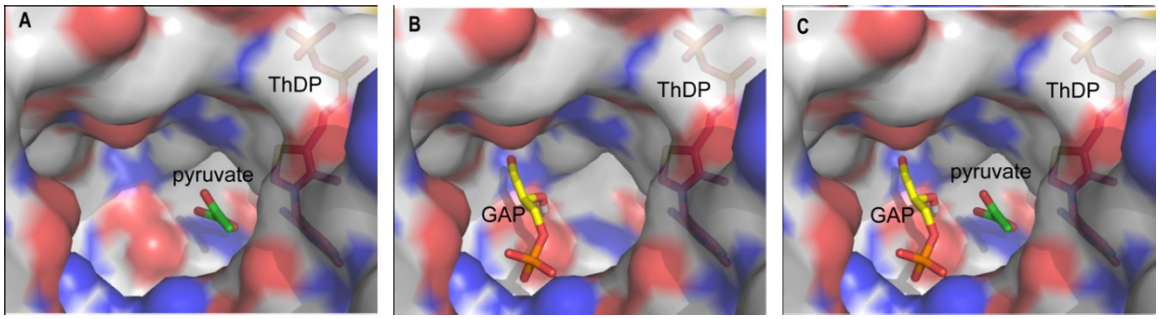

Figure 2-16 [21]. Pyruvate (A) and D-GAP (B) docked to the active site of *D. radiodurans* DXP synthase. Each substrate apparently accesses the active site without blocking access of the other (**C**).

Reanalysis of the kinetic data with respect to natural substrates provides additional insight. A global non-linear regression analysis supports a random sequential mechanism over an ordered mechanism with essentially irreversible pyruvate binding (**Figure 2-5**). However, this global non-linear regression analysis was executed with the idea that for *E. coli* DXP synthase the K_d $^{\text{D-GAP}}$ is comparable to the K_m $^{\text{D-GAP}}$, based on tryptophan fluorescent studies [21]. Subsequent studies have pointed to the instability of wild type *E. coli* DXP synthase and variants as probes in tryptophan fluorescence experiments. Thus, total protein fluorescence has been utilized to re-evaluate dissociation constants, leading to determination of a higher K_d $^{\text{D-GAP}}$ (2.0 ± 0.5 mM) [28]. This value is significantly higher than the K_m $^{\text{D-GAP}}$ (23.5 ± 1.7 μM) [21]. The K_d $^{\text{pyruvate}}$ measured using total protein fluorescence is higher than the K_m $^{\text{pyruvate}}$ (K_d $^{\text{pyruvate}}$ = 0.23 ± 0.07 mM; K_m

^{pyruvate} = 49 ± 8 μM) [21, 28]. These results suggest that while each substrate binds to DXP synthase, the E-pyruvate complex is apparently formed more readily that the E-GAP complex, supportive of a random sequential, preferred order mechanism [21].

Our results raised intriguing questions about the role of D-GAP binding in steps leading to the generation of the nucleophilic C2-α carbanion (**Figure 2-17**), including the ionization and tautomerization states of ThDP and timing of pyruvate activation. In all other ThDP-dependent enzymes that catalyze decarboxylation via a ping-pong mechanism, the aminopyrimidine ring of ThDP tautomerizes upon binding of the first substrate to promote the formation of a short lived predecarboxylation complex [49]. In the unique case of DXP synthase, accelerated decarboxylation of LThDP appears to occur only in the presence of the acceptor substrate D-GAP [6] ; however, it was not known whether D-GAP binding is required for tautomerization of the cofactor and formation of LThDP or if binding of D-GAP promotes decarboxylation of LThDP and formation of the C2-α carbanion.

In collaboration with Dr. Frank Jordan (Rutgers University, Department of Chemistry), the activation and tautomerization of the thiamin cofactor were studied using stopped flow circular dichroism (CD) to monitor enzyme events, and proton NMR was used to monitor ThDP-bound intermediates after release from the enzyme under acidic conditions [27]. In this study, formation of the LThDP intermediate was observed in the absence of D-GAP (**Figure 2-17**), and LThDP appears to be remarkably stable on DXP synthase, a characteristic that is unique among ThDP-dependent enzymes. On other ThDP-dependent enzymes, the LThDP intermediate is "extremely short lived and marginally accumulated at steady state, rendering a structural characterization of LThDP

under steady state turnover or single turnover conditions almost impossible" [27]. It was also discovered that D-GAP promotes a 600-fold rate increase in CO_2 release. Both of these findings support a mechanistic model in which a ternary complex is formed between the enzyme and both substrates prior to decarboxylation, and this is unique among ThDP-dependent enzymes.

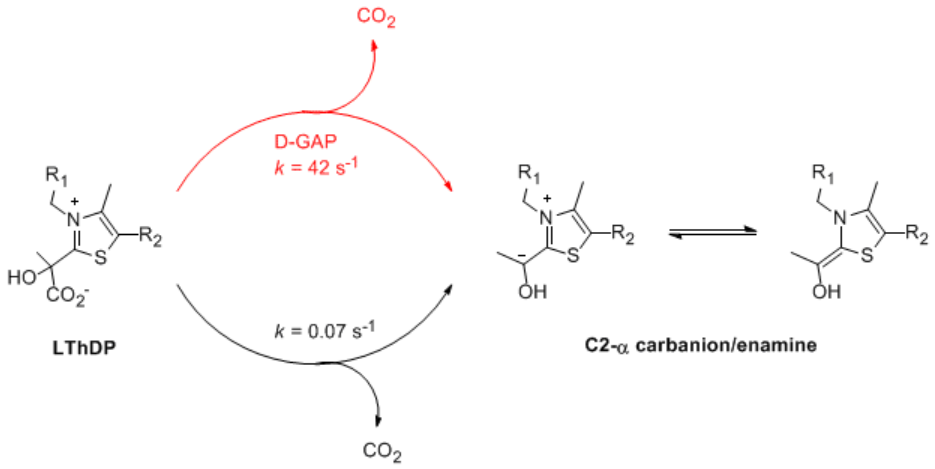

Figure 2-17. Direct observation of the predecarboxylation LThDP intermediate on DXP synthase [27].

Finally, although steady state kinetic analysis of *E. coli*, *Y. pestis*, *S. typhimurium*, and *M. tuberculosis* DXP synthase enzymes suggest these behave similarly, *M. tuberculosis* Dxs1 is predicted to have subtle structural differences around the ThDP cofactor binding site, apparently due to the Y177 residue (**Figure 2-15**). The CD method described above should prove to be especially useful for studying the role of this hydroxyl group during formation of LThDP and its subsequent decarboxylation on *M. tuberculosis* Dxs1. Tryptophan fluorescence analysis could further inform on conformational changes that take place near the ThDP binding pocket during formation of lactyl and phosphonolactyl intermediates.

In summary, the data presented in this chapter provide evidence for ternary complex formation in the kinetic mechanism of DXP synthase, and DXP synthase enzymes from a variety of different bacterial species exhibit similar kinetic behavior. Either substrate is capable of binding to the active site, and both are required prior to catalysis in decarboxylation and carboligation steps. These results are in striking contrast to all other ThDP-dependent enzymes, which supports the idea that it will be possible to develop selective inhibitors targeting this distinct ThDP-dependent enzyme toward the development of anti-infective agents targeting early stage isoprenoid biosynthesis.

Experimental Section

General Methods. Unless otherwise noted, all reagents were obtained from commercial sources. Primers were purchased from Integrated DNA Technologies. Spectrophotometric analyses were performed on a Beckman DU800 UV/Visible spectrophotometer. *E. coli* wild type DXP synthase and variants were purified as described previously [21, 30]. *E. coli* DXP reductoisomerase (IspC) was also prepared as described previously [30]. Molecular docking studies were performed using the program Autodock Vina (version 1.5.1) [50].

Cloning, overproduction, and purification of *M. tuberculosis* DXP synthase (Dxs1). Rv2682c was PCR amplified from H37Rv genomic DNA and ligated into the pET28a+ vector (Novagen), as previously reported [15]. *dxs1*-pET28a+ was then transformed into ArcticExpress competent cells (Agilent Technologies). Cells harboring the over-

expression plasmid were grown in LB broth at 30°C with shaking at 220 rpm until OD_{600} = 0.8, then cooled for 30 minutes on ice. After cooling, cultures were induced with 0.25 mM ispropylthiogalactoside (IPTG), and growth was continued with shaking at 13°C for 24 hours. Cells were harvested by centrifugation at 8 000 rpm for 10 min, and the cell pellet was stored at –20°C. The frozen cell pellet was suspended in lysis buffer (3 mL per gram of cells) containing 50 mM Tris HCl (pH =8), 5 mM $MgCl_2$, 10% glycerol v/v, 5 mM mM β-mercaptoethanol (BME), 1 mM PMSF, 1 mM ThDP, 1x protease inhibitor cocktail, 100 mM NaCl, and 0.01% Igepal-CA630. Cells were lysed by sonication and centrifuged for 45 minutes at 18 000 rpm to pellet cell debris. The supernatant was incubated with nickel-nitrilotriacetic (NTA) acid resin in 20 mM imidazole at 4°C for 2 hours, and Dxs1 was eluted from the resin over a stepwise gradient of 5 to 500 mM imidazole. Fractions containing Dxs1 (as determined by 10% SDS-PAGE) were combined and subjected to dialysis overnight at 4°C against 1 liter of 50 mM Tris (pH 8.0), 10 mM $MgCl_2$, 10% glycerol, 1 mM ThDP, and 100 mM NaCl. A second dialysis was carried out against 1 liter of 50 mM Tris (pH 8.0), 10 mM $MgCl_2$, 10% glycerol, 1 mM ThDP, and 100 mM NaCl and 1 mM for an additional 4 h. After dialysis, protein concentration was determined using the Bio-Rad Protein Assay with bovine serum albumin as a standard (yield 1.0 mg/liter of culture). Protein was flash frozen in liquid nitrogen and stored at -80 °C.

Cloning, overproduction, and purification of *Yersinia pestis,* and *Salmonella typhimurium* DXP synthase. The *Y. pestis* and S. *typhimurium* DXP synthase genes were cloned into the pMCSG28 vector using ligation independent cloning (LIC) methods

as previously described [51, 52] and the resulting plasmids were transformed into Single Step KRX competent cells (Promega). Cells harboring the overexpression plasmid were grown in TB broth containing 100 μg/mL ampicillin, 34 μg/mL chloramphenicol, and 0.1% L(+)arabinose. After growth reached OD_{600} = 0.6 at 37°C, the cultures were cooled to room temperature and induced with 0.5 mM IPTG and 0.25% rhamnose, and shaking was continued for 16 hours. Cells were harvested, lysed, and purified using the same method as described for *M. tuberculosis* Dxs1.

Overproduction and Purification of IspC [30]. *E. coli* BL21 cells harboring *ispC*-pET16b were grown to A_{600} = 0.6 and induced with isopropylthiogalactoside (100 μM) at 37°C. Shaking was continued for 5 h, and the cells were harvested at 4°C and stored overnight at -20 °C. Thawed cells were resuspended in protein purification buffer (25 mM Tris, pH 8.0, 400 mM NaCl, 10% glycerol), lysed by ultrasonication, and cell debris was removed by centrifugation at 4 °C. The supernatant was incubated with nickel-nitrilotriacetic acid resin in 20 mM imidazole at 4 °C for 2 h, and IspC was eluted from the resin over a stepwise gradient of 5 to 500 mM imidazole. Fractions containing IspC (as determined by 10% SDS-PAGE) were combined and subjected to dialysis overnight at 4 °C against 1 liter of 50 mM Tris, pH 8.0, 100 mM NaCl, 1 mM EDTA, and 10% glycerol. A second dialysis was carried out against 1 liter of 50 mM Tris, pH 8.0, 100 mM NaCl, 1 mM EDTA, 10% glycerol, and 1 mM β-mercaptoethanol for an additional 4 h. After dialysis, protein concentration was determined using the Bio-Rad Protein Assay with bovine serum albumin as a standard (yield 33 mg/liter of culture). Protein was then flash frozen in liquid nitrogen and stored at -80 °C.

Kinetic Analyses. Wild type DXP synthase activity was measured spectrophotometrically using IspC as a coupling enzyme as reported previously [23] with minor modifications [21]. The concentration of D-GAP in stock solutions was determined as reported previously [30]. DXP synthase reaction mixtures containing HEPES (100 mM, pH 8.0), 1 mg/mL BSA, 2 mM MgCl2, 2.5 mM tris(2-carboxyethyl)phosphine, 1 mM ThDP, 100 μM NADPH, 1 μM IspC, D,L-GAP, and pyruvate were preincubated at 37 °C for 5 min. DXP synthase (100 nM) was added to initiate each reaction, and the rate of NADPH depletion in the coupled step was monitored spectrophotometrically at 340 nm at 37°C. The rate of NADPH depletion was used to calculate initial rates of DXP formation. All experiments were performed in triplicate. Double reciprocal analysis was performed using GraFit from Erithacus Software (version 7). Non-linear regression analysis of initial velocities and model discrimination analyses were performed using the computer simulation software DynaFit (version 3.28.06) [29]. The pH-rate profile for *M. tuberculosis* Dxs1 was determined using a tri-buffered system and HPLC based assay as previous reported [30, 42].

Inhibition Studies. DXP synthase reaction mixtures containing 100 mM HEPES buffer, pH 8.0 (described above) were preincubated at 37°C for 5 min with β-fluoropyruvate (2, 3, 4, and 6 μM), MAP (2, 5, 10, and 12 μM), or D-glyceraldehyde (2.5, 5, 10, and 15 mM). Inhibition of the coupling enzyme, IspC, by β-fluoropyruvate, MAP, or D-glyceraldehyde was not observed up to 0.5 mM inhibitor. DXP synthase (100 nM) was added to initiate each reaction, and the rate of NADPH depletion was monitored

spectrophotometrically at 340 nm at 37°C. All experiments were performed in triplicate. Double reciprocal analysis of data was carried out using GraFit from Erithacus Software (version 7).

References

1. Sprenger, G. A., *et al*. Identification of a thiamin-dependent synthase in *Escherichia coli* required for the formation of the 1-deoxy-D-xylulose 5-phosphate precursor to isoprenoids, thiamin, and pyridoxol. *Proc. Natl. Acad. Sci. U. S. A*. **94**, 12857 (1997).

2. Xiang, S., Usunow, G., Lange, G., Busch, M. & Tong, L. Crystal structure of 1-deoxy-D-xylulose 5-phosphate synthase, a crucial enzyme for isoprenoids biosynthesis. *J. Biol Chem*. **282**, 2676-2682 (2007).

3. Brown, A. and Parish, T. Dxr is essential in *Mycobacterium tuberculosis* and fosmidomycin resistance is due to a lack of uptake. *BMC Microbiol*. **8**, 78 (2008).

4. Brown, A. C., Eberl, M., Crick, D. C., Jomaa, H. & Parish, T. The nonmevalonate pathway of isoprenoid biosynthesis in *Mycobacterium tuberculosis* is essential and transcriptionally regulated by Dxs. *J Bacteriol*. **192**, 2424-2433 (2010).

5. Lange, B. M., Rujan, T., Martin, W. & Croteau, R. Isoprenoid biosynthesis: The evolution of two ancient and distinct pathways across genomes. *Proc. Natl. Acad. Sci. U. S. A*. **97**, 13172-7 (2000).

6. Eubanks, L. M. and Poulter, C. D. *Rhodobacter capsulatus* 1-deoxy-D-xylulose 5-phosphate synthase: steady-state kinetics and substrate binding. *Biochemistry*. **42**, 1140-9 (2003).

7. Sisquella, X., *et al*. A single-molecule force spectroscopy nanosensor for the identification of new antibiotics and antimalarials. *FASEB J*. **24**, 4203-4217 (2010).

8. Matsue, Y., *et al*. The herbicide ketoclomazone inhibits 1-deoxy-D-xylulose 5-phosphate synthase in the 2-*C*-methyl-D-erythritol 4-phosphate pathway and shows antibacterial activity against *Haemophilus influenzae*. *J. Antibiot*. **63**, 583-8 (2010).

9.Mundle, S. O. C., Rathgeber, S., Lacrampe-Couloume, G., Sherwood Lollar, B. & Kluger, R. Internal return of carbon dioxide in decarboxylation: catalysis of separation and 12-C/13-C kinetic isotope effects. *J. Am. Chem. Soc.* **131**, 11638-9 (2009).

10. Kluger, R. and Rathgeber, S. Catalyzing separation of carbon dioxide in thiamin diphosphate promoted decarboxylation. *FEBS J*. **275**, 6089-6100 (2008).

11. Banerjee, A., *et al.* Feedback inhibition of 1-deoxy-D-xylulose-5-phosphate synthase regulates the methylerythritol 4-phosphate pathway. *J. Biol.Chem.* **288**, 16926-36 (2013).

12. Bouvier, F., d'Harlingue, A., Suire, C., Backhaus, R. A. & Camara, B. Dedicated roles of plastid transketolases during the early onset of isoprenoid biogenesis in pepper fruits. *Biochem J.* **370**, 679–86 (2003).

13. Cane, D. E., Chow, C., Lillo, A. & Kang, I. Molecular cloning, expression and characterization of the first three genes in the mevalonate-independent isoprenoid pathway in *Streptomyces coelicolor*. *Bioorg. Med. Chem*. **9**, 1467-1477 (2001).

14. Kuzuyama, T., Takagi, M., Takahashi, S. & Seto, H. Cloning and characterization of 1-deoxy-D-xylulose 5-phosphate synthase from Streptomyces sp. strain CL190, which uses both the mevalonate and nonmevalonate pathways for isopentenyl diphosphate biosynthesis. *J. Bacteriol*. **15**, 891 (2000).

15. Bailey, A. M., Mahapatra, S., Brennan, P. J. & Crick, D. C. Identification, cloning, purification, and enzymatic characterization of *Mycobacterium tuberculosis* 1-deoxy-D-xylulose 5-phosphate synthase. *Glycobiology*. **12**, 813-820 (2002).

16. Smith, J. M., *et al*. Targeting DXP synthase in human pathogens: enzyme inhibition and antimicrobial activity of butylacetylphosphonate. *J. Antibiot*. 2013. Advance online publication. doi: 10.1038/ja.2013.105.

17. Centers for Disease Control and Prevention. Emergency Preparedness and Response. Plague. 2013 (2005).

18. Ribot, E. M., Wierzba, R. K., Angulo, F. J. & Barrett, T. J. *Salmonella enteric*a serotype Typhimurium DT104 Isolated from Humans, United States, 1985, 1990, and 1996. Emerging Infectious Disease8, (2002).

19. Centers for Disease Control and Prevention. Core curriculum on tuberculosis: what the clinician should know. **24** (2011).

20. Bubb, W. A., Berthon, H. A. & Kuchel, P. W. Tris buffer reactivity with low-molecular weight aldehydes: NMR characterization of the reactions of glyceraldehyde 3-phosphate. *Bioorg. Chem.* **23**, 119–130 (1995).

21. Brammer, L. A., Smith, J. M. & Meyers, C. F. 1-deoxy-D-xylulose 5-phosphate synthase: a novel random sequential mechanism in thiamine diphosphate-dependent enzymology. *J. Biol. Chem*. **42**, 36522-31 (2011).

22. Patton, C., Thompson, S. & Epel, D. Some precautions in using chelators to buffer metals in biological solutions. *Cell Calcium*. **35**, 427-31 (2004).

23. Altincicek, B., *et al*. Tools for discovery of inhibitors of the 1-deoxy-D-xylulose 5-phosphate (DXP) synthase and DXP reductoisomerase: an approach with enzymes from the pathogenic bacterium *Pseudomonas aeruginosa*. FEMS Microbiol. Lett. **190**, 329-333 (2000).

24. Segel, I. H. in Ordered Bi Bi Systems That Appear to be Ping Pong. Enzyme kinetics: Behavior and analysis of rapid equilibrium and steady-state enzyme systems (John Wiley & Sons, Inc, New York, 1975).

25. Segel, I. H. in Rapid equilibrium bireactant and terreactant systems. Enzyme kinetics: Behavior and analysis of rapid equilibrium and steady-state enzyme systems (John Wiley & Sons, Inc, New York, 1975).

26. Copeland, R. A. Evaluation of enzyme inhibitors in drug discovery: a guide for medicinal chemists and pharmacologists (2005).

27. Patel, H., Nemeria, N. S., Brammer, L. A., Meyers, C. F. & Jordan, F. Observation of thiamin-bound intermediates and microscopic rate constants for their interconversion on 1-deoxy-D-xylulose 5-phosphate synthase: 600-fold rate acceleration of pyruvate decarboxylation by D-glyceraldehyde-3-phosphate. *J. Am. Chem. Soc.* **134**, 18374-9 (2013).

28. Brammer Basta, L. A., Patel, H., Kakalis, L., Jordan, F. & Freel Meyers, C. L. Defining critical residues for substrate binding to 1-deoxy-D-xylulose 5-phosphate synthase: Active site substitutions stabilize the pre-decarboxylation intermediate C2 alpha-lactylthiamin diphosphate. Submitted 2013.

29. Kuzmic, P. Program DYNAFIT for the analysis of enzyme kinetic data: Application to HIV proteinase. *Anal Biochem*. **237**, 260 (1996).

30. Brammer, L. A. and Meyers, C. F. Revealing substrate promiscuity of 1-deoxy-d-xylulose 5-phosphate synthase. *Org Lett*. **11**, 4748-51 (2009).

31. Arjunan, P., *et al.* A thiamin-bound, pre-decarboxylation reaction intermediate analogue in the pyruvate dehydrogenase E1 subunit induces large scale disorder-to-order transformations in the enzyme and reveals novel structural features in the covalently bound adduct. *J. Biol. Chem*. **281**, 15296 (2006).

32. O'Brien, T. A., Kluger, R., Pike, D. C. & Gennis, R. B. Phosphonate analogues of pyruvate. Probes of substrate binding to pyruvate oxidase and other thiamin pyrophosphate-dependent decarboxylases. *Biochim Biophys Acta.* **613**, 10-17 (1980).

33. Kale, S., Arjunan, P., Furey, W. & Jordan, F. A dynamic loop at the active center of the *Escherichia coli* pyruvate dehydrogenase complex E1 component modulates substrate utilization and chemical communication with the E2 component. *J. Biol. Chem*. **282**, 28106-28116 (2007).

34. Gish, G., Smyth, T. & Kluger, R. Thiamin diphosphate catalysis. Mechanistic divergence as a probe of substrate activation of pyruvate decarboxylase. *J. Am. Chem. Soc*. **110**, 6230-4 (1988).

35. Flournoy, D. S. and Frey, P. A. Inactivation of the pyruvate dehydrogenase complex of *Escherichia coli* by fluoropyruvate. *Biochemistry*. **28**, 9594-602 (1989).

36. Nemeria, N. S., Korotchkina, L. G., Chakraborty, S., Patel, M. S. & Jordan, F. Acetylphosphinate is the most potent mechanism-based substrate-like inhibitor of both the human and *Escherichia coli* pyruvate dehydrogenase components of the pyruvate dehydrogenase complex. *Bioorg. Chem*. **34**, 362-379 (2006).

37. Nemeria, N., *et al.* The 1',4'-iminopyrimidine tautomer of thiamin diphosphate is poised for catalysis in asymmetric active centers on enzymes. *Proc. Natl. Acad. Sci. U. S. A*. **104**, 78-82 (2007).

38. Hahn, F. M., *et al.* 1-deoxy-D-xylulose 5-phosphate synthase, the gene product of open reading frame (ORF) 2816 and ORF 2895 in *Rhodobacter capsulatus*. *J. Bacteriol*. **183**, 1-11 (2001).

39. Garbe, T., *et al.* Expression of the *Mycobacterium tuberculosis* 19-kilodalton antigen in *Mycobacterium smegmatis*: immunological analysis and evidence of glycosylation. *Infect Immun*. **61**, 260-7 (1993).

40. Noens, E. E., *et al.* Improved mycobacterial protein production using a *Mycobacterium smegmatis* groEL1ΔC expression strain. *BMC Biotechnol*. **25**, 1472 (2011).

41. Joseph, R. E. and Andreotti, A. H. Bacterial expression and purification of Interleukin-2 Tyrosine kinase: Single step separation of the chaperonin impurity. *Protein Expr. Purif.* **60**, 194-197 (2008).

42. Kuo, L. C., Herzberg, W. & Lipscomb, W. N. Substrate specificity and protonation state of ornithine transcarbamoylase as determined by pH studies. *Biochemistry*. **24**, 4754-61 (1985).

43. Shin, W., Pletcher, J., Sax, M., Blank, G. & Wood, M. Stereochemistry of intermediates in thiamine catalysis. Crystal structure of D,L-2-(alpha-hydroxybenzyl)thiamine chloride hydrochloride trihydrate. *J. Am. Chem. Soc.* **99**, 1396-403 (1977).

44. Guo, F., Zhang, D., Kahyaoglu, A., Farid, R. S. & Jordan, F. Is a hydrophobic amino acid required to maintain the reactive V conformation of thiamin at the active center of thiamin diphosphate-requiring enzymes? Experimental and computational studies of isoleucine 415 of yeast pyruvate decarboxylase. *Biochemistry*. **37**, 13379-91 (1998).

45. Crosby, J., Stone, R. & Lienhard, G. E. Mechanisms of thiamine-catalyzed reactions. Decarboxylation of 2-(1-carboxy-1-hydroxyethyl)-3,4-dimethylthiazolium chloride. *J. Am. Chem. Soc.* **92**, 2891-900 (1970).

46. Smith, J. M., Vierling, R. J. & Meyers, C. F. Selective inhibition of *E. coli* 1-deoxy-D-xylulose-5-phosphate synthase by acetylphosphonates. *Med. Chem. Commun*. **3**, 65-67 (2012).

47. Andrews, F. H., Tom, A. R., Gunderman, P. R., Novak, W. R. & McLeish, M. J. A bulky hydrophobic residue is not required to maintain the V-conformation of enzyme-bound thiamin diphosphate. *Biochemistry*. **52**, 3028-30 (2013).

48. Morris, F., Vierling, R., Boucher, L., Bosch, J. & Freel Meyers, C. L. DXP synthase-catalyzed C-N bond formation: nitroso substrate specificity studies guide selective inhibitor design. *Chem. Bio. Chem*. **14**, 1309-1315 (2013).

49. Nemeria, N. S., Chakraborty, S., Balakrishnan, A. & Jordan, F. Reaction mechanisms of thiamin diphosphate enzymes: Defining states of ionization and tautomerization of the cofactor at individual steps. *FEBS Lett.* **76**, 2432-3446 (2009).

50. Trott, O. and Olson, A. J. AutoDock Vina: improving the speed and accuracy of docking with a new scoring function, efficient optimization and multithreading. *J Comput Chem.* **31**, 455-61 (2010).

51. Dieckman, L., Gu, M., Stols, L., Donnelly, M. I. & Collart, F. R. High throughput methods for gene cloning and expression. *Protein Expr. Purif*. **25**, 1-7 (2002).

52. Stols, L., *et al.* A new vector for high-throughput, ligation-independent cloning encoding a tobacco etch virus protease cleavage site. *Protein Expr. Purif.* **25**, 8-15 (2002).

Chapter 3. Development and evaluation of selective inhibitors of DXP synthase.

Introduction:

Although numerous efforts have been made to identify inhibitors of pathogen isoprenoid biosynthesis, few potent inhibitors of the MEP pathway have been reported. Fosmidomycin potently inhibits the second enzyme in the pathway (IspC), and is the only MEP pathway inhibitor under clinical evaluation [1-3]. A previous study by Mai *et al* [4] attempted to develop selective *M. tuberculosis* DXP synthase inhibitors using a target-based approach starting from a known, thiamin-based transketolase inhibitor, 3-(4-chloro-phenyl)-5-benzyl-4H-pyrazolo[1,5-a]pyrimidin-7-one [4]. While the most potent enzyme inhibitor in this study showed *in vivo* activity against *M. tuberculosis* cultures (IC_{50} 7.6 = μM), these thiamin analogs also exhibited toxicity against mammalian cells, suggesting off-target activity against mammalian ThDP-dependent enzymes. This observation underscores the challenge in gaining selectivity of inhibition at the cofactor binding site which is highly conserved within the ThDP-dependent enzyme class [5].

In principle, selective inhibition can be achieved by targeting the unique kinetic mechanism and/or conformational dynamics of DXP synthase. As outlined in Chapter 2, DXP synthase follows a unique kinetic mechanism in the ThDP-dependent class, requiring a ternary complex prior to catalysis for C-C bond formation [6, 7]. Our group also demonstrated flexibility in the active site of *E. coli* DXP synthase toward non-polar acceptor substrates, including aliphatic aldehdyes [8]. On the basis of the relaxed specificity and the knowledge that DXP synthase requires formation of a ternary complex, we hypothesized that covalently linking substrate mimics through an aliphatic

chain will create an unnatural bisubstrate analog that exhibits high affinity for a unique DXP synthase conformation that accommodates both substrates. In this work, initial studies evaluated commercially available bisubstrate analogs as DXP synthase inhibitors. These compounds incorporate a carboxylate group as the GAP mimic (the natural acceptor substrate) and α-keto acids as the pyruvate mimic (the donor substrate) (**Figure 3-1, series A**).

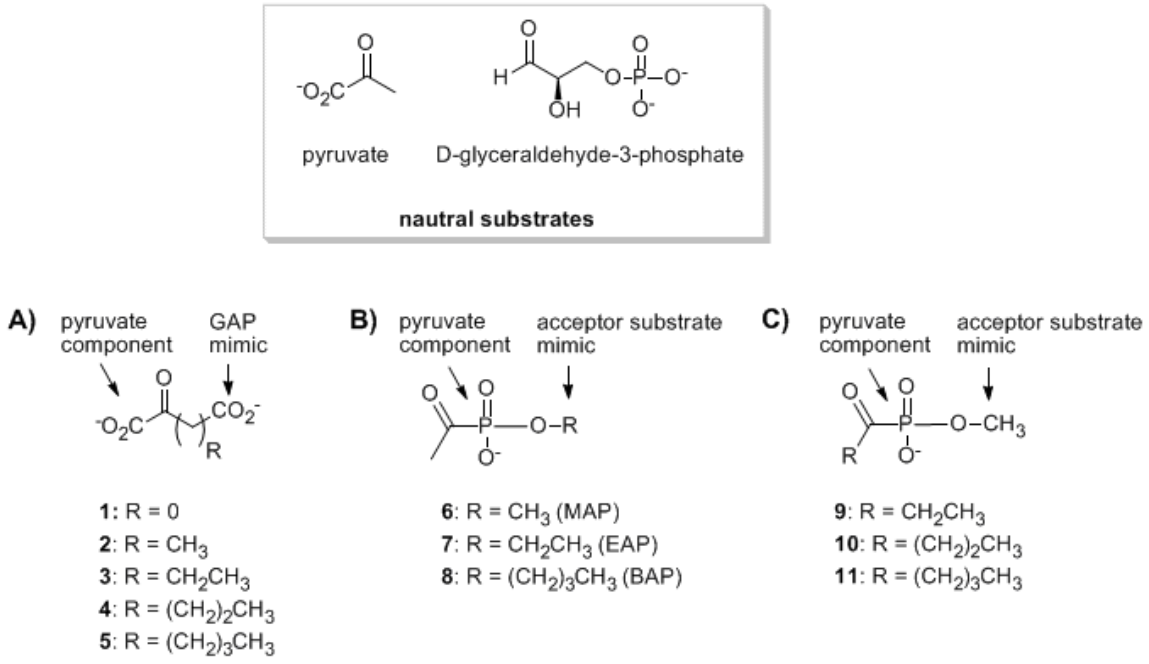

Figure 3-1. Bisubstrate analogs of DXP synthase [9]**. A**) carboxylate bisubstrate analogs **B**) analogs linked through an acyl phosphonate group **C**) analogs linked through phosphonate ester group.

Additionally, analogs that incorporate elements of the donor substrate, pyruvate, and a non-polar acceptor substrate were also evaluated. Methylacetylphosphonate (MAP) is a pyruvate analog that is incapable of undergoing activation by decarboxylation, and is

a well-characterized inhibitor of ThDP-dependent enzymes that utilize pyruvate as substrate [10-15]. As discussed in Chapter 2, we have investigated the inhibitory activity of MAP against DXP synthase during studies to elucidate the mechanism of this enzyme (see 2.2.1) [7]. The observation that MAP potently inhibits DXP synthase prompted speculation about the potential utility of alkylacylphosphonates as bisubstrate analogs for selective inhibition of DXP synthase. Two compound series were envisioned that incorporate an acylphosphonate group as the pyruvate mimic (**Figure 3-1**). Modification of either the acyl or alkyl groups of the phosphonate could mimic a non-polar acceptor substrate and test the importance of acylphosphonate orientation in bisubstrate analogs. Although DXP synthase exhibits relaxed substrate specificity for non-polar acceptor substrates, α-ketoacids modified at the acyl position are poor alternative donor substrates for this enzyme [8]. On this basis, we hypothesized that phosphonates modified at the alkyl position (**Figure 3-1, series B**) should have more potent inhibitory activity against DXP synthase compared to phosphonates modified at the acyl position (**Figure 3-1, series C**). This chapter will describe the evaluation of commercially available dicarboxylates, as well as the design and synthesis of acetylphosphonate analogs in order to achieve selective inhibition against DXP synthase.

Results

3.1. Dicarboxylates are poor bisubstrate inhibitors of E. coli DXP synthase.

Bisubstrate analogs bearing two carboxylate groups as mimics of GAP and pyruvate (**Figure 3-1, series A**) were evaluated as inhibitors of *E. coli* DXP synthase (**Table 3-1**). Results from this analysis suggest that the carboxylate group may not be a

suitable mimic for phosphate in this system. Substrate specificity studies carried out using carboxylate-bearing aldehydes (Leighanne Brammer Batsa, PhD) also reach this conclusion. For future mechanistic studies using bisubstrate analogs, the more challenging synthesis of a phosphate-bearing (GAP mimic) bisubstrate analog could be pursued. It should also be noted that oxaloacetate (**2**) exhibited time dependent inhibition. However, inhibition of the enzyme was first determined using an IspC-coupled assay [2, 7] and after evaluating activity using a discontinuous HPLC based assay [8], it was determined that oxaloacetate is in fact a poor alternative donor substrate for DXP synthase, and further studies were not pursued.

compound	#	slow inhibition?	IC_{50}
mesoxalic acid	**1**	no	> 3 mM
oxaloacetate	**2**	yes	N.D.*
alpha-ketoglutarate	**3**	no	> 3 mM
oxoadipic acid	**4**	no	> 3 mM
2-oxoheptanedioc acid	**5**	yes	2 ± 0.9 mM

Table 3-1. Carboxylate bisubstrate analogs are poor inhibitors of *E. coli* DXP synthase. *alternative substrate. For slow inhibition, DXP synthase was incubated with the dicarboxylate analog for 5 minutes and initiated with D-GAP.

3.2. Acetylphosphonates selectively inhibit E. coli DXP synthase.

Alkylacylphosphonates **6-8** were evaluated as inhibitors of *E. coli* DXP synthase using a spectrophotometric, coupled assay [2, 7]. As shown in mechanistic studies of DXP synthase [7], MAP (**6**) is a potent competitive inhibitor against pyruvate (K_i^{MAP} = 0.96 ± 0.3 μM, **Figure 3-2**). As expected, increasing the length of the acyl group (**9-11**, **Figure**

3-1) results in dramatic reduction of inhibitory activity against DXP synthase (**Table 3-2**), highlighting the importance of the small acetyl group in this pyruvate mimic. In contrast, compounds bearing a non-polar acceptor substrate mimic at the alkylphosphonate group (**6-8, Figure 3-1**) are potent inhibitors of DXP synthase. Ethylacetylphosphonate (**EAP**, **7**) and butylacetylphosphonate (**BAP**, **8**) exhibit comparable inhibitory activity to MAP, with K_i values of 6.7 ± 0.03 μM (**Figure 3-3**) and 5.6 ± 0.8 μM (**Figure 3-4**), respectively (**Table 3-2**). Similarly, both compounds show a competitive mode of inhibition with respect to pyruvate.

The goal of this work is to demonstrate selective inhibition of DXP synthase over other members of the ThDP-dependent class of enzymes. Compounds bearing an acylphosphonate mimic of pyruvate are not expected to exhibit inhibitory activity against transketolase as this enzyme does not recognize pyruvate as a substrate. As expected, none of the compounds reported here shows inhibitory activity against transketolase at concentrations up to 1 mM (**Table 3-2**). In contrast, pyruvate dehydrogenase E1 subunit (PDH) uses pyruvate as its natural substrate, and the pyruvate analogs MAP and the related phosphinates are known inhibitors of this enzyme [10, 11, 14-16]. However, the kinetic mechanism of PDH is distinct from DXP synthase, and small hydrogen and methyl phosphinates show a marked increase in inhibitory activity against PDH compared to MAP. We hypothesized that EAP and BAP may exhibit high affinity for DXP synthase which is known to accommodate both substrates in its active site prior to decarboxylation of pyruvate; however, these sterically demanding analogs should be less potent inhibitors of PDH. Indeed, all three alkylacylphosphonates tested, MAP, EAP and BAP, are considerably less potent inhibitors of porcine PDH compared to DXP synthase, with K_i

values against PDH of 29.9 ± 12.6 μM, 46.6 ± 1.9 μM and 335.4 ± 7.9 μM, respectively (**Table 3-2**). Even the smallest alkylacylphosphonate, MAP, exhibits selective inhibition toward DXP synthase ($K_i^{\text{PDH}}/K_i^{\text{DXP synthase}} = 31$). Selectivity of inhibition increases with increasing chain length, as demonstrated by the greatly reduced inhibitory activity of BAP against PDH compared to DXP synthase ($K_i^{\text{PDH}}/K_i^{\text{DXP synthase}} = 60$). Compounds **9-11** bearing modified acyl groups are not inhibitors of porcine PDH at concentrations up to 1 mM (**Table 3-2**).

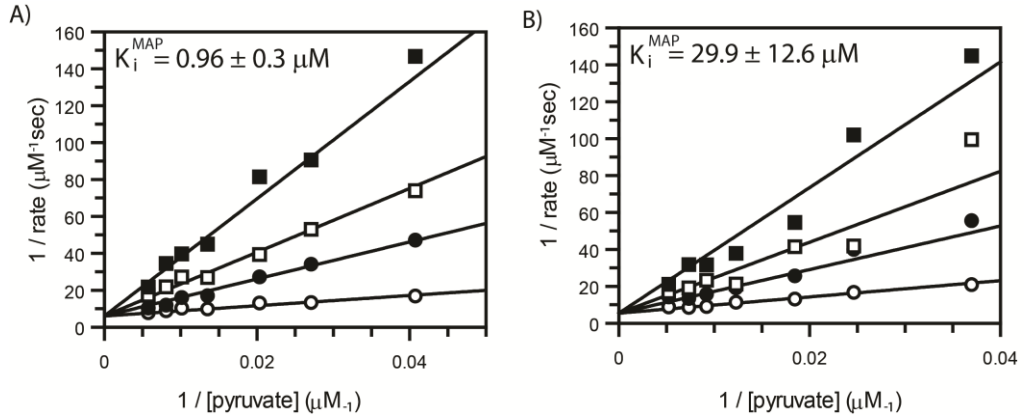

Figure 3-2. Competitive inhibition by methylacetylphosphonate (MAP) [9]**. A**) DXP synthase. The concentration of pyruvate was varied with increasing concentrations of MAP: 0 (○), 2.5 (●), 5 (□), and 10 (■) μM. **B**) E1 subunit of pyruvate dehydrogenase. The concentration of pyruvate was varied with increasing concentrations of MAP: 0 (○), 50 (●), 100 (□), and 200 (■) μM.

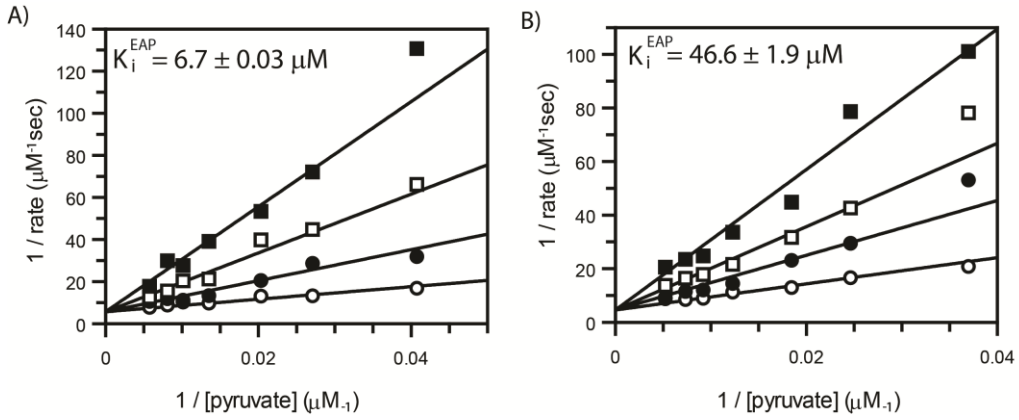

Figure 3-3. Competitive inhibition by ethylacetylphosphonate (EAP) [9]. A) DXP synthase. The concentration of pyruvate was varied with increasing concentrations of EAP: 0 (○), 10 (●), 25 (□), and 50 (■) μM. **B**) E1 subunit of pyruvate dehydrogenase. The concentration of pyruvate was varied with increasing concentrations of EAP: 0 (○), 50 (●), 100 (□), and 200 (■) μM.

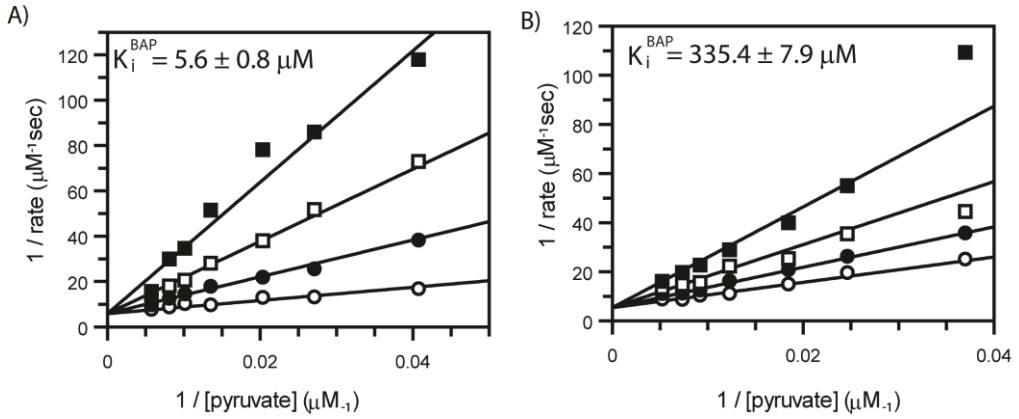

Figure 3-4. Competitive inhibition by butylacetylphosphonate (BAP) [9]. A) DXP synthase. The concentration of pyruvate was varied with increasing concentrations of BAP: 0 (○), 10 (●), 25 (□), and 50 (■) μM BAP. **B**) E1 subunit of pyruvate dehydrogenase. The concentration of pyruvate was varied with increasing concentrations of BAP: 0 (○), 0.2 (●), 0.5 (□), and 1.0 (■) mM BAP.

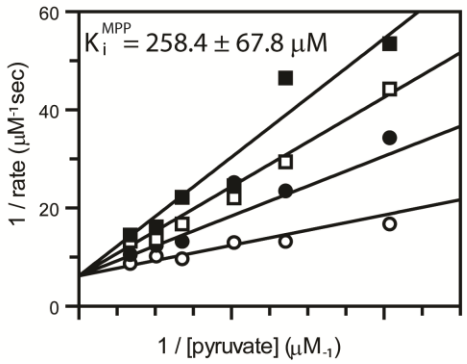

Figure 3-5. Competitive inhibition of DXP synthase by methyl proprionylphosphophosphate (4, MPP) [9]. The concentration of pyruvate was varied with increasing concentrations of MPP: 0 (○), 250 (●), 500 (□), and 750 (■) μM.

***E. coli* DXP synthase (Km = 40.8 ± 4.6 μM)**		**porcine PDH (Km = 54.0 ± 5.3 μM)**		***S. cerevisiae* transketolase**	
compound	**K_i (μM)**	**compound**	**K_i (μM)**	**compound**	**K_i**
1 (MAP)	1.1 ± 0.2	**1** (MAP)	38.5 ± 5.5	**1** (MAP)	> 1 mM
2 (EAP)	6.4 ± 0.5	**2** (EAP)	44.1 ± 5.3	**2** (EAP)	> 1mM
3 (BAP)	5.5 ± 0.9	**3** (BAP)	291.8 ± 30.7	**3** (BAP)	> 1 mM
4	258.4 ± 67.8	**4**	> 1 mM	**4**	> 1 mM
5	> 1 mM	**5**	> 1 mM	**5**	> 1 mM
6	> 1 mM	**6**	> 1 mM	**6**	> 1 mM

Table 3-2. Inhibition of ThDP-dependent enzymes: *E. coli* DXP synthase, porcine pyruvate dehydrogenase (PDH), and transketolase (TK) by alkylacylphosphonates [9].

3.2.1. Butylacetylphosphonate (BAP) inhibition is conserved among pathogenic DXP synthase.

Our work has established alkyl acetylphosphonates as selective inhibitors of *E. coli* DXP synthase [9], suggesting that it is possible to achieve selective inhibition of this

ThDP-dependent enzyme on the basis of differences in substrate usage and mechanism. In order to ensure alkylacetylphosphonates have broad spectrum activity against a variety of bacterial DXP synthase, inhibitory activity of BAP was characterized against DXP synthase from *M. tuberculosis*, *Y. pestis*, and *S. typhimurium* (**Figure 3-6**). In all cases, low micromolar inhibitory activity of BAP is observed that is comparable to the inhibitory activity of BAP against *E. coli* DXP synthase. As expected, the mode of inhibition is competitive with respect to pyruvate and noncompetitive with respect to D-GAP (for *M. tuberculosis* DXP synthase, $K_i^{BAP} = 4 \pm 2$ μM; for *Y. pestis* DXP synthase, $K_i^{BAP} = 7.5 \pm 0.9$ μM; for *S. enterica* DXP synthase, $K_i^{BAP} = 8.4 \pm 0.4$ μM).

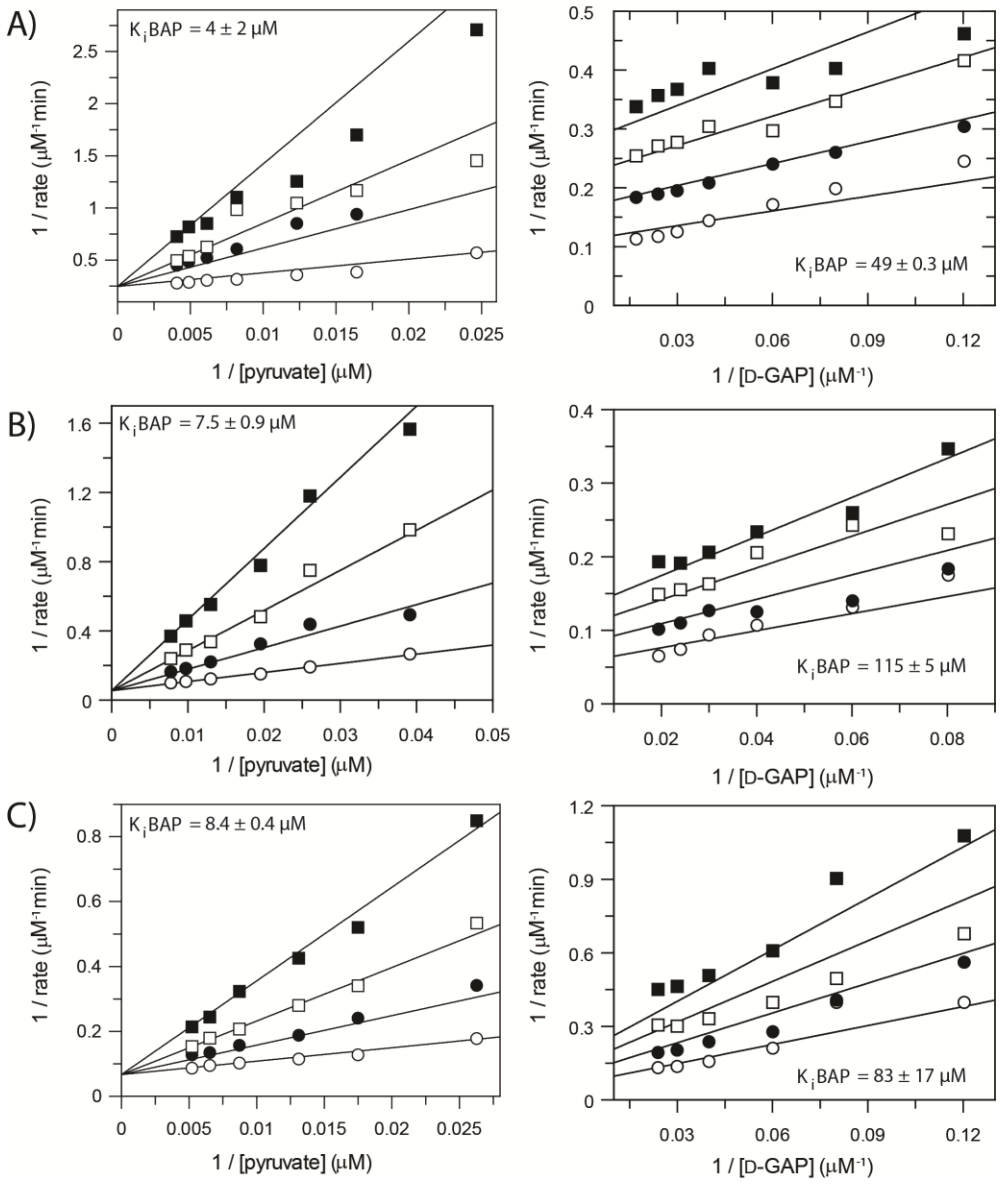

Figure 3-6. **Enzyme inhibitory activity of BAP** [17]. Representative inhibition kinetics are shown for BAP with respect to pyruvate or D-GAP against DXP synthase from **A**) *M. tuberculosis* **B**) *Y. pestis* **C**) *S. enterica*. The mean and standard deviation of three replicates was used to calculate K_i, and the average of the three replicates is shown.

Conclusions

This work shows that alkylacetylphosphonates selectively target DXP synthase [9]. Presumably these analogs exhibit high affinity for a DXP synthase active site that uniquely accommodates both donor and acceptor substrates. The results indicate that modification of the acetyl group abrogates inhibitory activity of acetylphosphonates, consistent with the observation that acyl-modified α-ketoacids are not substrates for DXP synthase [8]. However, lengthening the carbon chain of the alkyl phosphonate produces inhibitors with comparable activity to MAP. These analogs are considerably less potent inhibitors of porcine PDH and do not exhibit measurable inhibitory activity against transketolase. We also characterized the inhibitory activity of butylacetylphosphonate (BAP) against pathogenic DXP synthase to demonstrate comparable inhibitory activity, an important finding if acetylphosphonates are to be developed as broad spectrum anti-infectives. BAP displays low micromolar inhibitory activity against DXP synthase from *M. tuberculosis*, *S. enterica,* and *Y. pestis*, [17] and this is consistent with the idea that BAP targets a mechanism common to all pathogenic DXP synthase enzymes, but distinct from mammalian ThDP-dependent enzymes. Not surprisingly, BAP acts as a competitive inhibitor with respect to pyruvate in all cases, indicating that the acetylphosphonate moiety of BAP acts as a pyruvate mimic in this unnatural bisubstrate analog.

Taken together, these results are consistent with a unique inhibition mechanism in ThDP-dependent enzymology, and suggest an exciting new direction for the development of a new class of inhibitors targeting early-stage isoprenoid biosynthesis. Toward this end, structure activity relationship (SAR) studies will be carried out in order to improve efficacy and selectivity of acetylphosphonate analogs against DXP synthase. Reports on

substrate specify and reaction promiscuity will provide a foundation for SAR [8, 18]. For example, it has been shown that aromatic nitroso compounds are high affinity acceptor substrates of *E. coli* DXP synthase [18]. In future studies, high affinity aromatic elements will be incorporated to impart selectivity of inhibition.

Experimental Section

General Methods. Pyruvate dehydrogenase from porcine heart and transketolase from baker's yeast (*S. cerevisiae*) were obtained from Sigma Aldrich.

Kinetic Analyses. DXP synthase activity was measured spectrophotometrically using IspC as a coupling enzyme as previously reported [2, 7]. The concentration of D-GAP in stock solutions was determined as previously reported [8]. All experiments were performed in duplicate. Pyruvate dehydrogeanse activity was measured spectrophotometrically as previously reported [19] by measuring changes in optical density at 340 nm. The basic assay medium (30°C), contained 100 mM HEPES (pH = 8.0), 1 mg/mL BSA, 0.2 mM ThDP, 0.1 mM coenzyme A, 1 mM MgCl2, 2 mM cysteine, 0.3 mM TCEP. The reaction was initiated with enzyme. Transketolase activity was measured as previously reported by measuring changes in optical density at 340 nm [20]. The basic assay medium (37°) contained 50 mM glycylgylcine (pH = 7.7), 10 mM sodium arsenate, GADPH, 3.2 TCEP, 2.5 CaCl2, 80 μM ThDP, 70 μM xylulose-5-phosphate, 0.5 mM ribose-5-phosphate, 0.4 mM β-nicotinamide adenine dinucleotide phosphate sodium salt hydrate (NAD+). The reaction was initiated with enzyme.

Inhibition Studies. Suppression of DXP synthase activity was measured spectrophotometrically using IspC as a coupling enzyme and monitoring NADPH consumption by IspC. Chemical synthesis (compounds **6-11**) was carried out by Ryan Vierling [9]. DXP synthase reaction mixtures containing 100 mM HEPES buffer, pH 8.0 (described above) were pre-incubated at 37°C for 5 minutes with each compound. The reaction was initiated with enzyme. For the bisubstrate analogs that possessed carboxylate as a GAP mimic (compounds **1-5**), inhibitory activity was evaluated using a range of 0 – 5 mM at 0.15 mM pyruvate and 75 μM D-GAP. For analysis of time-dependent inhibition by these compounds, DXP synthase was included in the reaction mixture and the reaction was initiated with substrates. For the acetylphosphonate studies the following concentrations were used to obtain K_i: compound **6** (2.5, 5, and 10 μM), compound **7** (10, 25, and 50 μM), compound **8** (10, 25, and 50 μM), and compound **9** (250, 500, and 750 μM). Inhibition of DXP synthase by compounds **10 - 11** was not observed. Suppression of pyruvate dehydrogenase activity was measured spectrophotometrically by measuring changes in optical density at 340 nm. Pyruvate dehydrogenase reaction mixtures containing 100 mM HEPES buffer, pH 8.0 (described above) were pre-incubated at 30°C for 5 minutes with compound **6** (50, 100, 250 μM), compound **7** (50, 100, 250 μM), compound **8** (200, 500, 1000 μM). Inhibition of porcine pyruvate dehydrogenase by compounds **9 -11** was not observed up to 1 mM. Inhibition of the coupling enzyme (IspC) and transketolase from baker's yeast by compounds **6 -11** was not observed up to 1 mM. All experiments were performed in duplicate. Double reciprocal analysis of data was carried out using GraFit version 7 from Erithacus Software.

Synthesis

General Experimental. All compound synthesis was carried out by Ryan Vierling. Trialkyl phosphites, acyl chlorides and lithium bromide were obtained from commercial sources and used without further purification. Anhydrous acetonitrile was purchased in Sure-Seal bottles. All reactions were carried out in oven-dried glassware under an inert argon atmosphere. NMR spectra were recorded on a Bruker 400 MHz spectrometer for dialkyl acyl phosphonate intermediates, or a Varian 500 MHz spectrometer for final compounds. Chemical shifts are reported in units of parts per million (ppm), relative to a standard reference point. ^{1}H NMR chemical shifts are reported relative to tetramethylsilane (TMS, $\delta = 0$ ppm) as internal reference. ^{31}P chemical shifts are reported relative to triphenylphosphine oxide (TPPO, $\delta = 0$ ppm) as an external standard. Mass spectrometry analysis was carried out at University of Illinois at Urbana-Champagne, School of Chemical Sciences, Mass Spectrometry Laboratory. Chemical synthesis and characterization of compound (**6**) (MAP) was reported previously [7]. Compound (**9**) (MBP) was prepared according to published protocol [21].

Synthesis of ethyl acetyl phosphonate (7). An oven-dried flask was equipped with a stir-bar and charged with 0.21 mL of acetyl chloride (0.24g, 3.0 mmol). Triethyl phosphite (0.52 mL, 3.0 mmol) was added drop-wise at room temperature. The solution was stirred at room temperature for about 1 hour, until triethyl phosphite had disappeared (as indicated by ^{31}P NMR analysis). Diethyl acylphosphonate was isolated as a pale yellow oil following vacuum distillation (241.6mg, 97% pure as determined by ^{31}P NMR,

45% yield) and was carried on without further purification. ^{31}P-NMR ($CDCl_3$): δ -27.84 (s) ^{1}H-NMR ($CDCl_3$): δ 1.08 (t, 6H), 2.182 (d, 3H), 4.02 (m, 4H).

Diethyl acylphosphonate was dissolved in 1.7 mL of anhydrous acetonitrile. Lithium bromide (106.8 mg, 1.2 mmol) was added in one portion, and the reaction mixture was heated to 70 ^{o}C and stirred overnight. The resulting white solid was filtered and washed with two 10 mL portions of anhydrous acetonitrile followed by two 10 mL portions of diethyl ether. Ethyl acetylphosphonate (**7**) was isolated as a white solid (132.5 mg, 69% yield). ^{31}P-NMR (D_2O): δ -27.08 (s); ^{1}H-NMR (D_2O): 1.17 (t, 3H), 2.34 (d, 3H), 3.84 (m, 2H). HRMS (ESI), calculated m/z for $C_4H_9LiO_4P$ (free acid form), $[M+H]^+$ = 159.0399; observed: 159.0398.

Synthesis of butyl acetylphosphonate (8). An oven-dried flask was equipped with a stir-bar and charged with 0.40 mL of acetyl chloride (0.44g, 5.6 mmol). Tributyl phosphite (1.5 mL, 6.0 mmol) was added drop-wise at room temperature. The solution was stirred at room temperature for about 1 hour, until tributyl phosphite had disappeared (as indicated by ^{31}P NMR analysis). Dibutyl acylphosphonate was isolated as a pale yellow oil following vacuum distillation (754mg, 90% pure as determined by ^{31}P NMR, 64% yield) and was carried on without further purification. ^{31}P-NMR ($CDCl_3$): δ -28.75 (s) ^{1}H-NMR ($CDCl_3$): δ 0.94 (t, 6H), 1.42 (m, 4H), 1.71 (m, 4H), 2.49 (d, 3H), 4.16 (m, 4H).

Dibutyl acylphosphonate was dissolved in 4 mL of anhydrous acetonitrile. Lithium bromide (269.7 mg, 3.1 mmol) was added in one portion, and the reaction mixture was

heated to 70 ^{o}C and stirred overnight. The resulting white solid was filtered and washed with two 10 mL portions of anhydrous acetonitrile followed by two 10 mL portions of diethyl ether. Butyl acetylphosphonate (**8**) was isolated as a white solid (261.1 mg, 44%). ^{31}P-NMR (D_2O): δ -27.01(s); ^{1}H-NMR (D_2O): 0.76 (t, 3H), 1.22 (m, 2H), 1.47 (m, 2H), 2.29 (d, 3H), 3.76 (m, 2H). HRMS (ESI), calculated m/z for $C_6H_{13}LiO_4P$ (free acid form), $[M+H]^+$ = 187.0712; observed: 187.0709.

Synthesis of methyl propionylphosphonate (9). An oven-dried flask was equipped with a stir-bar and charged with 0.50 mL of propionyl chloride (0.53g, 5.5 mmol). Trimethyl phosphite (0.60 mL, 5.1 mmol) was added drop-wise at room temperature. The solution was stirred at room temperature for about 1 hour, until trimethyl phosphite had disappeared (as indicated by ^{31}P NMR analysis). Dimethyl propionylphosphonate was isolated as a pale yellow oil following vacuum distillation (542.3 mg, 98% pure as determined by ^{31}P NMR, 64% yield) and was carried on without further purification. ^{31}P-NMR ($CDCl_3$): δ -26.77 (s)

Dimethyl propionylphosphonate was dissolved in 4 mL of anhydrous acetonitrile. Lithium bromide (269.7 mg, 3.1 mmol) was added in one portion, and the reaction mixture was heated to 70 ^{o}C and stirred overnight. The resulting white solid was filtered and washed with two 10 mL portions of anhydrous acetonitrile followed by two 10 mL portions of diethyl ether. Methyl propionylphosphonate (**3**) was isolated as a white solid (241.0 mg, 47%). ^{31}P-NMR (D_2O): δ -27.01; ^{1}H-NMR (D_2O): 0.76 (t, 3H), 1.22 (m, 2H),

1.47 (m, 2H), 2.29 (d, 3H), 3.76 (m, 2H). ESI (M/S) calculated m/z for C4H9LiO4P (free acid form), $[M+H]^+$ = 159.04

Synthesis of methyl valeroylphosphonate (10). An oven-dried flask was equipped with a stir-bar and charged with 0.3 mL of valeroyl chloride (0.3g, 2 mmol), to which 0.3mL of trimethyl phosphite (0.3g, 2 mmol) was added. After one hour, reaction mixture was diluted with 3.1 mL of anhydrous acetonitrile. To this solution, 220 mg of LiBr (2.53 mmol) was added in one portion. The reaction mixture was warmed to 70^{o}C overnight. The solid white precipitate was filtered with two 10 mL portions of anhydrous acetonitrile, followed by two 10 mL portions of diethyl ether. Methyl valeroylphosphonate was isolated as a white solid (110.3mg, 23% overall yield). ^{31}P-NMR (D_2O): δ -25.89 (s); ^{1}H-NMR (D_2O): 0.79 (t, 3H), 1.18 (m, 2H), 1.46 (m, 2H), 2.73 (t, 2H), 3.52 (d, 3H). HRMS (ESI), calculated m/z for $C_6H_{13}LiO_4P$ (free acid form), $[M+H]^+$ = 187.0712; observed: 187.0708.

References

1. Okuhara, M., *et al*. Studies on new phosphonic acid antibiotics. *J. Antibiot*. **33**, 13 (1980).

2. Altincicek, B., *et al*. Tools for discovery of inhibitors of the 1-deoxy-D-xylulose 5-phosphate (DXP) synthase and DXP reductoisomerase: an approach with enzymes from the pathogenic bacterium *Pseudomonas aeruginosa*. *FEMS Microbiol Lett*. **190**, 329-333 (2000).

3. Albert Schweitzer Hospital. Efficacy of fosmidomycin-clindamycin for treating malaria in gabonese children. Clinical trial number NCT00214643. (2009).

4. Mao, J., *et al*. Structure–activity relationships of compounds targeting *Mycobacterium tuberculosis* 1-deoxy-D-xylulose 5-phosphate synthase. *Bioorg. Med. Chem. Lett*. **18**, 5320-5323 (2008).

5. Xiang, S., Usunow, G., Lange, G., Busch, M. & Tong, L. Crystal structure of 1-deoxy-D-xylulose 5-phosphate synthase, a crucial enzyme for isoprenoids biosynthesis. *J. Biol Chem*. **282**, 2676-2682 (2007).

6. Eubanks, L. M. and Poulter, C. D. *Rhodobacter capsulatus* 1-deoxy-D-xylulose 5-phosphate synthase: steady-state kinetics and substrate binding. *Biochemistry*. **42**, 1140-9 (2003).

7. Brammer, L. A., Smith, J. M. & Meyers, C. F. 1-deoxy-D-xylulose 5-phosphate synthase: a novel random sequential mechanism in thiamine diphosphate-dependent enzymology. *J. Biol. Chem*. **42**, 36522-31 (2011).

8. Brammer, L. A. and Meyers, C. F. Revealing substrate promiscuity of 1-deoxy-d-xylulose 5-phosphate synthase. *Org Lett*. **11**, 4748-51 (2009).

9. Smith, J. M., Vierling, R. J. & Meyers, C. F. Selective inhibition of *E. coli* 1-deoxy-D-xylulose-5-phosphate synthase by acetylphosphonates. *Med. Chem. Commun*. **3**, 65-67 (2012).

10. O'Brien, T. A., Kluger, R., Pike, D. C. & Gennis, R. B. Phosphonate analogues of pyruvate. Probes of substrate binding to pyruvate oxidase and other thiamin pyrophosphate-dependent decarboxylases. *Biochimica et Biophysica Acta (BBA) Enzymology*. **613**, 10-17 (1980).

11. Kale, S., Arjunan, P., Furey, W. & Jordan, F. A Dynamic Loop at the Active Center of the Escherichia coli Pyruvate Dehydrogenase Complex E1 Component Modulates Substrate Utilization and Chemical Communication with the E2 Component. *J. Biol. Chem*. **282**, 28106-28116 (2007).

12. Gish, G., Smyth, T. & Kluger, R. Thiamin diphosphate catalysis. Mechanistic divergence as a probe of substrate activation of pyruvate decarboxylase. *J. Am. Chem. Soc.* **110**, :6230-4 (1988).

13. Flournoy, D. S. and Frey, P. A. Inactivation of the pyruvate dehydrogenase complex of *Escherichia coli* by fluoropyruvate. *Biochemistry*. **28**, 9594-602 (1989).

14. Nemeria, N., *et al.* The 1',4'-iminopyrimidine tautomer of thiamin diphosphate is poised for catalysis in asymmetric active centers on enzymes. *Proc. Natl. Acad. Sci. U. S. A*. **104**, 78-82 (2007).

15. Kluger, R. and Pike, D. C. Active site generated analogs of reactive intermediates in enzymic reactions. Potent inhibition of pyruvate dehydrogenase by a phosphonate analog of pyruvate. *J. Am. Chem. Soc.* **99**, 504-6 (1977).

16. Arjunan, P., *et al.* A thiamin-bound, pre-decarboxylation reaction intermediate analogue in the pyruvate dehydrogenase E1 subunit induces large scale disorder-to-order transformations in the enzyme and reveals novel structural features in the covalently bound adduct. *J. Biol. Chem.* **281**, 15296 (2006).

17. Smith, J. M., *et al*. Targeting DXP synthase in human pathogens: enzyme inhibition and antimicrobial activity of butylacetylphosphonate. *J. Antibiot*. 2013. Advance online publication. doi: 10.1038/ja.2013.105.

18. Morris, F., Vierling, R., Boucher, L., Bosch, J. & Freel Meyers, C. L. DXP synthase-catalyzed C-N bond formation: nitroso substrate specificity studies guide selective inhibitor design. *Chem. Bio. Chem*. **14**, 1309-1315 (2013).

19. Strumilo, S., Czerniecki, J. & Dobrzyn, P. Regulatory effect of thiamin pyrophosphate on pig heart pyruvate dehydrogenase complex. *Biochem. Biophys. Res. Commun*. **256**, 341-345 (1999).

20. Sprenger, G. A., Schörken, U., Sprenger, G. & Sahm, H. Transketolase a of *Escherichia coli* K12. *Eur. J. Biochem*. **230**, 525-32 (1995).

21. Fang, M., *et al.* Succinylphosphonate esters are competitive inhibitors of MenD that show active-site discrimination between homologous alpha-ketoglutarate-decarboxylating enzymes. *Biochemistry*. **49**, 2672-9 (2010).

Chapter 4: Antimicrobial activity of butylacetylphosphonate.

Introduction

In many bacterial pathogens, DXP synthase is a branch point in metabolism; DXP is a precursor to pyridoxal phosphate (PLP) biosynthesis and, interestingly, also a precursor to its own essential cofactor, thiamin diphosphate [1-3] (for additional information, see section 1.4. Despite its importance in bacterial metabolism, DXP synthase is underdeveloped as a drug target. Ostensibly, this is largely due to perceived challenges in achieving selective inhibition of DXP synthase over mammalian ThDP-dependent enzymes, such as the E1 subunit of pyruvate dehydrogenase (E1 PDH) and transketolase (TK), and few reports describe inhibitors of this enzyme [4-7]. However, DXP synthase appears unique amongst ThDP-dependent enzymes (for additional information, see Chapter 2) [6-9]. Indeed, we have demonstrated that selective inhibition of *E. coli* DXP synthase is achievable with unnatural bisubstrate analogs including butylacetylphosphonate (BAP) [10] and benzylacetylphosphonate (BnAP) [8], both bearing an acetylphosphonate mimic of pyruvate [11-13] and a sterically demanding unnatural acceptor substrate (for additional information, see Chapter 3). Presumably, sterically demanding acetylphosphonates bind in the large DXP synthase active site and react with bound ThDP, in a manner similar to methylacetylphosphonate [14-18], to form a stable phosphonolactyl-thiamin diphosphate (PLThDP) intermediate, effectively trapping the enzyme at a pre-decarboxylation complex (**Figure 4-1**).

In this chapter, we describe studies to evaluate the antimicrobial activity of BAP against several bacterial pathogens, both in our lab and with a collaborator (Dr. Andrew

Koppisch, Northern Arizona University). Our results indicate that BAP possesses modest antibacterial activity via a mechanism that appears to involve inhibition of DXP synthase, and drug synergism is evident with BAP-fosmidomycin combinations in *E. coli*. These results suggest that selective inhibitors of DXP synthase could be effective in antibiotic combinations.

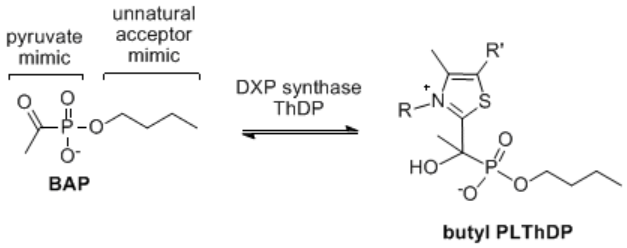

Figure 4-1. Proposed mechanism of selective inhibition of DXP synthase by butylacetylphosphonate [19].

Results

4.1. BAP exhibits weak antimicrobial activity. As a starting point, BAP was evaluated for antimicrobial activity against the Escherichia *coli* ATCC strain MG 1655 using the macrodilution method [20, 21]. BAP exhibits minimum inhibitory concentrations (MIC = [BAP] causing growth inhibition) of ~1 000 µg/mL in cation-adjusted Mueller Hinton Broth (**Table 4-1)** and a significantly lower MIC of 122 µg/mL in M9 minimal media. BAP was evaluated against several clinically isolated pathogens (Dr. Andrew Koppisch, **Table 4-1**), and BAP exhibits an MIC of 4 000 µg/mL against *Salmonella enterica* serovar Typhimurium and *Micrococcus sp.*, 1 000 µg/mL against *Bacillus anthracis* Sterne, and 4 000 µg/mL against *Pseudomonas aeruginosa* in cation adjusted Mueller Hinton Broth.

organism	MIC (μg/mL)
Bacillus anthracis Sterne [1]	1000
Bacillus subtillis	> 2000
Bacillus thuringiensis HD34 [1]	> 4000
Enterobacter cloacae	> 4000
Escherichia coli	1000
Klebsiella oxytoca	> 4000
Klebsiella pneumonia	> 4000
Micrococcus sp.	2000
Mycobacterium smegmatis	> 2000
Pseudomonas aeruginosa	4000
Pseudomonas fluorescens	> 4000
Rhizobium radiobacter [1]	> 4000
Salmonella typhimurium	4000
Staphylococcus aureus[2]	> 4000

Table 4-1. Antimicrobial activity of BAP [(19)]. [1] Fractional growth was determined as outlined in the Experimental Section, but with slightly longer incubations (22-24 hrs) at 37 °C. [2] Does not use the MEP pathway.

We considered the possibility that the weak antimicrobial activity of BAP is attributed to poor cellular uptake. Small phosphorylated (or phosphonylated) molecules, including the phosphonate fosmidomycin, are actively transported via the glycerol 3-phosphate transporter (*glpT*) [(22-24)]. BAP was evaluated for antimicrobial activity against a *glpT* knockout strain (JW2234-2) and its parent strain (BW25513) (Yale, Coli Genetic Stock Center) to determine whether this is a possible uptake mechanism. However, while fosmidomcyin is inactive against the *glpT* knockout strain, BAP exhibits comparable antimicrobial activity against the *glpT* knockout and parent strains (**Figure 4-2**). This result indicates the glycerol 3-phosphate transporter is not likely a mechanism of entry for BAP.

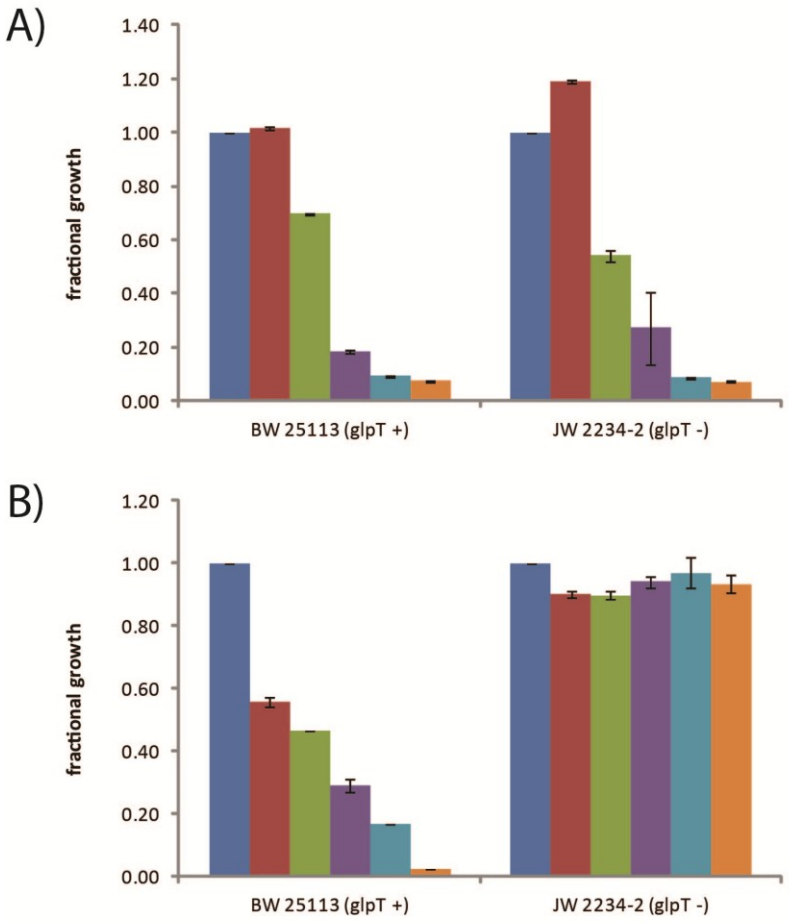

Figure 4-2. **BAP and fosmidomycin (FOS) antimicrobial activity against glycerol 3-phosphate transporter knockout (glpT-). A**) BAP evaluated for antimicrobial activity against a *glpT* knockout strain (JW2234-2) and its parent strain (BW25513) (Yale, Coli Genetic Stock Center). Fractional growth was determined with increasing BAP: 0 mM (blue), 0.16 mM (red), 0.33 mM (green), 1.31 mM (purple), 2.63 mM (teal), 5.25 mM (orange). **B**) Fractional growth was determined with increasing fosmidomycin: 0 mM (blue), 3 µM (red), 6 µM (green), 12.5 µM (purple), 25 µM (teal), 50 µM (orange). Studies were carried out as described in Materials and Methods (see Antimicrobial

susceptibility studies). The mean and standard deviation of two biological replicates is shown.

4.2. DXP synthase is an intracellular target of BAP. Experiments to rescue the growth inhibitory effects of BAP against *E. coli* MG1655 were performed to provide evidence for DXP synthase as an intracellular target.

4.2.1. Rescue by downstream metabolites.

Previous reports demonstrate labeling of downstream MEP pathway intermediates in *E. coli* in feeding experiments using labeled 1-deoxy-D-xylulose (DX), suggesting DX is cell permeable and undergoes intracellular phosphorylation at some level to produce DXP [25, 26]. Here, partial rescue of BAP inhibitory activity is observed when the growth medium is supplemented with DX (50% reduction in growth inhibition by BAP in the presence of DX) (**Figure 4-3A**). As DXP synthase is a branch point in bacterial metabolism, additional biosynthetic pathways including thiamin diphosphate and pyridoxal phosphate biosynthesis [1-3] should be affected by inhibition of DXP synthase. Further, inhibition of ThDP biosynthesis might potentiate the loss of DXP synthase activity as this cofactor is also required for DXP synthase-catalysis. Complete rescue of growth inhibitory effects of 31.25 μg/mL BAP (165 μM) is observed in the presence of thiamin (**Figure 4-3B**). *E. coli* growth rates in the presence or absence of thiamin are similar (**Figure 4-3C**), suggesting intracellular thiamin concentration is sufficient to support normal growth under conditions where ThDP biosynthesis is not inhibited. Cells treated with BAP display severely delayed growth (**Figure 4-3C**). While growth of BAP

treated cells is restored by 16 hours in the presence of thiamin, there is a clear delay in growth under these conditions. This may reflect the time required for intracellular phosphorylation of thiamin under growth inhibitory conditions. Under conditions of higher BAP concentration, thiamin supplementation does not rescue growth by 16 hours (**Figure 4-3C**).

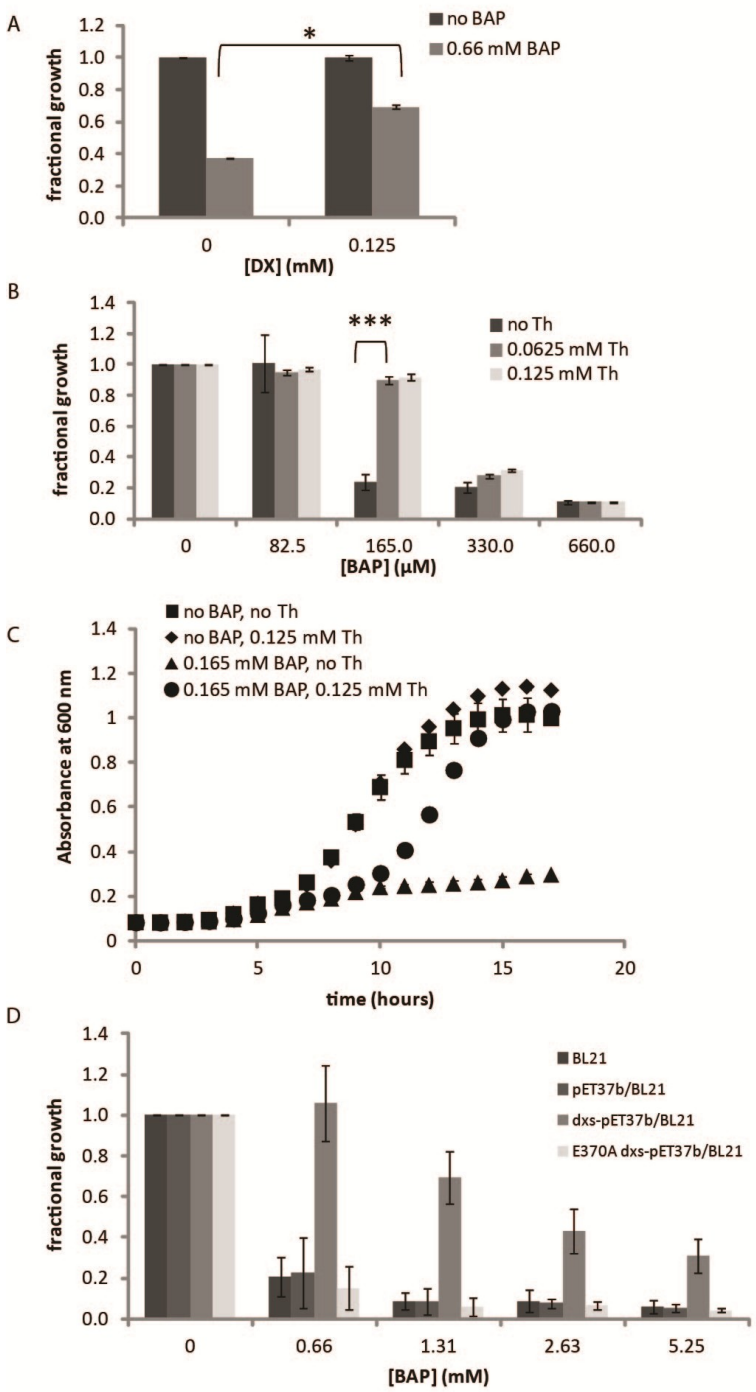

Figure 4-3. Butylacetylphosphonate (BAP) inhibition of *E. coli* MG1655 growth is rescued by 1-deoxy-D-xylulose (DX), thiamin (Th) and *E. coli* DXP synthase (Dxs) overexpression. **A**) Fractional growth at 12.5 hours in the presence and absence of BAP

and DX. Mean and standard error of four replicates are shown. $^{*}p = 0.022$ (unpaired *t* test comparing DX treated and untreated cultures at 0.66 mM BAP). **B**) Fractional growth at 16 hours in the presence and absence of BAP and thiamin. Mean and standard error of four replicates is shown. $^{***}p = 0.0000258$ (unpaired *t* test comparing thiamin treated and untreated cultures at 165 μM BAP). **C**) Growth curve over 16 hours, in the absence or presence of BAP and thiamin. **D**) Fractional growth at 16 hours determined for *E. coli* BL21 cells only, cells transformed with empty pET37b vector, vector expressing recombinant *E. coli* DXP synthase protein (*dxs*-pET37b), or vector expressing the catalytically inactive [9] E370A variant (E370A *dxs*-pET37b). Mean and standard error of four replicates is shown.

4.2.2. Metabolites that failed to rescue growth.

In addition to DX, a number of additional downstream metabolites were supplemented to cell culture media in attempt to rescue growth. A wide range of metabolite concentrations were examined at a variety of different BAP concentrations, under different assay conditions (**Table 4-2)**. None of these intermediates were able to rescue the growth inhibitory effects caused by BAP and there are several explanation for this. It is possible that under these experimental conditions there is inefficient turnover of the metabolite or insufficient uptake by the cell. Furthermore, studies involving rescue by metabolites in the isoprenoid pathway [5, 27-30] have been known to yield inconsistent results.

metabolite	range tested (mM)	media	pathway	structure
methylerythritol	0 - 0.5	M9, CAMHB	MEP/isoprenoid biosynthesis	
methylerythritol phosphate	0 - 2	M9, CAMHB		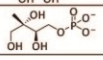
1-deoxy-D-xylulose phosphate	0 - 2	M9, CAMHB		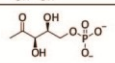
pyridoxine	0 - 0.5	M9	PLP/vitamin B_6 salvage	
pyridoxal	0 - 1	M9		
pyridoxamine	0 - 1	M9		
pyridoxal phosphate (PLP)	0 - 1	M9		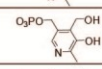
geranylgeraniol	0 - 0.25	M9	isoprenoid biosynthesis	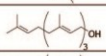
farnesol	0 - 0.5	M9	isoprenoid biosynthesis	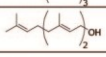
ubiquinone-8	0 - 0.25	M9	downstream product	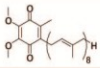

Table 4-2. Metabolites that failed to rescue growth of *E. coli* treated with butylacetylphosphonate (BAP).

4.2.3. Rescue by overexpression of E. coli DXP synthase.

Overexpression of DXP synthase should rescue growth of BAP-treated *E. coli* [31] if BAP acts by inhibition of DXP synthase. Indeed, increasing intracellular levels of DXP synthase results in rescue of bacterial growth (**Figure 4-3D**) compared to *E. coli* harboring empty vector (pET37b) or the catalytically inactive E370A mutant [9]. It should be noted that the T7 promoter, a *lac* promoter that is used in the pET plasmid systems, is known for background expression of recombinant protein. Under the conditions used here, the *E. coli dxs*-pET37b plasmid is capable of expressing DXP synthase in the absence of inducer, such as IPTG (**Figure 4-4**) and this basal expression is sufficient to rescue growth that is inhibited by BAP.

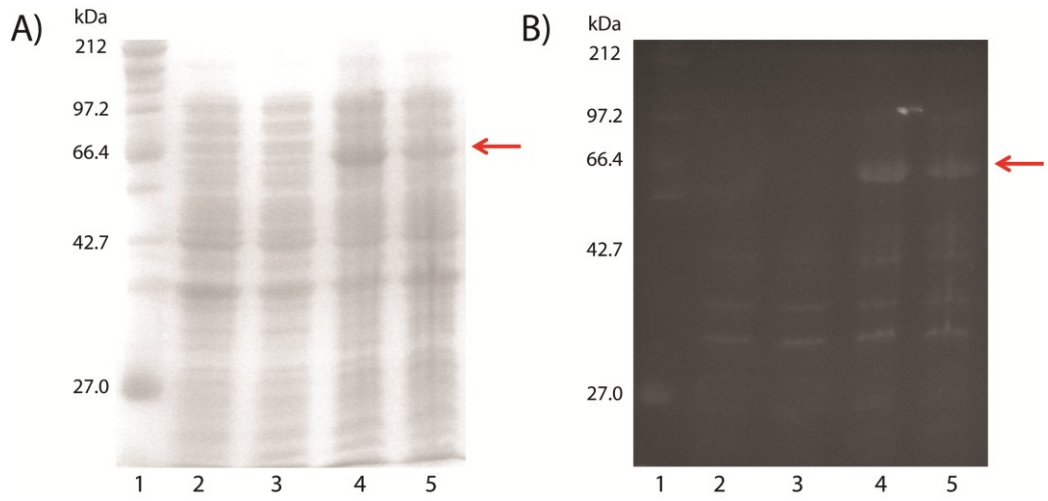

Figure 4-4. **DXP synthase overexpression confirmed by 10% SDS-PAGE**. Standardized inoculum was prepared as described in Material and Methods (see Antimicrobial susceptibility studies), and 5 mL cultures were analyzed after 16 hours in the absence of inducer. **1**) protein marker (2-212 kDa) **2**) *E. coli* BL21 cells only **3**) cells transformed with empty pET37b vector **4**) vector expressing recombinant *E. coli* DXP synthase protein (*dxs*-pET37b) **5**) vector expressing the catalytically inactive E370A [9] variant (E370A *dxs*-pET37b). **A**) Visualization by coomassie stain **B**) Incorporation of the histidine tag was verified using the *InVision His-tag* In-gel Stain (Invitrogen). The red arrow denotes recombinant E. coli DXP synthase.

To allow expression to be dependent upon inducer concentration, this background expression of DXP synthase would need to be silenced. In attempt to silence this background expression, and show a clear dose response relationship between increasing amounts of DXP synthase and rescue of growth inhibition caused by BAP, a number of

modifications to this method were explored. It has been reported that addition of glucose to cell culture media will silence basal expression, a phenomenon known as catabolite repression. In the presence of glucose, cyclic AMP levels decrease and this should result in very low levels of transcription from the *lac* promoter. However, addition of 0.5 – 5 % glucose to cell culture media did not eliminate basal expression of *E. coli* DXP synthase. Additionally, cells containing T7 lysozyme (BL21 (DE3) *pLysS, Promega)* were used in attempt to silence this basal expression of DXP synthase. T7 lysozyme is a natural inhibitor of T7 RNA polymerase and lowers the basal expression level of genes under the control of the T7 promoter, but does not interfere with the level of expression achieved following induction by IPTG. In this cell line, basal expression was silenced and expression of DXP synthase became strictly inducible. However, rescue of growth inhibition by BAP was not observed when DXP synthase expression was induced with IPTG.

It is possible that under the growth inhibition conditions used for these studies, introduction of IPTG and subsequent initiation of protein overproduction machinery in the cell is a cause of toxicity. As a control, BL21 cells alone, BL21 cells transformed with pET37b, and BL21 cells transformed with *dxs*-pET37b were treated with and without IPTG under the growth inhibition conditions. IPTG had no effect on BL21 cells alone, while there was a 70% decrease in optical density (OD_{600}) for cells transformed with the pET37b plasmid and exposed to IPTG. This toxicity was even more pronounced for the BL21 cells harboring *dxs*-pET37b; we observed an 89% drop in optical density. These results are in agreement with previous studies that show overexpression plasmids can be inherently toxic in the presence of inducer [(32)].

4.3. Growth inhibition is significantly enhanced when BAP is administered in antibiotic combinations.

The weak antimicrobial activity of BAP on its own prompted a study to determine the synergistic effects of BAP in combination with several established antibiotics. As a starting point, we investigated synergistic effects of BAP in combination with fosmidomycin, ampicillin, and tetracycline using the checkerboard method [20, 21]. Fosmidomycin potently inhibits the second enzyme in the MEP pathway, MEP synthase (IspC) [33-35]. Given the established synergy that can take place between agents that target the same metabolic pathway, and in particular the synergy observed between fosmidomycin and inhibitors of isoprenoid biosynthesis enzyme farnesylpyrophosphate synthase (FPPS) [36], we hypothesized that BAP could synergize with fosmidomycin. Likewise, fosmidomycin has been shown to synergize with cell wall biosynthesis inhibitors, including ampicillin, to inhibit bacterial cell growth [37]. Those early observations established precedence for drug synergisms between agents targeting isoprenoid biosynthesis and cell wall biosynthesis (which relies upon the prenylated Lipid II) and suggest synergy between BAP and cell wall biosynthesis inhibitors is also possible. Finally, we considered the possibility that synergy could exist between BAP and the bacterial translation inhibitor tetracycline, on the basis that geranylation of tRNA is proposed to play a role to modulate codon recognition during translation [38], thus drawing a connection between isoprenoid biosynthesis and protein synthesis.

organism	MIC BAP (μg/mL)	combination	FIC index
Escherichia coli MG1655	1000	BAP-fosmidomycin	0.25
		BAP-ampicillin	0.31
		BAP-tetracycline	0.53

Table 4-3. Antimicrobial activity of BAP against pathogenic bacteria and FIC index values for antibiotics in combination with BAP [19].

Here, the fractional inhibitory concentration (FIC) index was determined for BAP-fosmidomycin, BAP-ampicillin, and BAP-tetracycline combinations against *E. coli* MG1655 to predict drug synergisms [20, 21, 39]. As expected, the antimicrobial activity of BAP is enhanced in combination with fosmidomycin (FIC index = 0.25, **Table 4-3**) or ampicillin (FIC index = 0.31, **Table 4-3**). Analysis by isobolograms suggests pronounced synergy in the BAP-fosmidomycin combination against *E. coli* MG1655 (**Figure 4-5**) [19, 20, 38]. However, examination of the BAP-ampicillin combination by isobologram indicates synergy is less pronounced, suggesting this combination may display additive effects. The FIC index for BAP in combination with tetracycline is 0.53, indicating an additive relationship (**Table 4-3**).

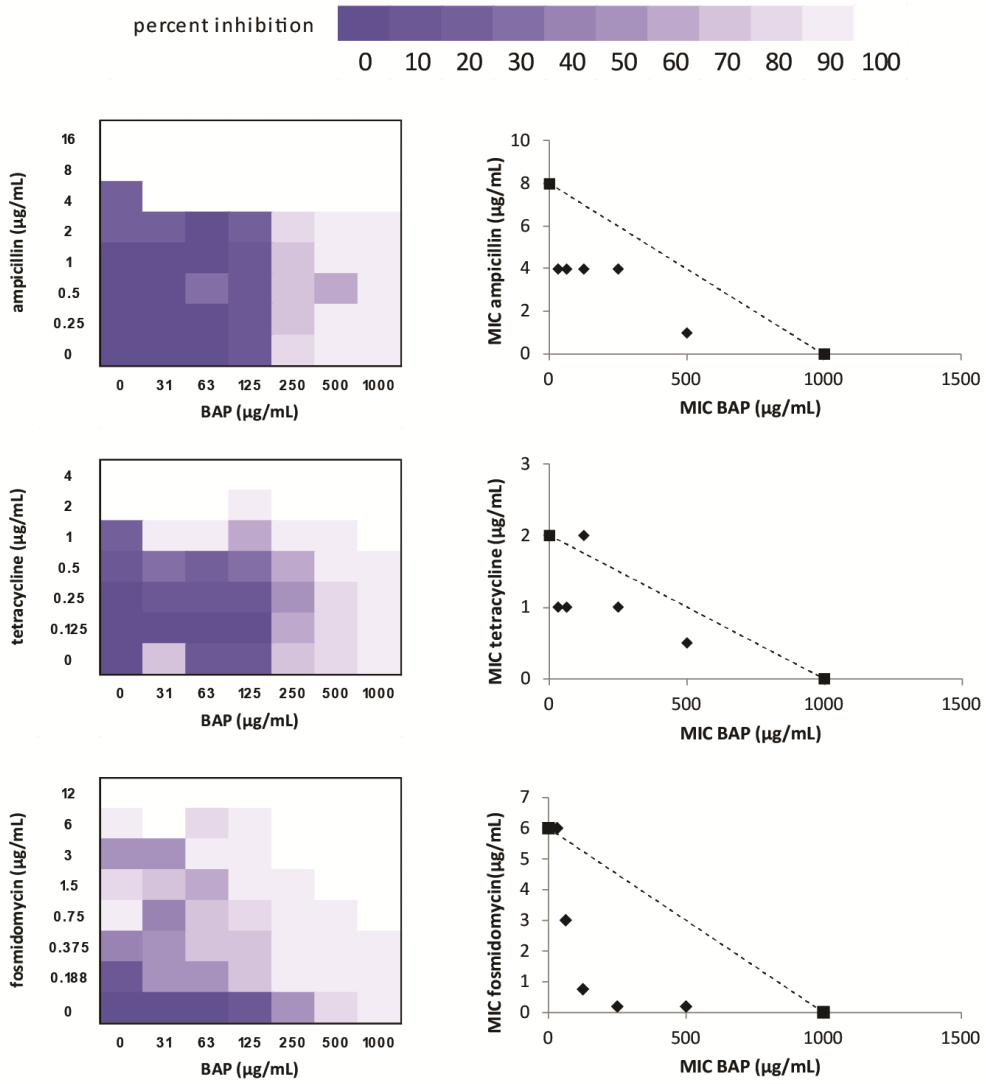

Figure 4-5. Checkerboard antibiotic combination studies [19]**. A**) Heat plots showing drug synergism for BAP-fosmidomycin and BAP-ampicillin, and additivity for BAP-tetracycline. **B**) Isobologram analysis suggests synergy in the BAP-fosmidomycin combinations against *E. coli* MG1655.

Conclusions

As the isoprenoid biosynthetic pathway is absent in mammals, but essential in many human pathogens, each of the seven enzymes in the pathway represents a prospective antibiotic target. Selective inhibition of DXP synthase could reduce flux through multiple metabolic pathways and is a potential advantage of targeting this first step of the MEP pathway. Here we have evaluated the inhibition and antimicrobial activity of butylacetylphosphonate (BAP), a DXP synthase inhibitor developed in our lab to selectively target the uniquely large active site of this enzyme [10].

BAP appears to exert antimicrobial activity against *E. coli* MG1655 through a mechanism that involves DXP synthase inhibition, as suggested by the observed rescue of its inhibitory effects in the presence of DX or thiamin, or under conditions of DXP synthase overexpression. Partial rescue is observed using nonphosphorylated 1-deoxy-D-xylulose (DX), implying DXP synthase as a target. More pronounced rescue is observed in the presence of thiamin or DXP synthase overexpression. In addition to rescuing the thiamin pathway and other thiamin-dependent cellular processes under these conditions, it is possible that ThDP generated under thiamin rescue conditions regenerates active DX synthase by competing with butylphosphonolactyl-thiamin disphosphate (butyl PLThDP) at the ThDP binding site. Alternatively, increasing intracellular ThDP levels could activate an apo-DXP synthase pool that presumably arises under conditions of DXP synthase inhibition and subsequent cofactor depletion. Not surprisingly, overexpression of active DXP synthase in *E. coli* also results in pronounced rescue of BAP growth inhibitory activity. The observation that rescue is less pronounced under all of these

conditions with increasing BAP is consistent with DXP synthase inhibition coupled with other nonspecific antimicrobial effects of BAP at high concentrations.

The reason for the observed weak antimicrobial activity of BAP on its own against the pathogens tested here is not entirely clear, although poor cell permeability is conceivable. Recent studies by Circello, et al. [40] reveal the natural product dehydrophos as a prodrug of the structurally related methyl acetylphosphonates (MAP), a mimic of pyruvate and known inhibitor of the ThDP-dependent enzymes that catalyze decarboxylation of pyruvate (see 1.9 for additional information) [14-18]. By extension, the acetylphosphonate scaffold of BAP may hamper efficient uptake in the absence of such a delivery mechanism. It is intriguing to contemplate a similar delivery strategy for enhancing cellular uptake of BAP and analogs, although it is also possible that incorporation of more hydrophobic substituents may enhance permeability.

Despite the weak antimicrobial effects of BAP on its own, a BAP-fosmidomycin combination is synergistic against *E. coli* MG1655. The synergistic BAP-fosmidomycin combination was anticipated, given that drug synergism in the MEP pathway has been previously reported with FPPS inhibitors and fosmidomycin [36]. Our previous work suggesting MEP activates and sustains IspF activity in a possible feed-forward regulatory mechanism in bacterial isoprenoid biosynthesis [41] could provide additional basis for this synergistic combination. It is conceivable that inhibition of upstream enzymes DXP synthase and IspC by BAP and fosmidomycin, respectively, not only reduces flux through the pathway at these points, but also effectively expedites the loss of IspF activity by rapidly depleting MEP levels. There is established precedence for drug synergisms between inhibitors of isoprenoid biosynthesis and cell wall biosynthesis [37],

given the requirement for isoprenoid precursors in Lipid II biosynthesis [31], and so the enhancement in activity observed with the BAP-ampicillin combination in this study was also anticipated. It is also plausible that ampicillin compromises cell wall integrity to permit more efficient uptake of BAP. These findings are significant given the necessity of combination therapies to prevent emergence of antimicrobial resistance [42]. Although inhibition of DXP synthase ought to simultaneously reduce flux through multiple essential pathways, the emergence of mechanisms to circumvent such an intervention in bacteria is inevitable [42-44].

This work highlights unnatural bisubstrate analogs as selective inhibitors of this unique ThDP-dependent enzyme and promising antimicrobial agents as components of synergistic antimicrobial combinations. While the acetylphosphonates were developed over 30 years ago as ketoacid mimics, and are powerful tools to study ThDP-dependent enzymes [14-18], in the case of dehydrophos, it is clear that Nature has already conceived of such an antimicrobial strategy to inhibit essential ThDP-dependent processes. Development of acetylphosphonates to increase selectivity, potency, and permeability is perhaps a new chapter in medicinal chemistry on natural product scaffolds.

Experimental Section

General Methods. Primers were purchased from Integrated DNA Technologies. *E. coli* wild-type DXP synthase and the variant E370A DXP synthase were purified as described previously [7, 45]. *E. coli* MEP synthase (IspC) was also purified as reported previously [45]. All microbial manipulation of pathogenic bacteria was conducted in a certified biosafety level 2 (BSL-2) laboratory with all associated safety protocols. *S. enterica* serovar Typhimurium LT2, *B. anthracis* Sterne, and all clinically isolated strains are maintained from an in-house bacterial strain library (NAU).

Antimicrobial susceptibility studies. Using aseptic technique, three to five isolated colonies were picked from a plate containing ATCC MG1655 *E coli* and *Bacillus subtilis* 168 were inoculated into 5 mL of cation adjusted Mueller Hinton Broth (CAMHB, Sigma) at 37°C. Incubation was continued until turbidity matched McFarland (MF) turbidity standard 0.5 (~OD_{600} = 0.10) [20, 21]. Colony counts were checked after 16 hours at 37°C for consistency between experiments. The standardized inoculums (MF = 0.5) contained approximately 1–2 x 10^8 CFU/mL. The final concentration in a well (or culture tube) was 5 x 10^5 CFU/mL [20, 21]. For these studies, the standardized inoculum (MF = 0.5) was diluted 1:100 in CAMHB and 0.25 mL of this adjusted inoculum was added to each tube containing 0.25 mL antimicrobial agent(s) for a final volume of 0.5 mL. These tubes were then incubated at 37°C for 16–18 hours, with shaking. Fractional growth was determined relative to the no drug control, and averaged values were used. The minimum inhibitory concentration (MIC) was determined to be the concentration at which growth

was ≤ 15% of the no drug growth controls (determined by OD_{600}) [20, 21, 39]. The concentration of BAP evaluated for these studies ranged from 0 - 5 mM (0 - 1 000 μg/mL). ATCC 70084 *Mycobacterium smegmatis* was evaluated in a similar manner outlined above, but using enriched Middlebrook 7H9 broth. A 24 hour culture (~ OD_{600} = 0.4) was diluted to OD_{600} = 0.1 and subcultured 1:100 for 1 x 10^6 colony forming units. The concentration of BAP was varied 0−10 mM (0 - 2 000 μg/mL). The *E. coli* glycerol 3-phosphate transporter knockout strain (JW2234-2) was evaluated along with the parent strain (BW25113) using the above method (Yale, Coli Genetic Stock Center, CGSC). Susceptibility studies were performed for *S. enterica* serovar Typhimurium LT2, *B. anthracis* Sterne, and all clinical isolates essentially as outlined above with the exception that the assays were conducted in 96-well plates with final volume of 0.2 mL, and concentrations of BAP ranged from 0 - 20 mM (0 – 4 000 μg/mL). All antimicrobial susceptibility assays were performed in triplicate.

***E. coli* growth rescue studies.** For the growth rescue experiments, 96-well plates were used with a final culture volume of 0.2 mL. The standardized inoculum (MF = 0.5) was prepared in the same manner as previously stated. These plates were then incubated in a SpectramaxPlus384 plate reader at 37°C for 16 hours, with shaking at 220 rpm every 30 minutes for 15 minutes. Less than 10% loss in volume was measured during this time. Fractional growth was then determined relative to the no BAP control in each case, and averaged fractional growth was plotted with standard experimental error as a function of BAP concentration. For the 1-deoxy-D-xylulose (DX) rescue experiments, a range of 0 - 1.0 mM DX was evaluated in the presence of 0 - 5.0 mM BAP in CAMHB media. For

the thiamin rescue experiments, a range of 0 - 1.0 mM thiamin was evaluated in the presence of 0 - 0.66 mM BAP in M9 minimal media (no thiamin). DX and thiamin rescue experiments were performed in quadruplicate. DXP synthase overexpression rescue experiments were carried out in LB broth, and the following cell types were treated with 0-5.0 mM BAP: BL21 (no vector), pET37b-BL21, wt *E. coli dxs*-pET37b/BL21, and E370A *E. coli dxs*-pET37b/BL21. Experiments were performed in triplicate.

DXP synthase overexpression was confirmed by 10% SDS-PAGE, and incorporation of the octa-histidine tag was verified using the *InVision His-tag* In-gel Stain (Invitrogen) (**Figure S2**). Site directed mutagenesis of the E370A residue was carried out as previously reported [7] using the QuikChange sitedirected mutagenesis kit (Stratagene), and the following primers (Integrated DNA technologies): 5' CGA CGT GGC AAT TGC CGC GCA ACA GCG GGT GAC CTT TGC 3' and 5' GCA AAG GTC ACC GCG TGT TGC GCG GCA ATT GCC ACG TCG 3'.

Checkerboard antibiotic combination studies. For the checkerboard antibiotic combination studies in *E. coli*, culture tubes were used with a final culture volume of 0.5 mL, prepared as described above. The concentration of ampicillin evaluated for these studies ranged from 0, 0.13, up to 8 μg/mL, tetracycline ranged from 0, 0.125, up to 4 μg/mL, and fosmidomycin ranged from 0, 0.19, up to 6 μg/mL.

For each antibiotic combination, the fractional inhibitory concentration (FIC) index was determined to predict drug synergism [20, 21, 39].

$$\frac{(BAP)}{(MIC_{BAP})} + \frac{(X)}{(MIC_X)} = FIC_{BAP} + FIC_X = FIC\ index\ (FICI) \qquad \text{Equation 1}$$

The FIC index was calculated using equation 1 [20, 21, 39]. MIC_{BAP} and MIC_X are the lowest concentrations of BAP or drug X (X = ampicillin, fosmidomycin, or tetracycline) showing ≤ 15% growth. The FIC_{BAP} was calculated as the [BAP in the presence of drug X] for a well showing ≤ 15% growth, divided by MIC_{BAP}. FIC_X was calculated as the [drug X in the presence of BAP] in the same well, divided by MIC_X. The FIC index is the sum of FIC_{BAP} and FIC_X. For each combination the FICI values were used to indicate drug synergism ($x < 0.5$), additivity ($0.5 < x < 1.0$), indifference ($1.0 < x < 2.0$), or antagonism ($x > 2$). Fractional growth was determined relative to the no drug growth control and average values were used. The BAP-ampicillin and BAP-tetracycline checkerboard assays were performed in duplicate. The BAP-fosmidomycin checkerboard assay was performed in quadruplicate.

References

1. Sprenger, G. A., *et al*. Identification of a thiamin-dependent synthase in *Escherichia coli* required for the formation of the 1-deoxy-D-xylulose 5-phosphate precursor to isoprenoids, thiamin, and pyridoxol. *Proc. Natl. Acad. Sci. U. S. A*. **94**, 12857 (1997).

2. Mukherjee, T., Hanes, J., Tews, I., Ealick, S. E. & Begley, T. P. Pyridoxal phosphate: biosynthesis and catabolism. *Biochimica et Biophysica Acta*. **1814**, 1585–1596 (2011).

3. Hill, R. E., *et al*. The biogenetic anatomy of vitamin B6. A 13C NMR investigation of the biosynthesis of pyridoxolin in *E. coli*. *J. Biol. Chem*. **271**, 30426 (1996).

4. Mao, J., *et al*. Structure–activity relationships of compounds targeting *Mycobacterium tuberculosis* 1-deoxy-D-xylulose 5-phosphate synthase. *Bioorg. Med. Chem. Lett*. **18**, 5320-5323 (2008).

5. Matsue, Y., *et al*. The herbicide ketoclomazone inhibits 1-deoxy-D-xylulose 5-phosphate synthase in the 2-*C*-methyl-D-erythritol 4-phosphate pathway and shows antibacterial activity against *Haemophilus influenzae*. *J. Antibiot*. **63**, 583-8 (2010).

6. Eubanks, L. M. and Poulter, C. D. *Rhodobacter capsulatus* 1-deoxy-D-xylulose 5-phosphate synthase: steady-state kinetics and substrate binding. *Biochemistry*. **42**, 1140-9 (2003).

7. Brammer, L. A., Smith, J. M. & Meyers, C. F. 1-deoxy-D-xylulose 5-phosphate synthase: a novel random sequential mechanism in thiamine diphosphate-dependent enzymology. *J. Biol. Chem*. **42**, 36522-31 (2011).

8. Morris, F., Vierling, R., Boucher, L., Bosch, J. & Freel Meyers, C. L. DXP synthase-catalyzed C-N bond formation: nitroso substrate specificity studies guide selective inhibitor design. *ChemBioChem* **14,** 1309-1315 (2013).

9. Xiang, S., Usunow, G., Lange, G., Busch, M. & Tong, L. Crystal structure of 1-deoxy-D-xylulose 5-phosphate synthase, a crucial enzyme for isoprenoids biosynthesis. *J. Biol Chem*. **282**, 2676-2682 (2007).

10. Smith, J. M., Vierling, R. J. & Meyers, C. F. Selective inhibition of E. coli 1-deoxy-D-xylulose-5-phosphate synthase by acetylphosphonates. *Med. Chem. Commun.* **3,** 65-67 (2012).

11. O'Brien, T. A., Kluger, R., Pike, D. C. & Gennis, R. B. Phosphonate analogues of pyruvate. Probes of substrate binding to pyruvate oxidase and other thiamin pyrophosphate-dependent decarboxylases. *Biochimica et Biophysica Acta (BBA) Enzymology*. **613**, 10-17 (1980).

12. Gish, G., Smyth, T. & Kluger, R. Thiamin diphosphate catalysis. Mechanistic divergence as a probe of substrate activation of pyruvate decarboxylase. *J. Am. Chem. Soc.* **110**, :6230-4 (1988).

13. Kluger, R. and Pike, D. C. Active site generated analogs of reactive intermediates in enzymic reactions. Potent inhibition of pyruvate dehydrogenase by a phosphonate analog of pyruvate. *J. Am. Chem. Soc.* **99**, 504-6 (1977).

14. Arjunan, P., *et al.* A thiamin-bound, pre-decarboxylation reaction intermediate analogue in the pyruvate dehydrogenase E1 subunit induces large scale disorder-to-order transformations in the enzyme and reveals novel structural features in the covalently bound adduct. *J. Biol. Chem.* **281**, 15296 (2006).

15. Kale, S., Arjunan, P., Furey, W. & Jordan, F. A Dynamic Loop at the Active Center of the Escherichia coli Pyruvate Dehydrogenase Complex E1 Component Modulates Substrate Utilization and Chemical Communication with the E2 Component. *J. Biol. Chem*. **282**, 28106-28116 (2007).

16. Nemeria, N. S., Korotchkina, L. G., Chakraborty, S., Patel, M. S. & Jordan, F. Acetylphosphinate is the most potent mechanism-based substrate-like inhibitor of both

the human and *Escherichia coli* pyruvate dehydrogenase components of the pyruvate dehydrogenase complex. *Bioorg. Chem*. **34**, 362-379 (2006).

17. Nemeria, N., *et al.* The 1',4'-iminopyrimidine tautomer of thiamin diphosphate is poised for catalysis in asymmetric active centers on enzymes. *Proc. Natl. Acad. Sci. U. S. A*. **104**, 78-82 (2007).

18. Bearne, S. L. and Kluger, R. Phosphoenol acetylphosphonates: Substrate analogues as inhibitors of phosphoenolpyruvate enzymes. *Bioorg. Chem*. **20**, 135-147 (1992).

19. Smith, J. M., *et al*. Targeting DXP synthase in human pathogens: enzyme inhibition and antimicrobial activity of butylacetylphosphonate. *J. Antibiot*. 2013. Advance online publication. doi: 10.1038/ja.2013.105.

20. Pilllai, S. K., Moellering, R. C. & Eliopoulos, G. M. in Antimicrobial combinations. *Antibiotics in Laboratory Medicine* (ed V. Lorian) (Lippincott Williams & Wilkins 2005).

21. Moody, J. in Synergism testing: broth microdilution checkerboard and broth macrodilution methods. *In* H. D. Isenberg, Clinical microbiology procedures handbook, vol. 2. American Society for Microbiology, Washington, DC. p. 5.12.1-5.12.23., (2004).

22. Venkateswaran, P. S. and Wu, H. C. Isolation and characterization of a phosphonomycin-resistant mutant of E*scherichia coli* K-12. *J. Bacteriol*. **110**, 935-944 (1972).

23. McKenney, E. S., *et al*. Lipophilic prodrugs of FR900098 are antimicrobial against *Francisella novicida in vivo* and *in vitro* and show GlpT independent efficacy. *PLoS One* **10,** 38167 (2012).

24. Sakamoto, Y., Furukawa, S., Ogihara, H. & Yamasaki, M. Fosmidomycin resistance in adenylate cyclase deficient (*cya*) mutants of *Escherichia coli*. *Biosci Biotechnol Biochem.* **67,** 2030-3 (2003).

25. Wungsintaweekul, J., *et al*. Phosphorylation of 1-deoxy-D-xylulose by D-xylulokinase of *Escherichia coli*. *Eur J Biochem*. **268**, 310-16 (2001).

26. Giner, J., Jaun, B. & Arigoni, D. Biosynthesis of isoprenoids in *Escherichia coli*: The fate of the 3-H and 4-H atoms of 1-deoxy-D-xylulose. *Chem.Commun.* 1857-1858 (1998).

27. Zhang, B., *et al.* A second target of the antimalarial and antibacterial agent fosmidomycin revealed by cellular metabolic profiling. *Biochemistry*. **50**, 3570-7 (2011).

28. Yeh, E. and DeRisi, J. L. Chemical rescue of malaria parasites lacking an apicoplast defines organelle function in blood-stage Plasmodium falciparum. *PLoS Biol*. **9** (2011).

29. Kang, S., Kim, E. S. & Moon, A. Simvastatin and lovastatin inhibit breast cell invasion induced by H-Ras. *Oncol Rep*. **21**, 1317-22 (2009).

30. Blanc, M., *et al.* Host defense against viral infection involves interferon mediated down-regulation of sterol biosynthesis. *PLoS Biol*. **9** (2011).

31. Campbell, T. L. and Brown, E. D. Characterization of the depletion of 2-C-methyl-D-erythritol-2,4-cyclodiphosphate synthase in *Escherichia coli* and *Bacillus subtilis*. *J. Bacteriol*. **184**, 5609-5618 (2002).

32. Miroux, B. and Walker, J. E. Over-production of proteins in *Escherichia coli*: mutant hosts that allow synthesis of some membrane proteins and globular proteins at high levels. *J Mol Biol*. **260**, 289-98 (1996).

33. Okuhara, M., *et al*. Studies on new phosphonic acid antibiotics. *J. Antibiot*. **33**, 13 (1980).

34. Kuroda, Y., *et al.* Studies on new phosphonic acid antibiotics: 4. Structure determination of FR-33289, FR-31564 and FR-32863. *J. Antibiot.* **33,** 29-35 (1980).

35. Kuzuyama, T., Shimizu, T., Takahashi, S. & Seto, H. Fosmidomycin, a specific inhibitor of 1-deoxy-D-xylulose 5-phosphate reductoisomerase in the nonmevalonate pathway for terpenoid biosynthesis. *Tetrahedron Lett.* **39,** 7913-7916 (1998).

36. Leon, A., *et al*. Isoprenoid biosynthesis as a drug target: bisphosphonate inhibition of *Escherichia coli* K12 growth and synergistic effects of fosmidomycin. *J. Med. Chem.* **25,** 7331-41 (2006).

37. Neu, H. and Kamimura, T. Synergy of fosmidomycin (FR-31564) and otherantimicrobial agents. *Antimicrob. Agents Chemother.* **22,** 560-563 (1982).

38. Dumelin, C., Chen, Y., Leconte, A., Chen, Y. & Liu, D. Discovery and biological characterization of geranylated RNA in bacteria. *Nat Chem Biol.* **11,** 913-9 (2012).39.Kalan, L. and Wright, G. D. Antibiotic adjuvants: multicomponent anti-infective strategies. Expert Reviews in Molecular Medicine13,n/a-e5 (2011)

40. Circello, B., Miller, C., Lee, J., van der Donk, W. & Metcalf, W. The antibioticdehydrophos is converted to a toxic pyruvate analog by peptide bond cleavage in *Salmonella enterica*. *Antimicrob Agents Chemother*. **55**, 3357 (2011).

41. Bitok, J. and Meyers, C. F. 2-C-methyl-D-erythritol 4-phosphate enhances and sustains cyclodiphosphate synthase IspF activity. *ACS Chem. Biol*. **7**, 1702 (2012).

42. Walsh, C. T. and Wencewicz, T. A. Prospects for new antibiotics: a molecule-centered perspective. *J. Antibiot.* In press. doi: 10.1038/ja.2013.49 (2013).

43. Perez-Gil, J., *et al*. Mutations in *Escherichia coli aceE* and *ribB* genes allow survival of strains defective in the first step of the isoprenoid biosynthesis pathway. *PLoS ONE*. 7, 43775 (2012).

44. Erb, T., *et al*. A RubisCO-like protein links SAM metabolism with isoprenoid biosynthesis. *Nat. Chem. Biol*. **8**, 926 (2012).

45. Brammer, L. A. and Meyers, C. F. Revealing substrate promiscuity of 1-deoxy-d-xylulose 5-phosphate synthase. *Org Lett*. **11**, 4748-51 (2009).

Chapter 5: Targeting DXP reductoisomerase (IspC) using fosmidomycin analogs.

Introduction

DXP reductoisomerase (IspC) is the second enzyme in the MEP pathway, and catalyzes the first committed step in non-mammalian isoprenoid biosynthesis to form 2C-methyl- D -erythritol 4-phosphate (MEP). IspC catalyzes the reduction and rearrangement of DXP to generate MEP in a magnesium and NAPDH dependent manner [(1)]. The first step of the reaction gives the branched aldose derivative, 2C-methyl- D -erythrose 4-phosphate, which is subsequently reduced to 2C-methyl-D-erythritol 4-phosphate (**Figure 5-1)**.

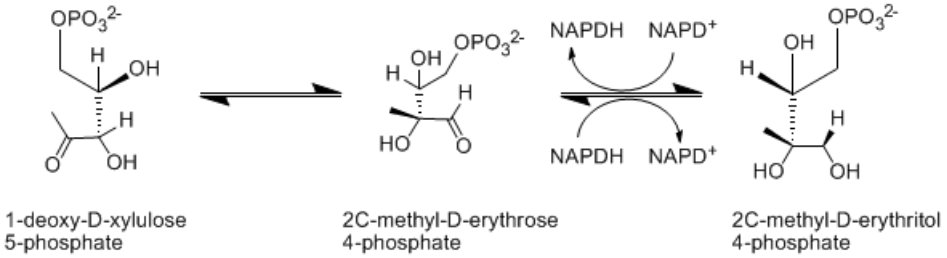

Figure 5-1. Reaction catalyzed by DXP reductoisomerase (IspC).

Fosmidomycin (**1**) is a potent inhibitor of IspC (K_m^{DXP} = 115 μM; $K_i^{fosmidomycin}$ = 57 nM for *Synechocystis* sp. PCC6803 IspC) [(2, 3)] and the most potent inhibitor of isoprenoid biosynthesis in human pathogens utilizing the MEP pathway. Currently, fosmidomycin is in phase 3 clinical trials for the treatment of uncomplicated malaria in combination with clindamycin (see section 1.4) [(4, 5)]. Crystallography studies report that fosmidomycin binds in a similar manner to DXP; the binding of DXP or fosmidomycin

induces a conformation change that closes a flexible loop over the active site [6]. Three regions in the active site have been identified that accommodate the hydroxamate, carbon linker, and phosphonate moiety of fosmidomycin. As discussed in 1.13, several structure activity relationship (SAR) studies have been carried out around this inhibitor (**Figure 1-13**) [2, 7-11] in efforts to address the poor pharmacokinetic properties of this phosphonyl-bearing inhibitor. Analogs of fosmidomycin include fosfoxacin and its *N*-acetyl congener (FR900098). Although these compounds are potent *in vitro* inhibitors of purified IspC, their potency against bacterial pathogens is limited, presumably due to poor cellular uptake [12].

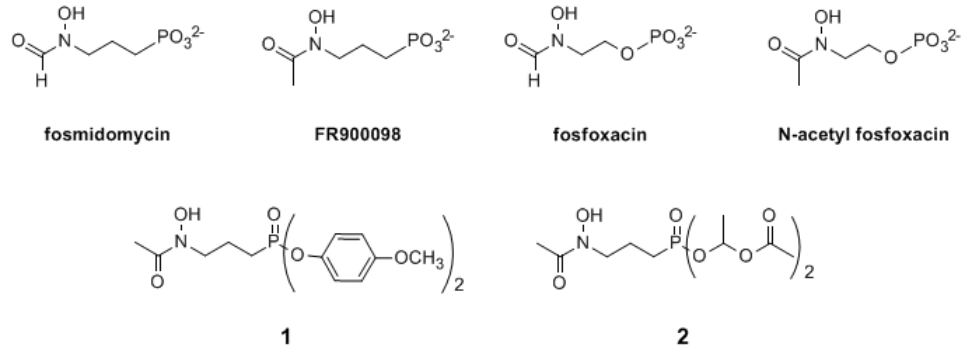

Figure 5-2. Diester prodrugs mask the phosphonate moiety of FR90098 [9, 10].

In order to improve the efficacy and bioavailability of fosmidomycin and its analogs, new tactics are required. Several strategies have been pursued to address pharmacokinetic issues. Alpha-substituted lipophilic analogs increase permeability, but these compounds are less potent inhibitors of purified IspC [11]. In a different approach, researchers sought to improve pharmacokinetic properties by masking the phosphonate moiety of FR900098 as a phosphodiarylester [10] or as a alkoxycarbonyloxyethyl ester [9].

These compounds were expected to be cell permeable and activated intracellularly via enzyme-catalyzed hydrolysis by non-specific plasma phosphatases or esterases, respectively [9, 10, 13]. Although one diarylester prodrug (**Figure 5-2, compound 1**) demonstrated efficacy in mice infected with the rodent malaria parasite *Plasmodium vinckei*, concerns were raised about toxicity of the phenol derivative released through P-O cleavage of this prodrug class. The alkoxycarbonyloxyethyl ester prodrugs **(Figure 5-2, compound 2)** displayed two-fold higher activity in a parasitic mouse model compared to FR900098, and a higher plasma concentration was measured after oral administration. Yet there are concerns regarding premature prodrug activation outside of the cell which creates membrane impermeable, toxic precursors. Another drawback of these masked FR900098 analogs includes the inefficient chemistry of activation. Two enzymatic activation events catalyzed by phosphatases or esterases are required to unmask these analogs, and the second of these events is often especially slow.

In this chapter, we present two approaches to combat the pharmacokinetic issues associated with fosmidomycin and fosfoxacin and their *N*-acetyl derivatives. The first approach takes advantage of the "two part" substrate hypothesis which has been previously reported [14, 15]. Taking triosephosphate isomerase (TIM) an example, it was proposed that the intrinsic binding energy of a phosphodianion group of the substrate is what drives the closing of a mobile loop and results in a protein conformational change [15]. More recently, this strategy has been used to investigate the role of the nonreacting phosphoryl group in the IspC-catalyzed formation of MEP from DXP [16]. The reaction of the truncated 1-deoxy-L-erythrulose (DE) substrate was monitored in the presence and absence of phosphite dianion. Kholodar *et al* [16] found that the conformation change

takes place upon substrate binding to IspC, and is driven by binding of the dianionic phosphoryl group. Likewise, binding of fosmidomycin induces a phosphonyl-dependent conformational change during inhibition. We have tested the hypothesis that membrane permeable, truncated fosmidomycin analogs lacking the dianionic phosphonyl group can be designed to inhibit IspC in a "two part" inhibitor mechanism. These analogs can be used in combination with intracellular anions that will facilitate analog binding and conformational changes (**Figure 5-3A**). The truncated *N*-hydroxyethyl fosfoxacin analog was designed to either act in a "two part" inhibitor mechanisms or undergo intracellular activation via phosphorylation to generate *N*-acetyl fosfoxacin (**Figure 5-3B**).

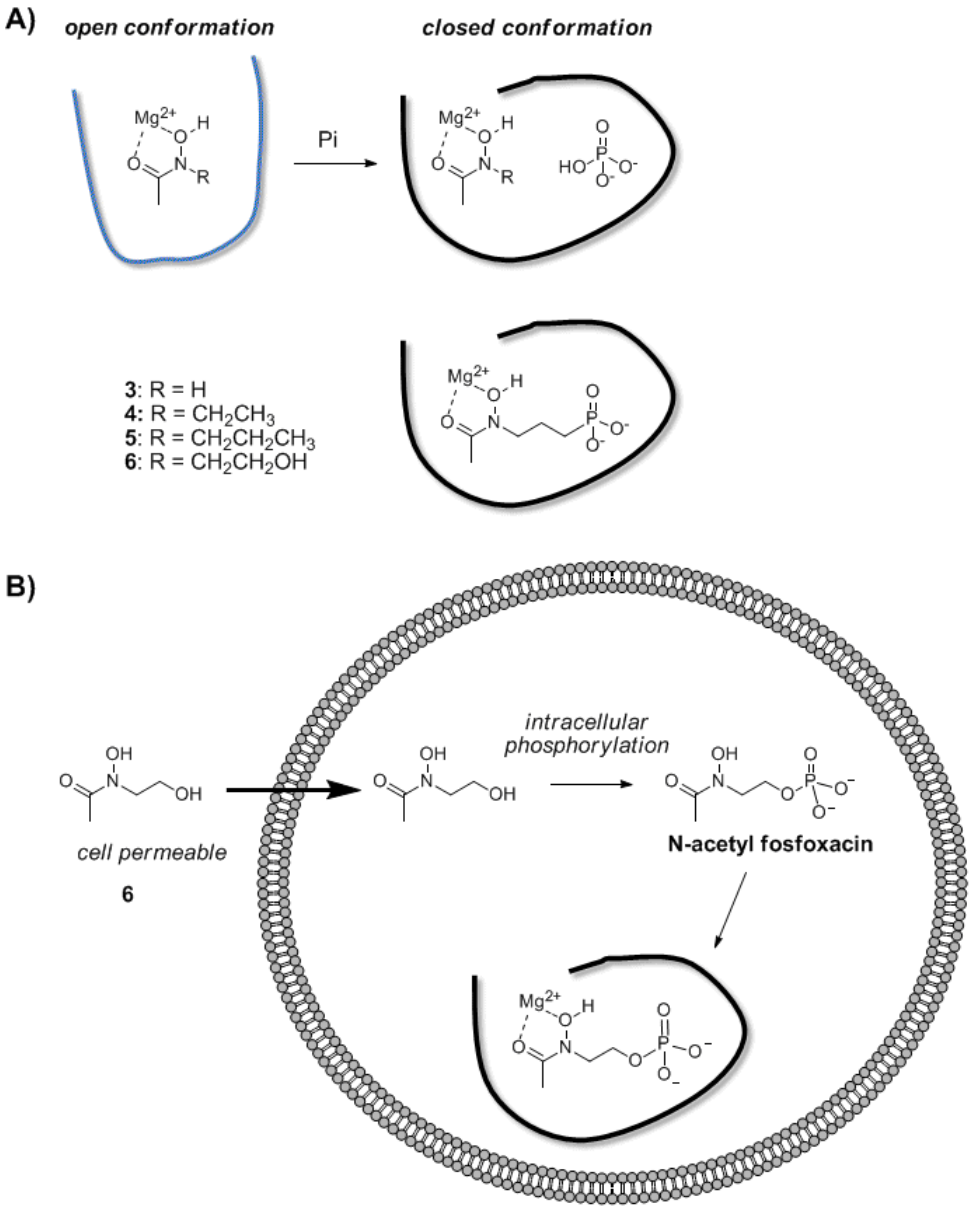

Figure 5-3. Truncated FR900098/fosfoxacin analogs target IspC. A) Binding of fosmidomycin induces a conformation change to close a flexible loop over the active site of IspC ("closed conformation") [6]. Binding of truncated analogs (**3-6**) in combination with intracellular anions is proposed to similarly induce the closure of the active site of IspC leading to inhibition of the enzyme. P_i : inorganic phosphate. **B**) Activation by intracellular phosphorylation of compound **6**.

In a distinct approach, we sought to mask the charges of the phosphonyl group by developing a phosphonamidate-based prodrug (**7**) requiring a single, efficient bioactivation event, rather than two bioactivation events. The prodrug is designed to incorporate a bioreducible delivery group susceptible to activation by intracellular reductases, and does not require activation by esterases or phosphatases which are also extracellular. After cellular uptake, bioreduction will result in the formation of the corresponding electron rich hydroxylamine, which rapidly undergoes elimination to release a phosphonamidate anion (**Figure 5-4**). Similar amidate-based prodrug strategies have been successfully implemented in previous studies for the intracellular delivery of nucleotide monophosphates [17-20] and highly polar, polyanionic bisphosphonates [21].

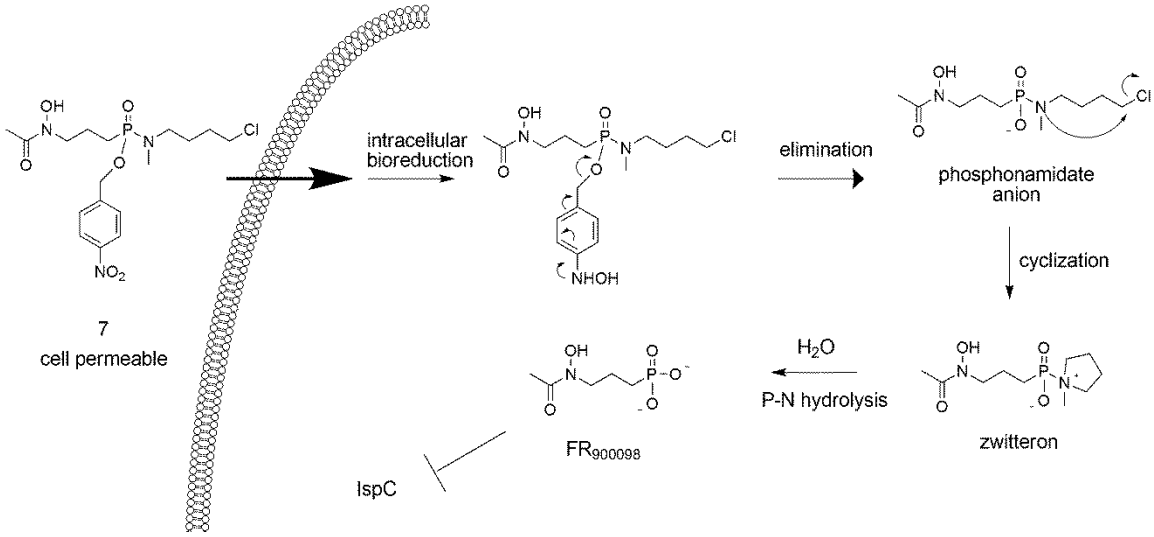

Figured 5-4. Proposed prodrug activation.

Results

5.1. Biochemical evaluation of truncated FR900098 analogs.

Prior to evaluating the inhibitory activity of FR900098 analogs, *E. coli* IspC was kinetically characterized with respect to its natural substrates (K_m ^{DXP} = 150 ± 9 µM, K_m ^{NADPH} = 4 ± 0.5 µM, k_{cat} = 9.3 ± 2.7 min^{-1}, **Figure 5-5**). The kinetic parameters for *E. coli* IspC with respect to NAPDH and DXP are comparable to those previously reported [2].

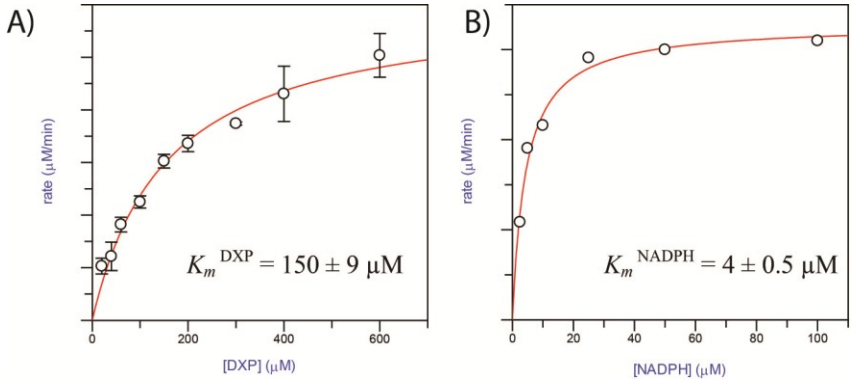

Figure 5-5. Kinetic characterization of *E. coli* IspC. **A**) DXP concentration was varied at 0.1 mM fixed NAPDH. **B**) NADPH concentration was varied at 0.5 mM fixed DXP.

As a starting point to test the "two part" inhibitor hypothesis, IspC activity was then examined in the presence of a variety of common intracellular anions that could potentially bind in the active site phosphonyl binding pocket and presumably act together with truncated FR900098 or *N*-acetyl fosfoxacin analogs to inhibit IspC. Anions selected for these studies included: chloride (intracellular concentration = 5 - 15 mM), bicarbonate (intracellular concentration = 12 mM), inorganic phosphate and diphosphate (intracellular concentration ~ 0.8 - 100 mM, although subject to debate due to difficulty measuring) [22, 23]. Although bicarbonate had no effect on IspC activity, inorganic phosphate and

diphosphate inhibit the enzyme (**Figure 5-6**). This was expected, as there is a well-defined phosphoryl binding pocket within the active site of IspC [6]. The enzyme was also inhibited 46% in the presence of 10 mM chloride.

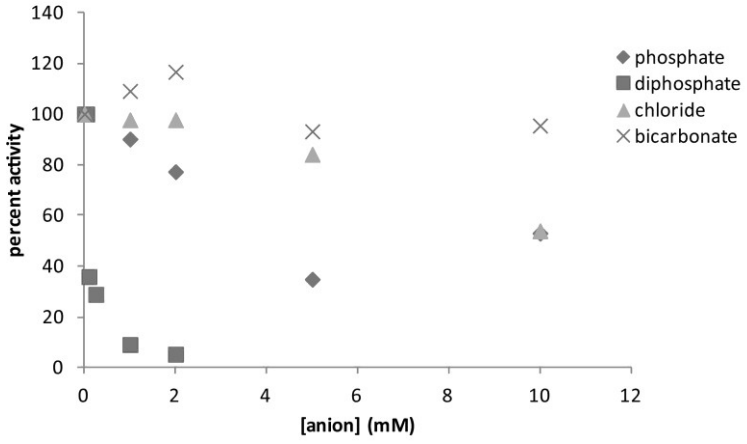

Figure 5-6. Activity of IspC in the presence of phosphate, chloride, bicarbonate, and diphosphate.

Truncated analogs (**3-6**, synthesized by Dr. David Meyers, Synthetic Core Facility) were then evaluated as inhibitors of IspC, and showed no inhibitory activity up to 10 mM. Following these experiments, truncated analogs (**3-6**) were then evaluated in combination with the previously tested anions. The inhibitory activity of compounds **4 - 6** is not enhanced in the presence of anions (**Figure 5-7**), although there is a slight decrease in the rate when compound **5** is combined with 0.25 μM diphosphate (**Figure 5-7D**). At 0.25 μM diphosphate, the enzyme is inhibited ~ 50%.

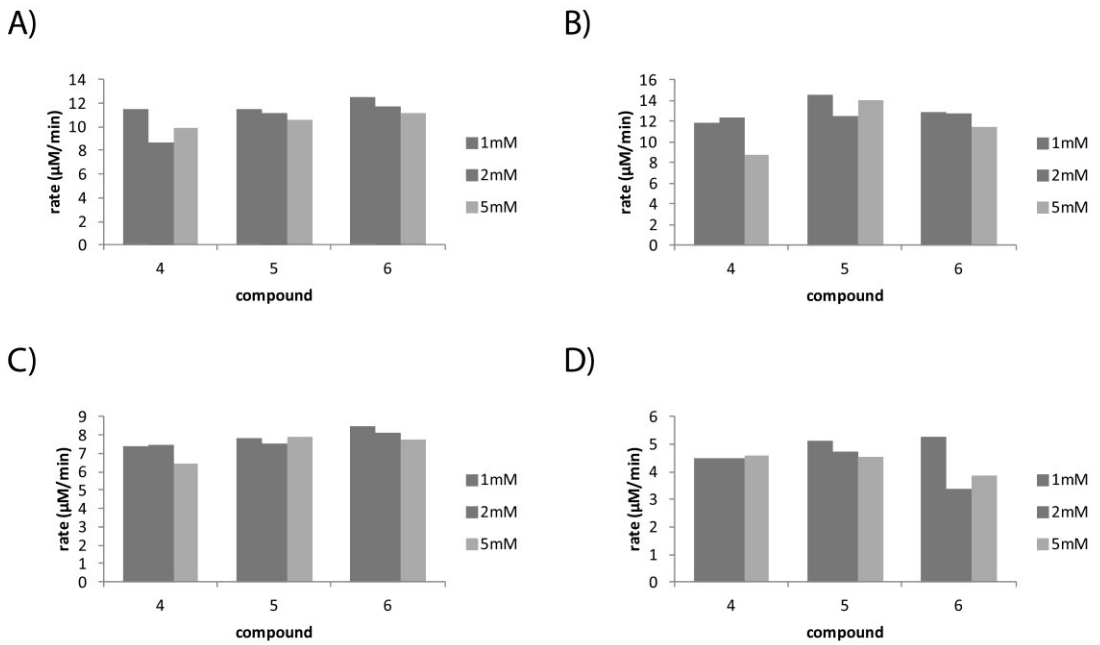

Figure 5-7. Evaluation of truncated FR900098 analogs 4 - 6 in combination with anions. Concentration of analog were varied from 0-5 mM. Activity assays were carried out in: **A**) 5 mM sodium chloride (NaCl), **B**) 5 mM bicarbonate, **C**) 5 mM inorganic phosphate, and **D**) 0.25 μM diphosphate.

The inhibitory activity of compound **3** is enhanced in the presence of inorganic phosphate (**Figure 5-8**). Further analysis indicates that enhanced inhibitory activity of **3** in the presence of inorganic phosphate is mutually dependent (using the Yonetani Theorell equation, Equation 1) [24].

$$v_i = {V_m}\Big/{\left[1 + \left(\frac{K_{mDXP}}{[DXP]}\right)\left(1 + \frac{[AHA]}{K_{iAHA}} + \frac{[P]}{K_{iP}} + \frac{[AHA][P]}{\alpha K_{iAHA} K_{iP}}\right)\right]} \qquad \textbf{Equation 1}$$

Where v_i = rate, V_m = maximum rate, and α = the interaction constant between AHA and phosphate in the E-AHA-phosphate complex. It is assumed that inhibitors and substrates are nonreactive with each other and that: ESI_1, ESI_2, and ESI_1I_2 are not formed in this

system [24]. For this analysis, terms were grouped into phenomenological variables to allow convergence. The Yonetani Theorell plot is shown in **Figure 5-8**. When $\alpha = 0$, two competitive inhibitors compete for the same site, and lines on the corresponding Yonetani Theorell plot will have parallel slopes. When $\infty > \alpha > 0$, two competitive inhibitors are interacting at different regions of a binding site in a mutually dependent relationship, and both the slope and intercept of the plots of $1/v_i$ versus AHA concentration will increase as linear functions of phosphate. A mutually dependent relationship is observed for AHA and phosphate, indicating they bind in different regions of the substrate binding site.

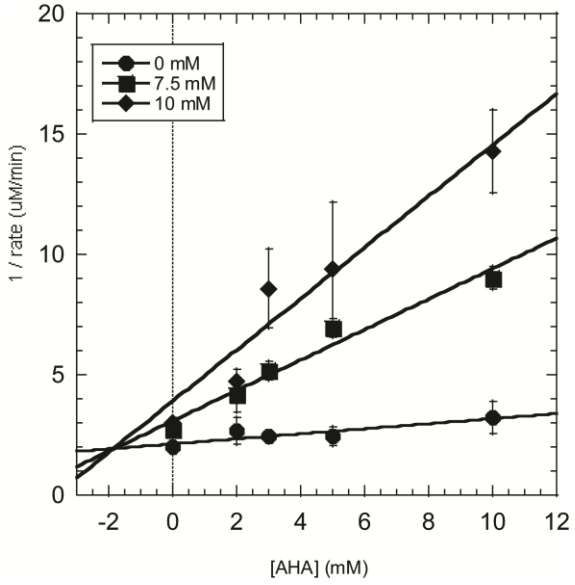

Figure 5-8. Inhibition of *E. coli* IspC by acetohydroxamic acid (AHA) is enhanced in the presence of phosphate. The Yonetani Theorell plot was generated using Equation 1 [24].

5.2. Confirming the reductive activation of FR900098 phosphonamidate prodrug.

Prodrug **7** (also synthesized by Dr. David Meyers, Synthetic Core Facility) was evaluated against IspC for inhibitory activity, and as expected, no inhibition was observed up to 0.5 mM prodrug. This was anticipated, as this prodrug is not activated to facilitate release of the IspC inhibitor FR900098 under standard IspC assay conditions. Inhibition of IspC under reducing conditions is more biologically relevant. Intracellular nitroreductases are known to reduce nitrogroups on diverse classes of substrates [(25)]; thus, these experiments were repeated following incubation of prodrug **7** with *E. coli* nitroreductase. The nitroreduction reaction was monitored at 340 nm to measure the disappearance of NADH. Under the conditions used here (see Experimental Section), the nitroreductase reaction was complete within 5 minutes. However, elimination, cyclization, and P-N hydrolysis events are also required to fully unmask compound **7** (**Figure 5-4**); thus, the incubation period was extended to 6 hours to ensure some amount of prodrug activation and FR900098 release. In these preliminary experiments, the apparent IC_{50} value for prodrug **7** post incubation is comparable to the IC_{50} values for fosmidomycin and FR900098 ($IC_{50}^{\text{fosmidomycin}} = 240 \pm 80$ nM; $IC_{50}^{\text{FR900098}} = 59 \pm 2.1$ nM ; $IC_{50}^{\text{apparent, prodrug 7}} = 270 \pm 90$ nM) (**Figure 5-9**). This preliminary result, combined with the observation that prodrug 7 is not an inhibitor of IspC in the absence of nitroreductase, indicates that reductive activation is required to release FR900098.

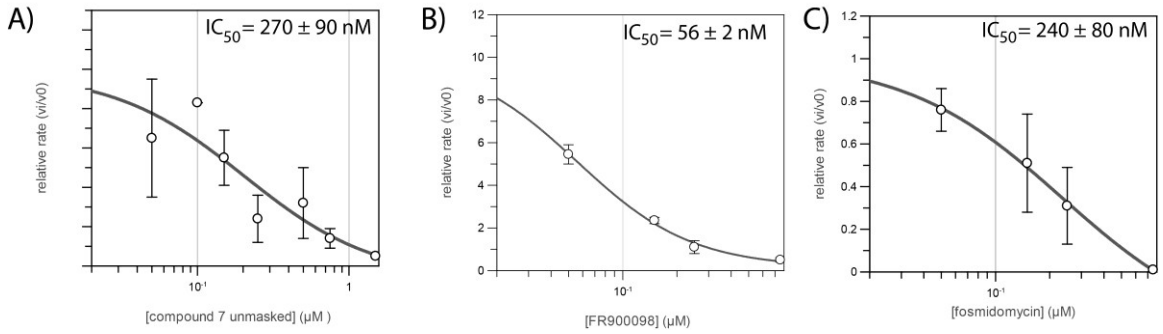

Figure 5-9. Apparent IC_{50} values for A) Unmasked FR900098 phosphonamidate prodrug, B) FR900098, and C) fosmidomycin. Experiments were performed in duplicate with representative plots shown.

5.3. Truncated FR900098 analogs evaluated against Plasmodium falciparum.

Compounds **3 - 7** were evaluated against *P. falciparum* (NF54), in collaboration with Prof. Theresa Shapiro, Johns Hopkins University, Dept. Pharmacology and Molecular Sciences (**Table 5-1**). Interestingly, prodrug **7** exhibits a comparable EC_{50} value to fosmidomycin ($EC_{50}^{FR900098}$ = 0.93 μM; EC_{50}^{7}= 1.03 μM). This suggests that after cellular uptake, the prodrug is capable of activation and subsequently inhibition of IspC. The EC_{50} of truncated analog **6** is ~27-fold higher than fosmidomycin, suggesting this membrane permeable analog can undergo phosphorylation to generate fosfoxacin, and then inhibit IspC. Compounds **3** and **4** also exhibited weak anti-parasitic activity with EC_{50} values 271 – 1119-fold higher than fosmidomycin.

compound	EC_{50} (μM)
fosmidomycin [+]	0.92 ± 0.02
FR900098 [+]	0.93
3*	250
4*	1030
6 [+]	25 ± 0
7 [+]	1.03 ± 0.07

Table 5-1. Anti-parasitic activity of fosmidomycin/FR900098 truncated analogs against NF54 *P. falciparum*. *performed in medium supplemented with 10% O^+ serum. [+]performed in medium supplemented with Albumax II.

It has been previously shown that fosmidomycin inhibition of *P. falciparum* can be chemically rescued by supplementation with isopentenyl diphosphate (IDP) [(26)]. This finding suggests an essential role of isoprenoids in parasites, and provides a valuable tool for validation of MEP pathway inhibitors. To validate the MEP pathway as the target of compounds **6** and **7**, and reduction of flux through the MEP pathway as the cause of anti-parasitic activity, rescue of anti-parasitic activity using isopentenyl diphosphate (IDP) was carried out (**Figure 5-10**). Parasite survival was observed for compounds **6** and **7** in the presence of IDP, as well as the fosmidomycin and FR900098 controls. Preliminary experiments to assess the antibacterial activity of prodrug **7** against *E. coli* MG1655 suggests weak growth inhibitory activity (MIC > 0.5 mM).

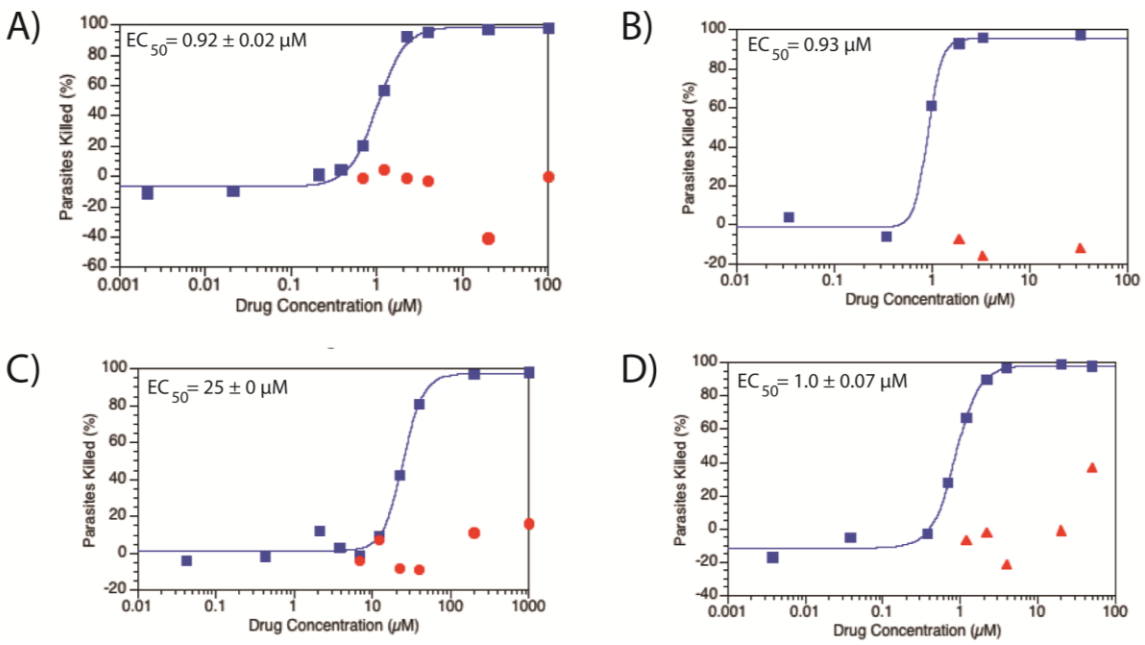

Figure 5-10. Percent *P. falciparum* killed with IDP rescue as a function of drug concentration. The dose response shown in blue for: **A)** fosmidomycin, **B)** FR900098, **C)** compound **6**, and **D)** compound **7**. Rescue by IDP is shown in red.

Conclusions

In this chapter we present alternatives to facilitate the intracellular entry of fosmidomycin and its analogs, toward improving pharmacokinetic propoerties. This was achieved by 1) taking advantage of the "two part" substrate mechanism that was recently elucidated for IspC [16] in which the dianion drives conformational changes of the active site, and 2) employing a prodrug strategy requiring intracellular phosphorylation of a hydroxyethyl precursor to fosfoxacin, and 3) using a phosphoamidite prodrug strategy for intracellular delivery of phosphonylated FR900098 [17-21]. We show that acetohydroxamic acid (AHA, **4**) inhibition of IspC is enhanced in the presence of inorganic phosphate. This

is an important finding because estimates of intracellular phosphate concentration are on the same order of magnitude as what is required to synergistically inhibit IspC in combination with AHA. Acetohydroxamic acid (AHA, **3**) is a potent and irreversible inhibitor of bacterial and plant urease [27]. Also known as Lithostat, it is used as an antibiotic to treat urinary tract infections [27]. Further, AHA is already an FDA approved antibiotic for the treatment of urinary tract infections, so it is possible that in addition to targeting bacterial urease, it might also act in combination with intracellular phosphate anion to inhibit IspC.

Additionally, we examined compound **7** as a prodrug of FR900098. As expected, compound **7**, bearing the masked phosphonyl group, does not inhibit recombinant *E. coli* IspC *in vitro* (IC_{50} > 0.5 mM); however, upon prodrug activation in the presence of *E. coli* nitroreductase, inhibition of IspC is indeed observed at a comparable activity to FR900098 under the same conditions ($IC_{50}^{apparent}$ = 0.27 ± 0.09 μM). This suggests that reduction of **7** leads to the expulsion of the active inhibitor. Importantly, prodrug **7** possesses potent anti-parasitic activity (EC_{50} = 1.0 ± 0.07 μM) that is rescued in the presence of IDP, suggesting prodrug **7** undergoes intracellular activation to release FR900098, a known inhibitor of isoprenoid biosynthesis.

Experimental Section

General Methods. Unless otherwise noted, all reagents were obtained from commercial sources. *E. coli* wild type DXP synthase was purified as described previously [28]. *E. coli* DXP reductoisomerase (IspC) was also prepared as described previously [29]. AHA was

purchased from Sigma. All other fosmidomycin/FR900098 analogs were chemically synthesized by Dr. David Meyers, Synthetic Core Facility.

Kinetic Analyses. DXP was generated using *E. coli* DXP synthase. DXP synthase reaction mixtures containing HEPES (100 mM, pH 8.0), 1 mg/mL BSA, 2 mM MgCl2, 2.5 mM tris(2-carboxyethyl)phosphine, 1 mM ThDP, 4 mM D,L-GAP, and 4 mM pyruvate were incubated at 37 °C for 90 minutes until reaction completion. After completion, DXP concentration was determined in a reaction mixture containing: HEPES (100 mM, pH 8.0), 1 mg/mL BSA, 2 mM MgCl2, 0.1 mM nicotinamide adenine dinucleotide phosphate (NAPDH), and 0.5 μM IspC. The final concentration of NAPDH was recorded at 340 nm and the concentration of DXP was determined. IspC was kinetically characterized as previously reported [(29)], with minor modifications: 10 nM enzyme was added to initiate each reaction, and the rate of NADPH depletion was monitored spectrophotometrically at 340 nm at 37°C. When NAPDH was the varied substrate, DXP was fixed at 0.5 mM. When DXP was the varied substrate, NAPDH was held at 0.1 mM. Double reciprocal analysis was performed using GraFit from Erithacus Software (version 7).

Inhibition Studies. IspC reaction mixtures were prepared as described above, with 0.18 mM NAPDH, 0.14 mM DXP, and 50 nM IspC. For inhibition assays, fosmidomycin was varied from 0 - 0.75 μM, compounds **4** – **7** were varied from 0 – 10 mM. The rate of IspC was also evaluated in the presence of chloride, bicarbonate, inorganic phosphate, and disphosphate, from 0 – 10 mM. Compound **4 - 6** were then evaluated in the presence of 5

mM sodium chloride (NaCl), 5 mM bicarbonate, 5 mM inorganic phosphate, and 0.25 μM diphosphate. Activation period of prodrug **7** was carried out over 6 hours, at 37 °C with the following reaction conditions: 100 mM HEPES (pH = 8.0), 0.25 mM NADH, 0.25 μM *E. coli* nitroreductase, and 0.25 mM prodrug **7**.

Evaluation of IspC inhibitors against *E. coli* and *P. falciparum*. Prodrug **7** was evaluated against *E. coli* MG1655 as outlined in Chapter 4. Evaluation of compounds **3** - **7** against *P. falciparum* was carried out as previously reported [30], in medium supplemented with either 10% O^+ serum or Albumax II, a serum substitute.

References

1. Takahashi, S., Kuzuyama, T., Watanabe, H. & Seto, H. A 1-deoxy-D-xylulose 5-phosphate reductoisomerase catalyzing the formation of 2-C-methyl-d-erythritol 4-phosphate in an alternative nonmevalonate pathway for terpenoid biosynthesis. *Proc. Natl. Acad. Sci. U. S. A*. **95**, 9879-9884 (1998).

2. Woo, Y. H., Fernandes, R. P. & Proteau, P. J. Evaluation of fosmidomycin analogs as inhibitors of the Synechocystis sp. PCC6803 1-deoxy-D-xylulose 5-phosphate reductoisomerase. *Bioorg Med Chem*. **14**, 2375-85 (2006).

3. Kuzuyama, T., Shimizu, T., Takahashi, S. & Seto, H. Fosmidomycin, a specific inhibitor of 1-deoxy-d-xylulose 5-phosphate reductoisomerase in the nonmevalonate pathway for terpenoid biosynthesis. *Tetrahedron Lett*. **39**, 7913-7916 (1998).

4. Albert Schweitzer Hospital. Efficacy of fosmidomycin-clindamycin for treating malaria in gabonese children. Clinical trial number NCT00214643. (2009).

5. Lanaspa, M., *et al.* Inadequate efficacy of a new formulation of fosmidomycin-clindamycin combination in Mozambican children less than three years old with uncomplicated *Plasmodium falciparum* malaria. *Antimicrob Agents Chemother.* **56**, 2923-8 (2012).

6. Mac Sweeney, A., *et al*. The Crystal structure of *E. coli* 1-deoxy-d-xylulose-5-phosphate reductoisomerase in a ternary complex with the antimalarial compound fosmidomycin and NADPH reveals a tight-binding closed enzyme conformation. *J. Mol. Biol.* **345**, 115-127 (2005).

7. Zingle, C., Kuntz, L., Tritsch, D., Grosdemange-Billiard, C. & Rohmer, M. Isoprenoid biosynthesis via the methylerythritol phosphate pathway: structural variations around phosphonate anchor and spacer of fosmidomycin, a potent inhibitor of deoxyxylulose phosphate reductoisomerase. *J. Org. Chem.* **75**, 3203-3207 (2010).

8. Umeda, T., *et al.* Molecular basis of fosmidomycin's action on the human malaria parasite *Plasmodium falciparum*. *Sci Rep*. 1-9 (2011).

9. Ortmann, R., *et al.* Acyloxyalkyl ester prodrugs of FR900098 with improved *in vivo* anti-malarial activity. *Bioorg Med Chem Lett*. **13**, 2163-6 (2003).

10. Reichenberg, A., *et al.* Diaryl ester prodrugs of FR900098 with improved *in vivo* antimalarial activity. *Bioorg Med Chem Lett*. **11**, 833-5 (2001).

11. Haemers, T., *et al.* Synthesis of alpha-substituted fosmidomycin analogues as highly potent Plasmodium falciparum growth inhibitors. *Bioorg Med Chem Lett.* **16**, 1888-91 (2006).

12. Jia, J., *et al.* Mechanisms of drug combinations: interaction and network perspectives. *Nat Rev Drug Discov*. **8**, 111-28 (2009).

13. Norén, J. O., Helgstrand, E., Johansson, N. G., Misiorny, A. & Stening, G. Synthesis of esters of phosphonoformic acid and their antiherpes activity. *J. Med. Chem*. **26**, 264-70 (1983).

14. Goryanova, B., Spong, K., Amyes, T. L. & Richard, J. P. Catalysis by orotidine 5'-monophosphate decarboxylase: effect of 5-fluoro and 4'-substituents on the decarboxylation of two-part substrates. *Biochemistry*. **22**, 537-46 (2013).

15. Amyes, T. L. and Richard, J. P. Enzymatic catalysis of proton transfer at carbon: activation of triosephosphate isomerase by phosphite dianion. *Biochemistry*. **46**, 841-54 (2007).

16. Kholodar, S. A. and Murkin, A. S. DXP reductoisomerase: reaction of the substrate in pieces reveals a catalytic role for the nonreacting phosphodianion group. *Biochemistry*. **52**, 2302-8 (2013).

17. Freel Meyers, C. L. and Borch, R. F. Activation mechanisms of nucleoside phosphoramidate prodrugs. *J. Med. Chem*. **43**, 4319-27 (2000).

18. Freel Meyers, C. L., Hong, L., Joswig, C. & Borch, R. F. Synthesis and biological activity of novel 5-fluoro-2'-deoxyuridine phosphoramidate prodrugs *J. Med. Chem*. **43**, 4313-8 (2000).

19. Tobias, S. C. and Borch, R. F. Synthesis and biological evaluation of a cytarabine phosphoramidate prodrug. *Mol Pharm*. **1**, 112-6 (2004).

20. Tobias, S. C. and Borch, R. F. Synthesis and biological studies of novel nucleoside phosphoramidate prodrugs. *J. Med. Chem*. **44**, 4475-80 (2001).

21.Webster, M. R., Zhao, M., Rudek, M. A., Hann, C. L. & Freel Meyers, C. L. Bisphosphonamidate clodronate prodrug exhibits potent anticancer activity in non-small-cell lung cancer cells. *J. Med. Chem*. **54**, 6647-56 (2011).

22. Auesukaree, C., *et al.* Intracellular phosphate serves as a signal for the regulation of the PHO pathway in*Saccharomyces cerevisiae. J. Biol. Chem*. **279**, 17289-94 (2004).

23. Tanokura, M. and Yamada, K. Changes in intracellular pH and inorganic phosphate concentration during and after muscle contraction as studied by time-resolved 31P-NMR. Alkalinization by contraction. *FEBS Lett*. **171**, 165-8 (1984).

24. Yonetani, T. The Yonetani-Theorell graphical method for examining overlapping subsites of enzyme active centers. *Methods Enzymol*. **87**, 500-9 (1982).

25. Race, P. R., *et al.* Structural and mechanistic studies of *Escherichia coli* nitroreductase with the antibiotic nitrofurazone. Reversed binding orientations in different redox states of the enzyme. *J. Biol. Chem*. **280**, 13256-64 (2005).

26. Yeh, E. and DeRisi, J. L. Chemical rescue of malaria parasites lacking an apicoplast defines organelle function in blood-stage Plasmodium falciparum. *PLoS Biol*. **9** (2011).

27. Lake, K. D. and Brown, D. C. New drug therapy for kidney stones: a review of cellulose sodium phosphate, acetohydroxamic acid, and potassium citrate. *Drug Intell Clin Pharm*. **19**, 530-9 (1985).

28. Brammer, L. A. and Meyers, C. F. Revealing substrate promiscuity of 1-deoxy-d-xylulose 5-phosphate synthase. *Org Lett*. **11**, 4748-51 (2009).

29. Brammer, L. A., Smith, J. M. & Meyers, C. F. 1-deoxy-D-xylulose 5-phosphate synthase: a novel random sequential mechanism in thiamine diphosphate-dependent enzymology. *J. Biol. Chem*. **42**, 36522-31 (2011).

30. Posner, G., Gonzalez, L., Cumming, J., Klinedinst, D. & Shapiro, T. A. Synthesis and antimalarial activity of heteroatom-containing bicyclic endoperoxides. *Tetrahedron*. **53**, 37-50 (1997).

CURRICULUM VITAE FOR Ph.D. CANDIDATES

The Johns Hopkins University School of Medicine

Jessica Mott Smith November 22, 2013

Educational History:

Ph.D.	2013	Program in Biochemistry, Cellular, and Molecular Biology (BCMB); Department of Pharmacology and Molecular Sciences Mentor: Dr. Caren L. Freel Meyers	Johns Hopkins University, School of Medicine
B.S.	2008	Department of Biology	University of Kentucky

Other Professional Experience:

Research Rotation	(2009) Lab of Dr. Robert Cotter, Johns Hopkins University
Research Rotation	(2009) Lab of Dr. Wade Gibson, Johns Hopkins University
Research Rotation	(2008) Lab of Dr. Geraldine Seydoux, Johns Hopkins University
Student Research	(2007-2008) Lab of Dr. Rebecca Kellum, University of Kentucky

Fellowships and Academic Honors:

2011-2013	National Institute of General Medical Sciences, Individual Predoctoral Kirschstein-NRSA Fellowship (F31 GM099467)
2013	1st place, BCMB Program Annual Recruiting poster session, JHU SOM.
2012	Faculty selected speaker, BCMB Program Annual Retreat, JHU SOM.
2011	1st place, BCMB Program Annual Retreat poster session, JHU SOM.
2011	1st place, third year and below. Annual Graduate Student Association poster session, JHU SOM.
2010	SACNAS Travel Award Recipient for the National Conference, Anaheim, CA

Publications:

Smith, J. M., Warrington, N.; Vierling, R.J.; Kuhn, M.L.; Anderson, W.F.; Koppisch, A.T.; Freel Meyers, C.L. (2013) Targeting DXP synthase in human pathogens: enzyme inhibition and antimicrobial activity of butylacetylphosphonate. *Journal of Antibiotics*. Advance online publication. doi: 10.1038/ja.2013.105.

Smith, JM*; Vierling, RJ*; Freel Meyers, C. (2012) Selective inhibition of *E. coli* 1-deoxy-D-xylulose-5-phosphate synthase by acetylphosphonates. *Medicinal Chemistry Communications.* **3**, 65-67. *these authors contributed equally

Brammer, LA*; **Smith, JM***; Wade, H; Freel Meyers, C. (2011) 1-Deoxy-D-xylulose 5-phosphate synthase: A novel random sequential mechanism in thiamine diphosphate-dependent enzymology. *Journal of Biological Chemistry*. **286**, 36522-31. *these authors contributed equally

Posters and Abstracts:

Smith, JM; Vierling, RJ; Freel Meyers, C. "Development and evaluation of butylacetylphosphonate (BAP) as a selective inhibitor of DXP synthase". Enzyme Mechanisms National Conference, Coronado Bay, CA. 2013.

Smith, JM; Vierling, RJ; Freel Meyers, C. "Selective inhibition of *E. coli* 1-deoxy-D-xylulose 5-phosphate synthase by acetylphosphonates". 2012.
Frontiers at the Chemistry and Biology Interface, University of Pennsylvania.
American Chemical Society, Middle Atlantic Regional Meeting.
BCMB Annual Retreat, selected for oral presentation, JHU SOM.

Smith, JM; Brammer, LA; Wade, H; Freel Meyers, C. "DXP Synthase: A new twist in thiamine diphosphate-dependent enzymology". Experimental Biology National Conference, Washington, D.C. 2011.

Smith, JM; Brammer, LA; Wade, H; Freel Meyers, C. "DXP Synthase: Investigating Substrate Binding and Catalysis".
SACNAS National Conference, Anaheim, CA. 2010.
Frontiers at the Chemistry and Biology Interface, JHU. 2010.

Service and Leadership

2013	Volunteer Board, Association for Women in Science, Bethesda, MD Chapter.
2009-2011	Event Organizer, BCMB monthly Student Colloquium Series.
2009-2010	Volunteer, The Ark Preschool for homeless children.